

**AN EXPERIMENTAL STUDY OF HEAT DRIVEN
ABSORPTION COOLING SYSTEMS.**

Thesis submitted for the degree of

MASTER OF SCIENCE

by

RAMÓN AYALA DELGADO

Department of Chemical & Gas Engineering

University of Salford

ENGLAND

JULY 1992.

**TO THE MEMORY
OF MY MOTHER**

CONTENTS

	Page
NOMENCLATURE	v
LIST OF TABLES	ix
LIST OF FIGURES	xi
ACKNOWLEDGMENTS	xiii
ABSTRACT	xv
CHAPTER 1 INTRODUCTION AND PERSPECTIVES FOR LOW	
ENTHALPY GEOTHERMAL ENERGY	
1.1 ENERGY RESOURCES	1
1.2 LOW ENTHALPY GEOTHERMAL ENERGY	1
1.3 GEOTHERMAL COOLING	2
1.4 PROSPECTS FOR LOW ENTHALPY GEOTHERMAL	
ENERGY	2
1.5 REFERENCES	3
CHAPTER 2 THERMODYNAMIC CONSIDERATIONS FOR HEAT	
DRIVEN ABSORPTION COOLING SYSTEMS.	
2.1 COOLING SYSTEMS	4
2.2 MECHANICAL VAPOUR COMPRESSION SYSTEMS ...	5
2.3 HEAT DRIVEN ABSORPTION COOLING SYSTEMS ...	7
2.4 AMMONIA-WATER HEAT DRIVEN ABSORPTION	
COOLING SYSTEMS	8
2.5 REFERENCES	10

**CHAPTER 3 THERMODYNAMIC CONSIDERATIONS FOR
FLUIDISED BED HEAT EXCHANGERS**

3.1	VERTICAL FLUIDISED BED HEAT EXCHANGERS . . .	15
3.2	PROPERTIES OF FLUIDISED BEDS	16
3.3	REFERENCES	18

**CHAPTER 4 EXPERIMENTAL STUDIES WITH AN ABSORPTION
SYSTEM FOR COLD STORAGE**

4.1	INTRODUCTION	21
4.2	EQUIPMENT	23
4.3	PROCEDURE	25
4.4	RESULTS AND DISCUSSIONS	25
4.5	CONCLUSIONS	27
4.6	REFERENCES	27

**CHAPTER 5 EXPERIMENTAL STUDIES WITH AN ABSORPTION
SYSTEM USED AS AN ICE MAKING MACHINE**

5.1	INTRODUCTION	44
5.2	VERTICAL TUBES ICE-GENERATOR	45
5.2.1	Introduction	45
5.2.2	Equipment	47
5.2.3	Procedure	48
5.2.4	Results and Discussions	48
5.3	INCLINED PLATE WITH TUBING COIL ICE- GENERATOR	50
5.3.1	Introduction	50

5.3.2	Equipment	52
5.3.3	Procedure	52
5.3.4	Results and Discussions	53
5.4	VERTICAL TUBE COIL ICE-GENERATOR	54
5.4.1	Introduction	54
5.4.2	Equipment	54
5.4.3	Procedure	55
5.4.4	Results and Discussions	56
5.5	ECONOMIC EVALUATION	58
5.6	CONCLUSIONS	59
5.6	REFERENCES	60

**CHAPTER 6 EXPERIMENTAL STUDIES WITH AN ABSORPTION
SYSTEM USING A FLUIDISED BED HEAT
EXCHANGER.**

6.1	INTRODUCTION	89
6.2	EQUIPMENT	89
6.3	PROCEDURE	91
6.4	RESULTS AND DISCUSSIONS	92
6.5	CONCLUSIONS	94
6.6	REFERENCES	94

CHAPTER 7 CONCLUSIONS AND RECOMMENDATIONS

7.1	CONCLUSIONS	99
7.2	RECOMMENDATIONS	101

APPENDIX 1 RAW EXPERIMENTAL DATA	103
--	-----

APPENDIX 2 SOFTWARE GENERATED

A2.1 NH3H ₂ O00 MODEL	132
A2.1.1 Introduction	132
A2.1.2 Programme Description	132
A2.1.3 How to Use the Programme	133
A2.1.4 Conclusions	134
A2.1.5 References	135
A2.1.6 Nomenclature	138
A2.1.7 Programme Listing	140
A2.2 REFRI00 MODEL	143
A2.2.1 Introduction	143
A2.2.2 Thermodynamic Considerations	143
A2.2.3 REFRI00 Programme Description	143
A2.2.3 How to Use the Programme	144
A2.2.4 Conclusions	146
A2.2.5 References	146
A2.2.6 REFRI00 Programme Print Out	151
A2.2.7 Programme Nomenclature	152
A2.2.8 Programme Listing	155

NOMENCLATURE

c	specific heat capacity [kJ kg ⁻¹]
COP	coefficient of performance [dimensionless]
CR	compression ratio P _{co} /P _{ev} [dimensionless]
d _p	particle diameter [m]
E	efficiency [dimensionless]
FR	flow ratio [dimensionless]
FS	solution flow rate [dimensionless]
g	gravitational acceleration [m s ⁻²]
H	enthalpy per unit mass [kJ kg ⁻¹]
h _{mf}	height of the bed at U _{mf} [m]
M	mass flow rate [kg s ⁻¹]
N	efficiency [dimensionless]
P	pressure [bar]
q	heat [kJ kg ⁻¹]
Q	heat load [kW]
r	latent heat of freezing [kJ kg ⁻¹]
R	radius [m]
S _o	surface area per unit volume [m ² m ⁻³]
t	time [min]
T	temperature [°C]
Th	thickness [m]
u _{mf}	the minimum superficial velocity [m s ⁻¹]

- u_t terminal (free-falling) velocity of a single particle in the fluid [m s^{-1}]
 w mass rate [kg]
 W rate of work delivered to the shaft of compressor, W or kW

SUBSCRIPTS

- a actual
- $_{AB}$ absorber
- $_{ACL}$ actual for cooling
- $_{AH}$ actual for heating
- b bed
- c constant
- c Carnot
- $_{CCL}$ Carnot for cooling
- co condenser
- $_{ECL}$ enthalpy based for cooling
- ev evaporator
- f freezing point
- f fluid
- $_{GE}$ generation
- $_{GEN}$ generator
- h for heating
- i ice
- if ice final
- $_{IG}$ ice-generator

k	refrigerant condensation
mf	minimum fluidization
p	particle
r	refrigerant
REC	recuperator
s	particle/solid
t	terminal
v	geothermal steam
w	water
w1	water initial
x	refrigerant evaporation

GREEK LETTERS

ΔP_b	vertical pressure drop [Pa]
δ_f	fluid density [kg m^{-3}]
δ_s	solid particles density [kg m^{-3}]
ϵ	bulk bed porosity [dimensionless]
ϵ_{mf}	bulk bed porosity at minimum fluidizing condition [dimensionless]
$1-\epsilon$	volume fraction of bed occupied by particles [dimensionless]
μ	the viscosity of the fluid [N s m^{-3}]

SUPERSCRIPTS

- n** Constant [dimensionless]

LIST OF TABLES

	Page
4.1 Main thermodynamic parameters of the absorption system as cold storage tests.	29
5.1 Characteristics of the equipment analyzed for economics analysis	61
5.2 PBP for a series of electricity costs	61
5.3 Ice-generator experimental data. September 10/91	62
5.4 Ice-generator experimental data. September 11/91	63
5.5 Ice-generator experimental data. October 31/91	64
5.6 Ice-generator experimental data. November 1/91	65
5.7 Ice-generator experimental data. November 12/91	66
5.8 Ice-generator experimental data. November 19/91	66
5.9 Ice-generator experimental data. November 20/91	67
6.1 Properties of sand particles	95
6.2 Brine chemical data in the LFBHE	95
A1.1 Raw experimental data 24-hour test August 17, 1990	104
A1.2 Raw experimental data 24-hour test August 21, 1990	107
A1.3 Raw experimental data August 29, 1990	110
A1.4 Raw experimental data August 30, 1990	111
A1.5 Raw experimental data August 31, 1990	112
A1.6 Raw experimental data September 6, 1990	113
A1.7 Raw experimental data September 7, 1990	114
A1.8 Raw experimental data September 10, 1990	115
A1.9 Raw experimental data September 11, 1990	116
A1.10 Raw experimental data September 11, 1990	117

A1.11	Experimental data and result of REFRI programme September 10, 1991	118
A1.12	Experimental data and result of REFRI programme September 11, 1991	118
A1.13	Experimental data and result of REFRI programme October 31, 1991	119
A1.14	Experimental data and result of REFRI programme November 1, 1991	119
A1.15	Experimental data and result of REFRI programme November 19, 1991	120
A1.16	Experimental data and result of REFRI programme November 20, 1991	120
A1.17	Experimental data and result of REFRI programme March 26, 1992	121
A1.18	Raw experimental data October 31, 1991	122
A1.19	Raw experimental data November 1, 1991	123
A1.20	Raw experimental data November 19, 1991	124
A1.21	Raw experimental data November 20, 1991	125
A1.22	Raw experimental data March 26, 1992	128
A1.23	Raw experimental data February 25, 1992	129
A1.24	Raw experimental data February 27, 1992	129
A1.25	Raw experimental data February 28, 1992	130
A1.26	Raw experimental data March 4 and 5, 1992	130
A1.27	Raw experimental data March 9 and 10, 1992	131
A1.28	Raw experimental data March 26, 1992	131
A2.1	NH ₃ H ₂ O programme ranges named and their localization in the worksheet	137
A2.2	REFRI00 programme ranges named and its localization into the worksheet	148
A2.3	Density of aqua ammonia solutions as a function of liquid concentration (%) , and temperature	150

LIST OF FIGURES

	Page
2.1 Mechanical vapour compression cooling system	11
2.2 Absorption system pressure temperature diagram	12
2.3 Schematic diagram for an absorption cooler system	13
2.4 Schematic diagram of the experimental absorption cooler	14
3.1 Vertical fluidised bed heat exchanger	19
3.2 Experimental fluidised bed heat exchanger	20
4.1 Schematic diagram of the experimental absorption cooler	30
4.2 Schematic diagram of the absorber	31
4.3 Schematic diagram of the generator	32
4.4 Schematic of the new separator rectifier	33
4.5 Experimental ammonia-water absorption refrigeration	34
4.6 Cooling water system	35
4.7 Theoretical flow ratio against actual flow ratio	36
4.8 Actual coefficient of performance against actual flow ratio	37
4.9 Generator efficiency against actual flow ratio	38
4.10 Actual coefficient of performance against recuperator efficiency	39
4.11 Recuperator efficiency against actual flow ratio	40
4.12 Coefficient of performance against generator temperature	41
4.13 Temperature against time (August 17, 1990)	42
4.14 Temperature against time (August 21, 1990)	43
5.1 Physical geometric characteristics	70
5.2 Schematic of vertical tubes ice-generator system	71
5.3 Schematic diagram of the ammonia-water absorption vertical tube prototype	72

5.4	Schematic diagram of the ammonia-water absorption vertical tube prototype with recirculation	73
5.5	Schematic diagram of the ammonia-water absorption vertical tube prototype with manual valves	74
5.6	Vertical tubes refrigerant flow diagram	75
5.7	Schematic diagram of the inclined plate ice generator	76
5.8	Stainless steel tubing coil distribution on the inclined plate ice generator . .	77
5.9	Schematic diagram of the ammonia-water absorption unit with the inclined plate ice generator	78
5.10	Vertical tube coil diagram	79
5.11	Vertical tube coil ice generator flow diagram	80
5.12	Ammonia-water absorption system with the vertical tube coil ice generator	81
5.13	Vertical tube coil ice-generator preliminary test (September 10, 1991) . . .	82
5.14	Vertical tube coil ice-generator preliminary test (September 11, 1991) . . .	83
5.15	Ice-generator evaluation test (October 31, 1991)	84
5.16	Ice-generator evaluation test (November 1, 1991)	85
5.17	Ice-generator evaluation test (November 12, 1991)	86
5.18	Ice-generator evaluation test (November 19, 1991)	87
5.19	Ice-generator evaluation test (November 20, 1991)	88
6.1	Brine separation system and LFBHE	96
6.2	Schematic diagram of the absorption system and the LFBHE	97
6.3	Particles classification system	98
A2.1	Main programme flowchart NH ₃ H ₂ O.	136
A2.2	Subroutines NH ₃ H ₂ O flowchart	136
A2.3	Flow diagram of REFRI00 programme	147

ACKNOWLEDGMENTS

I wish to express my deep thanks to the Instituto de Investigaciones Electricas Eléctricas, (IIE), for giving me the opportunity and supporting my participation in the IIE/University of Salford cooperative programme.

I also wish to thank the IIE Centro Cerro Prieto for the opportunity the use the experimental facilities.

I am grateful to Professor F. A. Holland for the supervision of this thesis and for his continuous valuable advice.

I am also grateful to Dr. Christopher Heard and Dr. Roberto Best for the cosupervision of this work and valuable advice.

Special thanks to Ing. Luis M. Lam for his invaluable help in the development of this work.

I extend my thanks to Mr. José Gpe. Sanchez, Mr. Benito Cañedo and Mr. José Figueroa for their help with the experimental equipment.

Thanks are also for IIE operators, technicians and secretaries, for their dedicated support during the project development.

ADDITIONAL ACKNOWLEDGMENTS

I wish to thank the Coordinadora Ejecutiva de Cerro Prieto, of Comision Federal de Electricidad (CFE), for providing the test site, the geothermal fluid, information on the field operation and for helping in the field operations.

ABSTRACT

The great need for cooling combined with Mexico's large availability of low enthalpy geothermal energy, makes it very attractive to utilize this resource for cooling using heat driven absorption systems. Mexico possesses large amounts of brine at temperatures which are too low to enable electricity to be generated efficiently and economically. Of the possible non electric uses of low and medium enthalpy geothermal energy are, to provide cold storage facilities for perishable foods and produce ice using the heat driven absorption cooling systems.

The main purpose of the work described in the thesis is to obtain experimental data on heat driven absorption cooling systems using geothermal energy for the design of large scale systems.

An experimental study on the performance of the ammonia-water absorption cooler operating on low enthalpy geothermal energy at the Cerro Prieto Geothermal Field was made. The system was used to cool a small storage unit at below freezing temperatures, during 8 hour tests and 24 hour tests.

An experimental study on the performance of the ammonia-water absorption cooler operating on low enthalpy geothermal energy at the Cerro Prieto Geothermal Field, has been made in order to operate it as an ice-making machine. Some prototypes of ice generators were designed, installed and operated.

An experimental study of a fluidized bed heat exchanger prototype connected to the ammonia-water absorption cooler was made in order to use the geothermal brine at the Cerro Prieto Geothermal Field.

Computer models based on LOTUS 123 worksheet were developed. These models were developed to calculate quickly and accurately the thermodynamic data from the water-ammonia absorption systems.

CHAPTER 1

INTRODUCTION AND PERSPECTIVES FOR LOW ENTHALPY GEOTHERMAL ENERGY

1.1 ENERGY RESOURCES

Even though Mexico has large reserves of hydrocarbons (about 420 EJ, where 1 EJ = 10^{18} J), a variety of energy sources and energy conservation measures are necessary for the following reasons. (i) There are technical and economical limits on the volume of hydrocarbons which can be extracted from the earth. (ii) There are also restrictions on the acquisition of foreign currency needed for industrial development. The by-products of the hydrocarbons industry are of great importance since they generate foreign currency. (iii) The cost per joule for non-renewable sources is likely to increase. (iv) An ecologically necessary limit to CO₂ emissions may be imposed. [Best (1990)]

1.2 LOW ENTHALPY GEOTHERMAL ENERGY

Geothermal energy in Mexico can be roughly classified as follows; [P. Mulas et al. (1985)]

- (1) low enthalpy (80-110°C) and medium enthalpy (110-170°C) fields approximately, 310 fields,

and

- (2) high enthalpy (170-350°C) fields, about 10 fields.

Most of the geothermal energy is at a temperature too low to produce electricity economically by conventional systems.

An attractive way of using low enthalpy geothermal energy is to produce refrigeration using heat driven absorption cooling systems. Since the most important geothermal fields are located in the vicinity of major agriculture areas, absorption coolers would enable geothermal energy to be used to provide cold storage systems for perishable foods products and ice production for food conservation during distribution.

1.3 GEOTHERMAL COOLING

Mexico possesses large amounts of geothermal brine at temperatures which are too low to enable electricity to be generated efficiently and economically. Of the possible non-electric uses of low and medium enthalpy geothermal energy, the one which appears to have the greatest potential is the use of heat driven absorption systems to provide cold storage facilities for perishable food and ice production for food conservation during the distribution process.

Most of the geothermal fields in Mexico are located near important agricultural areas. The largest geothermal field in Mexico is at Cerro Prieto which is near the growing city of Mexicali in Baja California. Mexicali is on the border with the U.S. state of California. It has a population in the region at 800,000 and rapidly growing.

At present the Cerro Prieto Geothermal field has an average production of $5,459 \text{ ton h}^{-1}$ of steam and $6,394 \text{ ton h}^{-1}$ of brine with 112 geothermal wells in operation. [CFE, (1991)].

1.4 PROSPECTS FOR LOW ENTHALPY GEOTHERMAL ENERGY.

In the middle of 1989, CFE (Comision Federal de Electricidad) analyzed the development of an industrial park adjacent to the Cerro Prieto geothermal field. The purpose of this

park was to make a comprehensive utilization of the residual heat from the brine produced by the power generation process. Presently, the legal and economic implications of this 580 hectare industrial park are being reviewed.

An industrial laundry is presently in operation in the Cerro Prieto geothermal field, and others projects are under consideration for using geothermal energy, including an ice plant.

1.5 REFERENCES

- 1.1 R. Best, An experimental study of heat driven absorption cooling systems, Ph.D. Thesis, University of Salford, England. pp 21-23. (1990).
- 1.2 P. Mulas, D. Nieva and F. A. Holland, Developments in geothermal energy in Mexico-Part one; General considerations, J. Heat Recovery Systems, 5(4) 285-297 (1985).
- 1.3 Comision Federal de Electricidad, Gerencia de proyectos geotermoelectricos, Residencia General de Cerro Prieto, Revista Informativa, Cerro Prieto Baja California Mexico, (1991).

CHAPTER 2

THERMODYNAMIC CONSIDERATIONS FOR HEAT DRIVEN ABSORPTION COOLING SYSTEMS.

2.1 COOLING SYSTEMS

Cooling systems are devices which are used to absorb or remove heat by evaporating the liquid refrigerant or refrigerant fluid, in the evaporator.

All cooling systems depend on five thermal laws, [Althouse et al (1982)].

- (i) Fluids absorb heat while changing from the liquid state to the vapour state and give up heat in changing from a vapour to a liquid.
- (ii) The temperature at which a change of state occurs is constant during the change provided the pressure remains constant.
- (iii) Heat flows only from a body which is at higher temperature to a body which is at a lower temperature (hot to cold).
- (iv) Metallic parts of the evaporating and condensing units use metals which have a high heat conductivity (copper, brass, aluminum).
- (v) Heat energy and other forms of energy are interchangeable. For example electricity may be converted to heat; heat to electrical energy and heat to mechanical energy.

Conventional prevalent large-scale cooling systems can be divided into two categories;

- (1) mechanical vapour compression systems,

and

- (2) heat driven absorption systems.

The first category has a compression cycle. The compression cycle is so named because it is the compressor which changes the refrigerant vapour from low pressure to high pressure. In the second category the increase in pressure is achieved by using a secondary circuit, in which a liquid absorbent is recirculated with a pump. [Best et al (1990)]

2.2 MECHANICAL VAPOUR COMPRESSION SYSTEMS

The most common type of cooling system is the vapour compression system using a mechanical compressor as shown schematically in Figure 2.1. It consists of two heat exchangers, a compressor, an expansion valve and a working fluid. In the evaporator heat exchanger, the working fluid evaporates at an absolute temperature T_{EV} extracting an amount of heat Q_{EV} from the source which may be in the gaseous, liquid or solid state. The working fluid is then compressed and gives up an amount of latent heat Q_{CO} at a higher absolute temperature T_{CO} in the condenser heat exchanger. The condensed working fluid is then expanded through the expansion valve and is returned to the evaporator to complete the cycle.

From the first law of thermodynamics, the amount of heat delivered Q_{CO} at higher temperature T_{CO} is related to the amount of heat extracted Q_{EV} at lower temperature T_{EV} and the amount of high grade energy input W by equation (2.1)

$$Q_{CO} = Q_{EV} + W \quad (2.1)$$

The coefficient of performance (COP) of a compressor driven vapour compression cooling system can be written in the forms

$$\text{COP}_H = \frac{Q_{CO}}{W} = \frac{Q_{CO}}{Q_{CO}-Q_{EV}} \quad (2.2)$$

and

$$\text{COP}_{ACL} = \frac{Q_{EV}}{W} = \frac{Q_{EV}}{Q_{CO}-Q_{EV}} \quad (2.3)$$

where COP_H is the coefficient of performance for heating and COP_{ACL} is the coefficient of performance for cooling.

From equations (2.1-2.3) the coefficient of performance for heating is related to the coefficient of performance for cooling by the equation (2.4)

$$\text{COP}_H = \text{COP}_{CL} - 1 \quad (2.4)$$

For the theoretically ideal case of zero increase in entropy, the Carnot coefficient of performance of the mechanical vapour compression system shown schematically in Fig. 2.1 can be written

$$\text{COP}_{CCL} = \frac{T_{EV}}{T_{CO}-T_{EV}} \quad (2.5)$$

2.3 HEAT DRIVEN ABSORPTION SYSTEMS

The absorption system is different from the compression system. It uses heat energy instead of mechanical energy to make the change in the conditions necessary to complete a refrigeration cycle. This less common type of refrigeration system is shown in Figs. 2.2 and 2.3. The condensation, expansion and evaporation are the same as in the conventional compressor driven system. However, in the absorption cycle, the compressor is replaced by a secondary circuit in which a liquid absorbent is circulated by a pump. The evaporated refrigerant is absorbed by the recirculating liquid and the pressure is increased by the pump prior to entering the generator. An amount of high grade heat Q_{GE} is added at an absolute temperature T_{GE} in the generator to produce the high pressure refrigerant vapour required to feed the condenser. [Best et al (1986)]

The mechanical energy required to pump the liquid is usually negligible compared to the input of high grade heat energy Q_{GE} .

The pump in the secondary circuit of an absorption heat pump provides the compression ratio $CR = P_{CO}/P_{EV}$.

The coefficient of performance of a conventional absorption cooler can be defined as

$$COP_{ACL} = \frac{Q_{EV}}{Q_{GE}} \quad (2.6)$$

The coefficient of performance of a conventional absorption system for heating can be defined as

$$\text{COP}_{\text{AH}} = \frac{Q_{\text{EV}} + Q_{\text{AB}}}{Q_{\text{GE}}} \quad (2.7)$$

The Carnot coefficient of performance of the heat driven absorption cooling system is shown schematically in Figs. 2.2 and 2.3, can be written as

$$\text{COP}_{\text{CCL}} = \left(1 - \frac{T_{\text{CO}}}{T_{\text{GE}}}\right) \left(\frac{T_{\text{EV}}}{T_{\text{CO}} - T_{\text{EV}}}\right) \quad (2.8)$$

2.4 AMMONIA-WATER HEAT DRIVEN ABSORPTION COOLING SYSTEMS.

The ammonia-water absorption system technique is a specific example where the vaporizing refrigerant is ammonia and the absorbent liquid is water, or dilute aqueous solution of ammonia (weak solution). The absorber then produces a concentrated solution of ammonia in water (strong solution). This rich solution is separated by evaporation and distillation into two streams-a liquid ammonia overhead product (recycled as refrigerant) and the water-rich (weak solution) used as absorbent. Figure 2.4 shows the basic flow sheet for the ammonia-water absorption system installed at Cerro Prieto Geothermal field. [Bogart (1981)].

The main parameters that define the performance of an ammonia-water absorption refrigeration system are as follows. From thermodynamics and from mass and heat balance considerations, with reference to Fig. 2.4, [Best et al (1986)] and using the above defined nomenclature, the actual coefficient of performance is given by equation.

$$\text{COP}_A = \frac{Q_{\text{EV}}}{Q_{\text{GE}}} \quad (2.9)$$

The actual coefficient of performance already defined by equation (2.9) can also be written as

$$\text{COP}_A = \frac{M_R (H_{17} - H_{15})}{M_{AB} (H_8 - H_7)} \quad (2.10)$$

where H_8 is the enthalpy per mass unit of the vapour-liquid mixture leaving the generator.

The Carnot coefficient of performance is given by

$$\text{COP}_{CCL} = \left(\frac{(T_{GE} - T_{AB})}{T_{GE}} \right) \left(\frac{T_{EV}}{(T_{CO} - T_{EV})} \right) \quad (2.11)$$

and the theoretical coefficient of performance based on enthalpies is

$$\text{COP}_{ECL} = \frac{(H_{17} - H_{15})}{H_{10} - H_{11} - (H_{11} - H_7) FR} \quad (2.12)$$

where FR is the flow ratio and is defined as the ratio of the mass flow rate of solution from the absorber to generator, to the mass flow rate of refrigerant from the condenser and to the evaporator.

Alternatively the flow ratio can be rewritten in terms of concentrations as:

$$FR = \frac{X_R - X_{GE}}{X_{AB} - X_{GE}} \quad (2.13)$$

The efficiency of the recuperator is given by

$$\eta_{REC} = \frac{H_5 - H_4}{H_5 - H_{43}} \quad (2.14)$$

where H_{43} is the enthalpy of the ammonia/water solution with concentration X_4 but at the temperature T_3 .

The efficiency of the generator is defined as

$$N_{GEN} = \frac{H_7 - H_8}{H_7 - H_{v8}} \quad (2.15)$$

where H_{v8} is the enthalpy of the vapour-liquid mixture leaving the generator at the geothermal vapor temperature T_v . [Best et al (1990)]

2.5 REFERENCES

- 2.1 R. Best, C. L. Heard, H. Fernandez and J. Siqueiros, Developments in geothermal energy in Mexico-Part five: The commissioning of an ammonia/water absorption cooler operating on low enthalpy geothermal energy, *J. Heat Recovery Systems* **6** (3) 209-216 (1986).
- 2.2 R. Best, C. L. Heard, P. Peña, H. Fernandez and F. A. Holland, Developments in geothermal energy in Mexico-Part twenty six: Experimental assessment of an ammonia/water absorption cooler operating on low enthalpy geothermal energy, *J. Heat Recovery Systems & CHP*, **10** (1) 61-70 (1990).
- 2.3 A. D. Althouse, C.H. Turnquist and A. F. Bracciano, Modern refrigeration and air conditioning, The Goodheart-Willcox, CO. Publ. South Holland II, pp 73-99, (1982).
- 2.4 M. Bogart, Ammonia absorption refrigeration in industrial process, Gulf Publ. Co. Houston, Tx, USA. pp 30-31, (1981).
- 2.5 R. Best, An experimental study of heat driven absorption cooling systems, Thesis for Ph.D. University of Salford, England. pp 21-23. (1990).

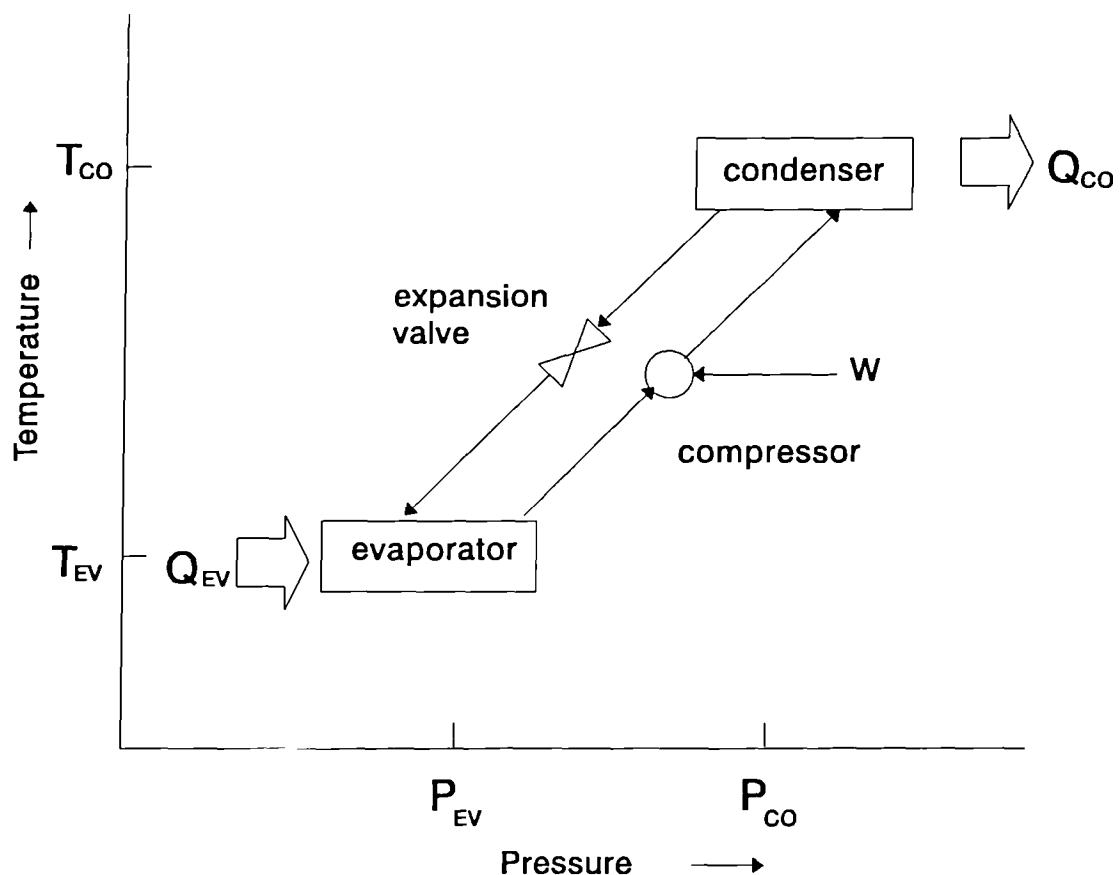


Fig. 2.1 Mechanical vapour compression cooling system

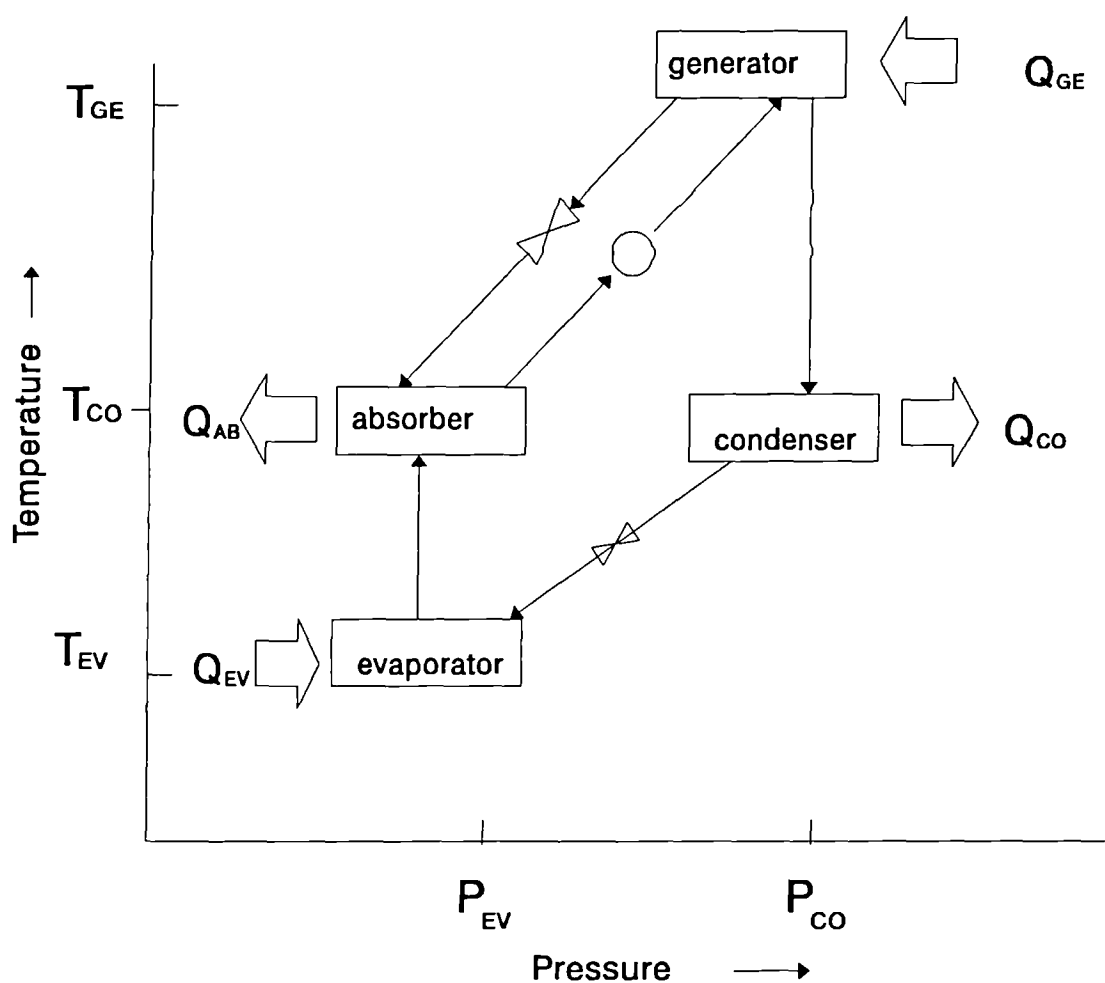


Fig. 2.2 Absorption system pressure temperature diagram

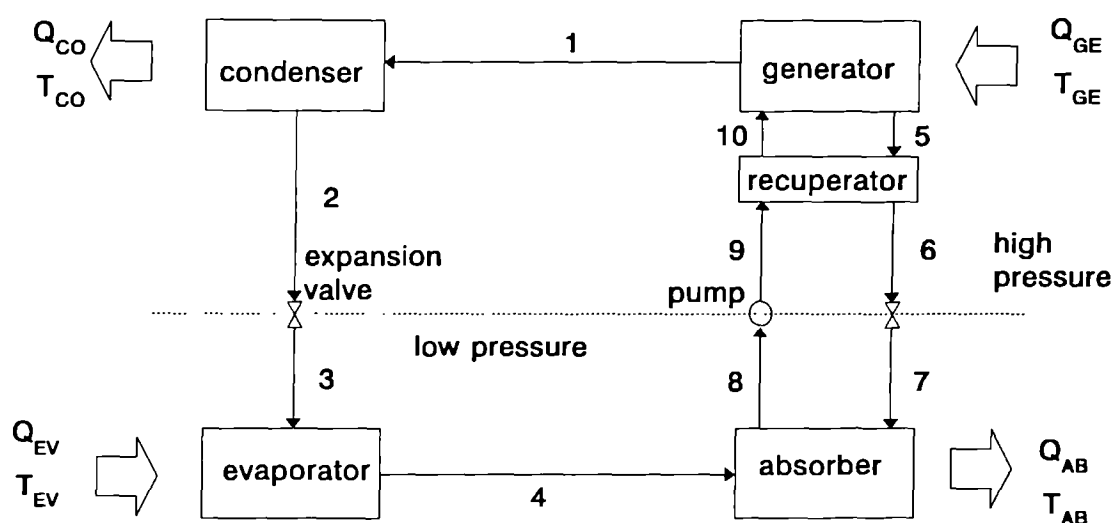


Fig. 2.3 Schematic diagram for a absorption cooler system

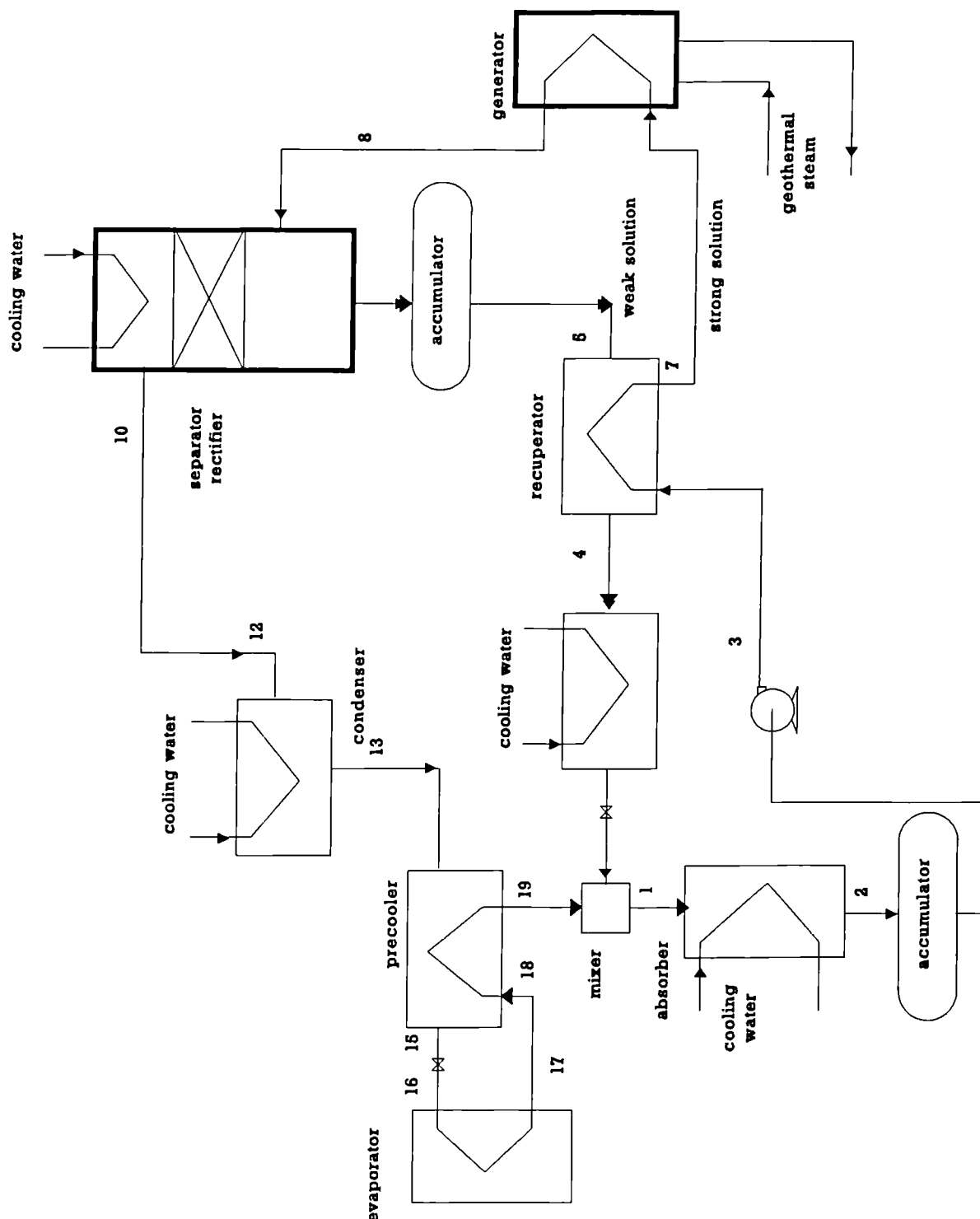


Fig. 2.4 Schematic diagram of the experimental absorption cooler

CHAPTER 3

THERMODYNAMIC CONSIDERATIONS FOR FLUIDISED BED HEAT EXCHANGERS.

3.1 VERTICAL FLUIDISED BED HEAT EXCHANGERS

The principle of operation of a typical vertical fluidised bed heat exchanger is shown in Fig. 3.1. [D. G. Claren, (1989)]. Externally the fluidised heat exchanger resembles a conventional vertical shell and tube heat exchanger. However, internally within the tubes small solid particles are kept in a quasistationary fluidised condition by the liquid passing up through the tubes. In this context, "quasistationary" means that the continuous swarm of particles is carried by the liquid in the tubes from the inlet channel to the lower section of the outlet channel. In the outlet channel the particles disengage from the liquid and are returned to the inlet channel through a number of downcomer tubes.

Practical application of this principle requires that the particles be evenly distributed over all the tubes. In this way the stability of the multiple parallel fluidised beds is guaranteed. The particles must not leave the outlet channel of the heat exchanger. This can be summarized as follows.

- (i) The solid particles have a slightly abrasive (or polishing) effect on the wall of the heat exchanger tubes, so that any deposit will be removed at an early stage.
- (ii) The solid particles regularly break through the boundary layer at the tube wall, so that heat transfer is improved despite comparatively low liquid velocities in the tubes.

In this work a vertical liquid fluidised bed heat exchanger was studied using sand particles as the bed material and the experimental equipment is a single concentric tube heat exchanger. See Fig 3.2, [C. Heard, (1989)]

3.2 PROPERTIES OF FLUIDISED BEDS

The fluidisation literature deals mostly with gas/solid systems for it is in these that most applications have arisen. The very few fundamental studies of liquid fluidised beds have involved particles of carefully characterized, uniform shapes and smooth surfaces.

In the present application silica sand was used because of its availability, low cost and surface affinity for silica deposition. However sand particles are neither smooth nor uniform and they do not behave in strict accordance with the correlations that describe more idealized fluidised systems.

Fluidisation Velocity

A major constraint on sizing a fluidised bed is u_{mf} , the minimum superficial velocity (i.e. the fluid velocity relative to the particles) for fluidisation. The vertical pressure drop in the bed is given by; [R. Axtmann, 1986]

$$\Delta P_b = (\delta_s - \delta_f) (1 - \epsilon_{mf}) H_{mf} (g/g_c) \quad (3.1)$$

where δ_s and δ_f are the densities of the solid particles and the fluid, ϵ_{mf} is the voidage (approximately 0.4 for most granular material at rest), H_{mf} is the height of the bed at u_{mf} , g is the acceleration of gravity and g_c the gravitational constant where in SI units $g_c = 1$ and dimensionless. As the bed expands with increasing fluid flow rate, the product $(1-\epsilon)H$

remains constant, as does ΔP_b .

According to the Carman-Kozeny equation for fine particle fluidisation,

$$u_{mf} = \frac{\epsilon^3_{mf} \Delta P_b}{5(1 - \epsilon_{mf})^2 S_o^2 \mu H_{mf}} \quad (3.2)$$

where S_o is the surface area per unit volume of a single particle and μ the viscosity of the fluid. Since $(1-\epsilon)H$ is constant, combining eqs 3.1 and 3.2 gives

$$u_{mf} = \frac{\epsilon^3_{mf} (\delta_s - \delta_f) g}{5(1 - \epsilon_{mf}) S_o^2 \mu g_c} \quad (3.3)$$

For uniform spherical particles, $S_o = 6/d_p$ where d_p is the particle diameter; then, for

$$\epsilon = 0.4$$

$$u_{mf} = 0.00059 \frac{d_p (\delta_s - \delta_f) g}{\mu g_c} \quad (3.4)$$

Voidage

Fluidised beds are universally characterized by an empirical equation that relates the voidage, ϵ , to u , the superficial velocity of the fluid, [J. Richardson, (1954)]

$$\epsilon^n = \frac{u}{u_t} \quad (3.4)$$

where the u_t is the terminal (free-falling) velocity of a single particle in the fluid. Equation 3.4 has no theoretical basis and the exponent n must be determined by experiment, i.e. by measuring the slope of a log - log plot of voidage vs superficial velocity.

3.3 REFERENCES

- 3.1 D. G. Claren and R.E. Bailie, The non-fouling fluidised bed heat exchanger, Heat transfer equipment fundamentals, Design, applications, and Operating problems. The American Society of Mechanical Engineers, Book No. H00500, pp 276-278, (1989).
- 3.2 C. Heard, preliminary design (1989)
- 3.3 R. C. Axtmann and D. Grant-taylor, Desalination of geothermal wastewaters in fluidised beds, Geothermics, **15**, No. 2, 185-191, (1986).
- 3.4 J. F. Richardson and W. N. Zaki, Sedimentation and fluidisation: part I, Trans. Inst. Chem. Engrs, London, **32**, 35-53 (1954).

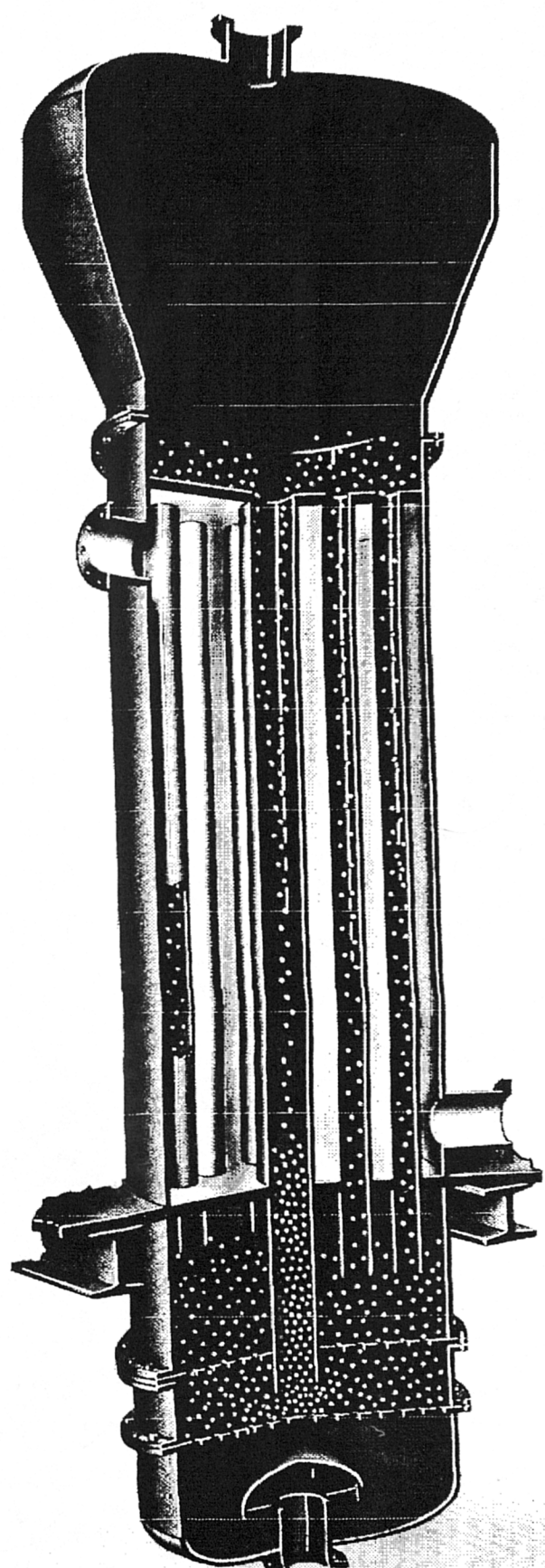


Fig 3.1 Vertical fluidised bed heat exchanger

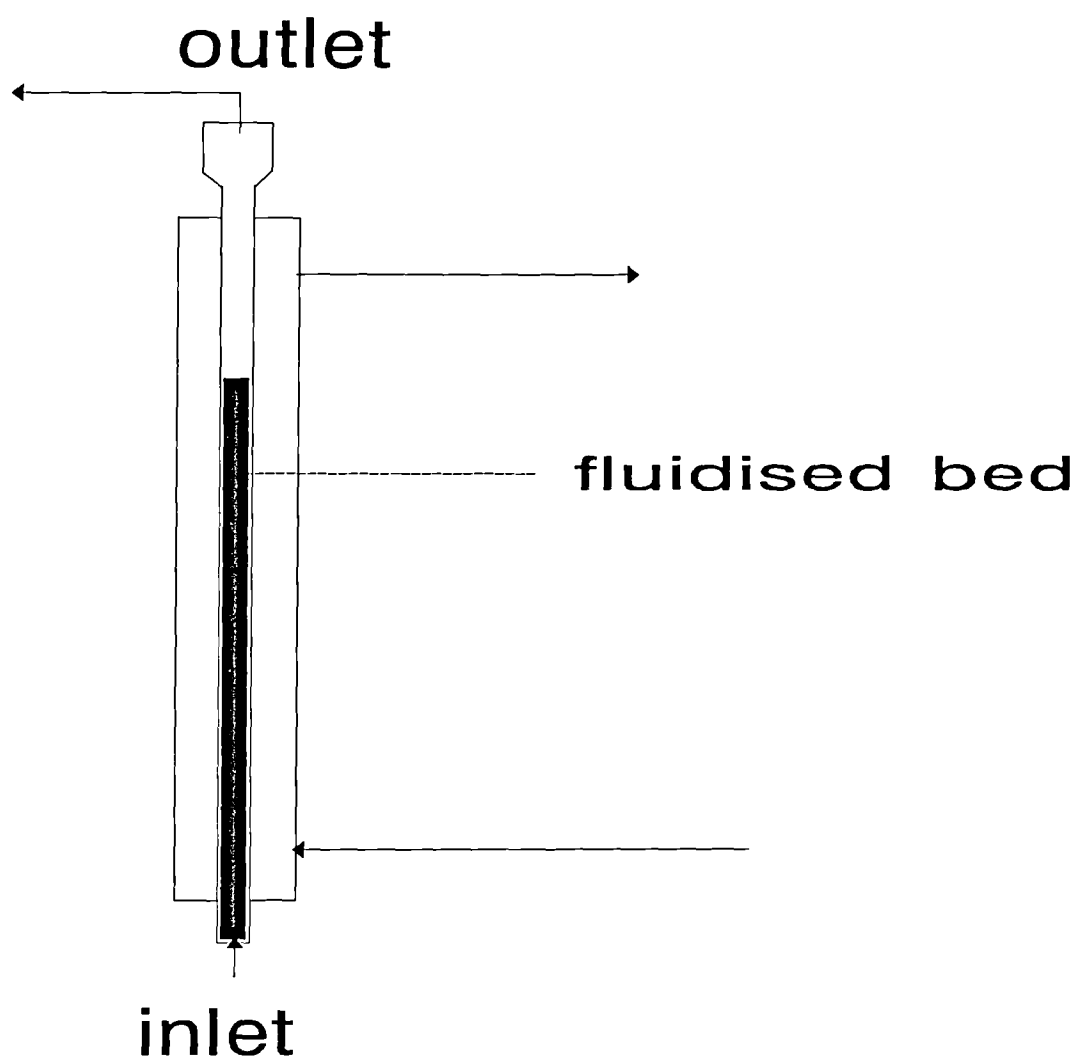


Fig 3.2 Experimental fluidised bed heat exchanger

CHAPTER 4

EXPERIMENTAL STUDIES WITH AN ABSORPTION SYSTEM FOR COLD STORAGE

4.1 INTRODUCTION

Mexico possesses large amounts of geothermal energy at temperatures which are too low to enable electricity to be generated efficiently and economically. Of the possible non-electric uses of low and medium enthalpy geothermal energy, the one which appears to have the greatest potential is to use the heat driven absorption systems to provide cold storage facilities for perishable food. It has been estimated that perishable food losses in Mexico, resulting from inadequate handling and cooling facilities, vary from 35 to 50% with sea food having the highest losses [R. Best, 1990]. Spauschus [Spauschus, (1987)] has published data on the world market for refrigeration and air conditioning equipment. The study showed that North America, Japan and Europe produce and purchase almost 90% of the refrigeration equipment in the world, although they account for less than 25% of the world population. The Middle East, Africa, China and the USSR, with 59% of the world population, produce and purchase less than 5% of the refrigeration equipment in the world. Latin America, with 10% of the world population, produces and purchases 6% of the refrigeration equipment in the world.

The enormous potential demand for refrigeration in the less developed regions of the world will need to be met by all the available technologies and energy sources. The low enthalpy heat from solar radiation, geothermal fluids and biomass can play an important role in meeting this demand.

Most of the geothermal fields in Mexico are located near important agricultural areas. The largest geothermal field in Mexico is at Cerro Prieto which is near the growing city of Mexicali in Baja California. Mexicali is on the border with the U.S. state of California.

In order to continue proving the technical feasibility of operating heat driven absorption cooling systems on low enthalpy geothermal energy, the prototype installed in the Cerro Prieto geothermal field was evaluated under other operating conditions.

This prototype ammonia-water absorption refrigerator used in previous experiments, was originally designed for, and installed in the Los Azufres geothermal field, [Best et al (1986)], and was operated successfully at the Cerro Prieto geothermal field using low enthalpy geothermal steam, under extreme hot weather conditions and high cooling water temperatures [Best et al (1990)].

In order to evaluate the ammonia-water absorption system installed at the Cerro Prieto geothermal field in long test periods, two 24-hour tests were performed to observe its efficiency with ambient temperature variations, and to find out how many changes to the system are required in order to maintain generation and evaporation temperatures. The previous testing periods ranged between 6 to 7 hours for each test.

Another series of tests was performed with the same system in order to complete the data base with generation temperatures between 125 and 90°C and $9.46 \times 10^{-5} \text{ m}^3 \text{ s}^{-1}$ (1.5 gpm) of weak solution.

The two 24-hour tests were performed with the following objectives,

- (i). to find the system parameters that are going to be corrected, in order to maintain the steady state conditions during ambient temperature variations,

- (ii) to estimate the total energy consumption of the system in order to evaluate its economic feasibility,

- (iii) to calculate the main parameters of the system in order to define its performance,

- and
- (iv) to observe how the modifications to the original unit *can help obtain a better performance from the system*

4.2 EQUIPMENT

Figure 4.1 is a schematic diagram of the experimental absorption cooler which was installed at the Cerro Prieto Geothermal field. The unit was designed for fabrication at minimum expense. The helicoidal coil in the generator and in the rectifier were the only components made of stainless steel. This was necessary to minimize corrosion and scaling during its contact with geothermal fluid. The other components were determined by the availability of materials.

The condenser and the evaporator were standard commercially available units. The condenser was a model CAH-06 shell and tube heat exchanger with a nominal capacity of 17.6 kW supplied by Herdel Co., Mexico. It consisted of a 0.27 m internal diameter shell and thirty 2.5 m long tubes with internal diameter of 0.016 m in a pass arrangement. The evaporator was model 1500 XRWA shell and tube heat exchanger supplied by Recold Co., Mexico, with a nominal capacity of 10.6 kW at 5.6 °C difference in temperature between

the air entering the evaporator and the saturation temperature of the working fluid in the evaporator.

The absorber is illustrated in Fig. 4.2. It consists of a vertical one pass shell and tube heat exchanger. The internal diameter of the shell was 0.20 m and the tube bundle contained thirty six tubes with an internal diameter of 0.2 m. Dilute ammonia solution was mixed with ammonia vapor before entering the absorber in order to enhance heat and mass transfer. The absorber was 1.8 m long.

The generator was a shell and tube heat exchanger. The generator is illustrated schematically in Fig. 4.3. The 1 m long shell was made of available tube with an internal diameter of 0.318 m. Geothermal steam entered at the bottom of the shell and was distributed through a perforate vertical pipe with internal diameter of 0.027 m in the centre of the surrounding coil. The ammonia-water solution circulated through the 17.3 m long stainless steel helicoidal coil which had an internal diameter of 0.0158 m.

The rectifier was a separator/rectifier unit. This consists of a single vessel with a larger inside volume for vapour-liquid separation than the one originally used. This unit was modified installing a stainless steel coil and a flange. The unit was filled in the upper part with stainless steel packing for a more efficient rectification, and to allow it to be operated over a wider range of strong solution flow rates M_{AB} (see Fig. 4.4).

The solution pump used was a piston pump unit. The evaporator was located inside a storage chamber with a volume of 19.2 m³. It was equipped with three low energy consumption fans to increase the air circulation rate and to make the temperature uniform.

The storage chamber was constructed with 0.05 m thick polyethylene and covered by a 0.06 m thick wood sheet.

Additionally there are two more detailed diagrams of the complete system Figs. 4.5 and 4.6.

4.3 EXPERIMENTAL PROCEDURE

The system was operated manually. Initially the system was charged with 49.3 kg of water and 37.5 of ammonia and 0.74 kg of sodium dichromate as a corrosion inhibitor. Geothermal steam was fed to the generator and the pressure and temperature were controlled until the required steam temperature was reached. When the pressure of the ammonia solution in the generator increased to the operating value, the solution pump and the evaporator fans were turned on. The system was controlled by fixing the solution and the refrigerant flow rates . This was accomplished by manipulating the liquid refrigerant expansion valve between the precooler and the evaporator and the ammonia-water solution expansion valve between the recuperator and the mixer.

The various temperatures, pressures and flows were continuously recorded during each run. For a particular geothermal steam temperature, steady state conditions were achieved when the flow readings in the rotameters and the liquid levels in the accumulators were constant.

4.4 RESULTS AND DISCUSSIONS

During system operation in 24-hour tests, only two parameters had to be controlled in order to keep the steady state; the refrigerant expansion valve and the geothermal steam valve at the generator entrance.

Table 4.1 shows the main thermodynamics parameters for each test, during 1990.

Tables A1-1 to A1-10 in Appendix 1 show all the data recorded during the experimentation; at the bottom of each column an average and standard deviation of every parameter are shown in order to see the stability of tests.

Figure 4.7 shows the relationship between the actual flow ratio FR_A compared with the thermodynamic flow ratio FR . The last test of September 10th and 11th, revealed some problems with the flow relations. The low generation temperature produced low refrigerant flows and since the flow meter scale begins at $6.31 \times 10^{-6} \text{ m}^3 \text{ s}^{-1}$ (0.1 gpm) it is hard to read the exact data, when the flow is lower than that.

Figure 4.8 is a plot of actual coefficient of performance COP_A against actual flow ratio FR_A . This confirms the observation made by Best [Best et al (1990)] that at lower values of the flow ratio the system operates at higher efficiencies.

Figure 4.9 is a plot of efficiency of the generator against flow ratio. It can be seen that the efficiency of heat transfer from the geothermal steam to the ammonia/water solution in the generator varied from 0.67 to 0.94. Evidently, the efficiency of the generator is also greater at lower flow rates due to heat losses and steam flow control problems at lower steam flow rates.

Figure 4.10 is a plot of the value of the actual coefficient of performance against the efficiency of the recuperator heat exchanger. This confirms the observation made by Best [Best et al (1990)] that at higher values of heat exchanger efficiency the coefficient of performance has higher values.

Figure 4.11 is a plot of the efficiency of the recuperator N_{REC} against values of actual flow ratio.

Figure 4.12 is a plot of the enthalpy coefficient of performance COP_{ECL} and actual coefficient of performance COP_A against generator temperatures. It can be seen that the coefficient increases with increasing generator temperatures.

Figure 4.13 and 4.14 are plots of ambient temperature, cooling water temperature and cold storage temperature against time in the two 24-hours tests. They show the stability of the system.

4.5 CONCLUSIONS

It can be shown that the ammonia-water absorption refrigerant system can have a good performance for long periods, with a minimum of control.

The experimental data obtained will be added to the data base and will be used to improve the design and operation of the system and will provide an excellent basis for the design of large scale heat driven absorption refrigeration systems.

4.6 REFERENCES

- 4.1 R. Best, C. L. Heard, H. Fernandez and J. Siqueiros, Developments in geothermal energy in Mexico-Part five: The commissioning of an ammonia/water absorption cooler operating on low enthalpy geothermal energy, *J. Heat Recovery Systems & CHP*, **6** (3) 209-216 (1986).
- 4.2 R. Best, C. L. Heard, P. Peña, H. Fernandez and F. A. Holland, Developments in geothermal energy in Mexico-Part twenty six: Experimental assessment of an

- ammonia/water absorption cooler operating on low enthalpy geothermal energy,
J. Heat Recovery Systems & CHP, **10** (1) 61-70 (1990).
- 4.3 H.O. Spauschus, Development in refrigeration: technical advances and opportunities for the 1990, Int, J, Refrig. 10 (5), 263-270 (1987).
- 4.4 International institute of refrigeration, Thermodynamic and physical properties of ammonia, Paris, France (1980)
- 4.5 Institute of Gas Technology, Physical and thermodynamic properties of ammonia-water mixtures, Research bulletin no.34 (1964).
- 4.6 CRANE, Flow of fluids through valves, fittings, and pipe, Crane Co. (1978).
- 4.7 Bogart M., Ammonia absorption refrigeration in industrial processes, Gulf Publishing Company (1981).

Table 4.1

Main thermodynamic parameters of the absorption system as cold storage tests.

Date:	Aug 17	Aug 21	Aug 29	Aug 30	Aug 31	Sep 6	Sep 7	Sep 10	Sep 11	Sep 11*
COP _A	0.348	0.421	0.413	0.340	0.280	0.345	0.367	0.333	0.327	*
COP _{CCL}	-0.175	-0.193	-0.178	-0.168	-0.225	-0.138	-0.170	-0.128	-0.135	*
COP _{ECL}	0.152	0.178	0.178	0.100	0.097	0.119	0.141	0.050	0.033	*
FR	7.113	5.876	7.263	11.897	12.333	10.303	8.253	21.667	32.526	*
N _{REC}	0.655	0.695	0.927	0.647	0.576	0.640	0.648	0.654	0.604	*
N _{GEN}	0.836	0.937	0.924	0.787	0.810	0.781	0.757	0.726	0.669	*
FR _A	6.839	5.031	7.065	8.955	10.000	8.411	8.654	10.510	12.000	*
T _G	113.8	116.2	121	118	125	114	111	107	101	*

* Unstable test.

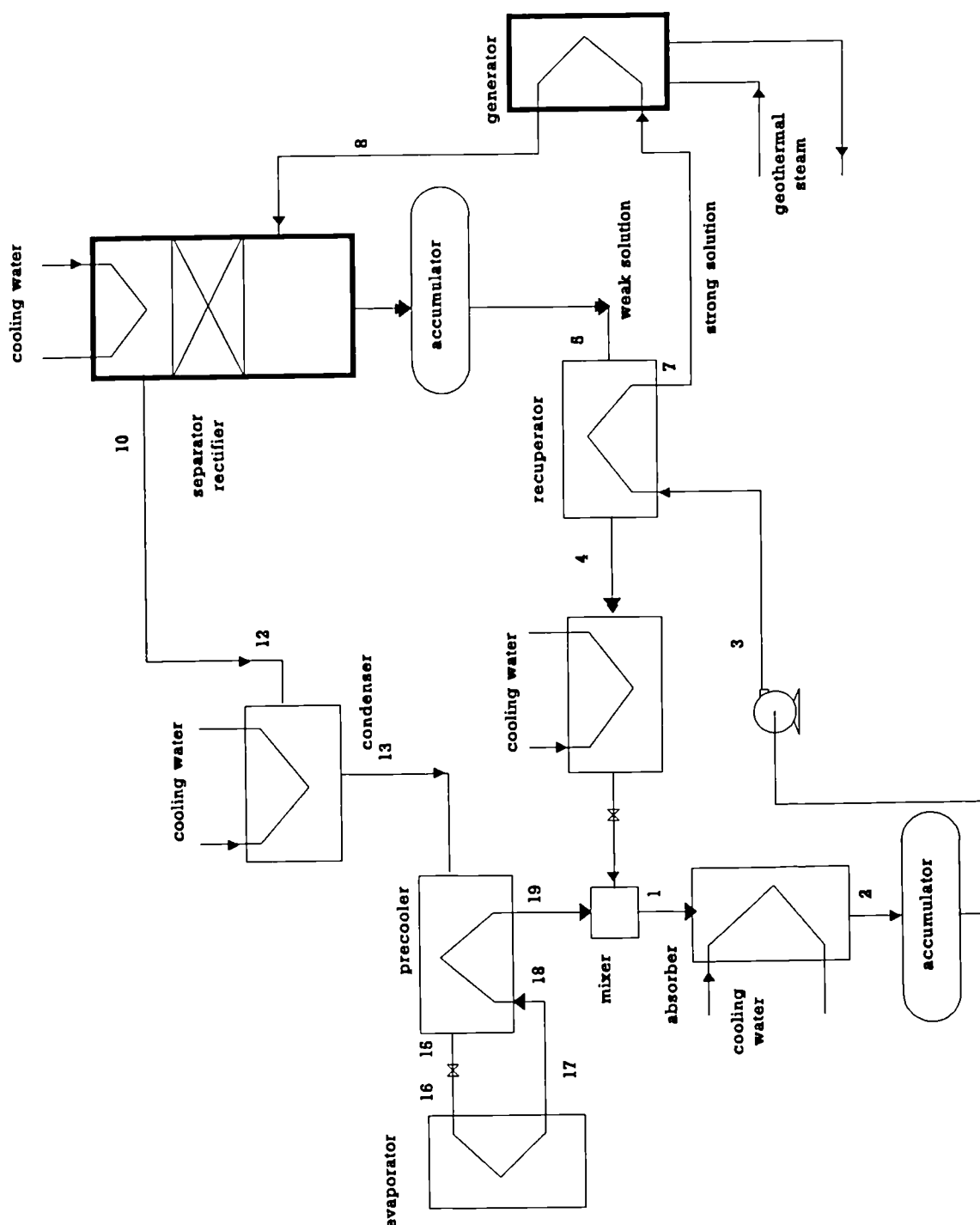


Fig. 4.1 Schematic diagram of the experimental absorption cooler

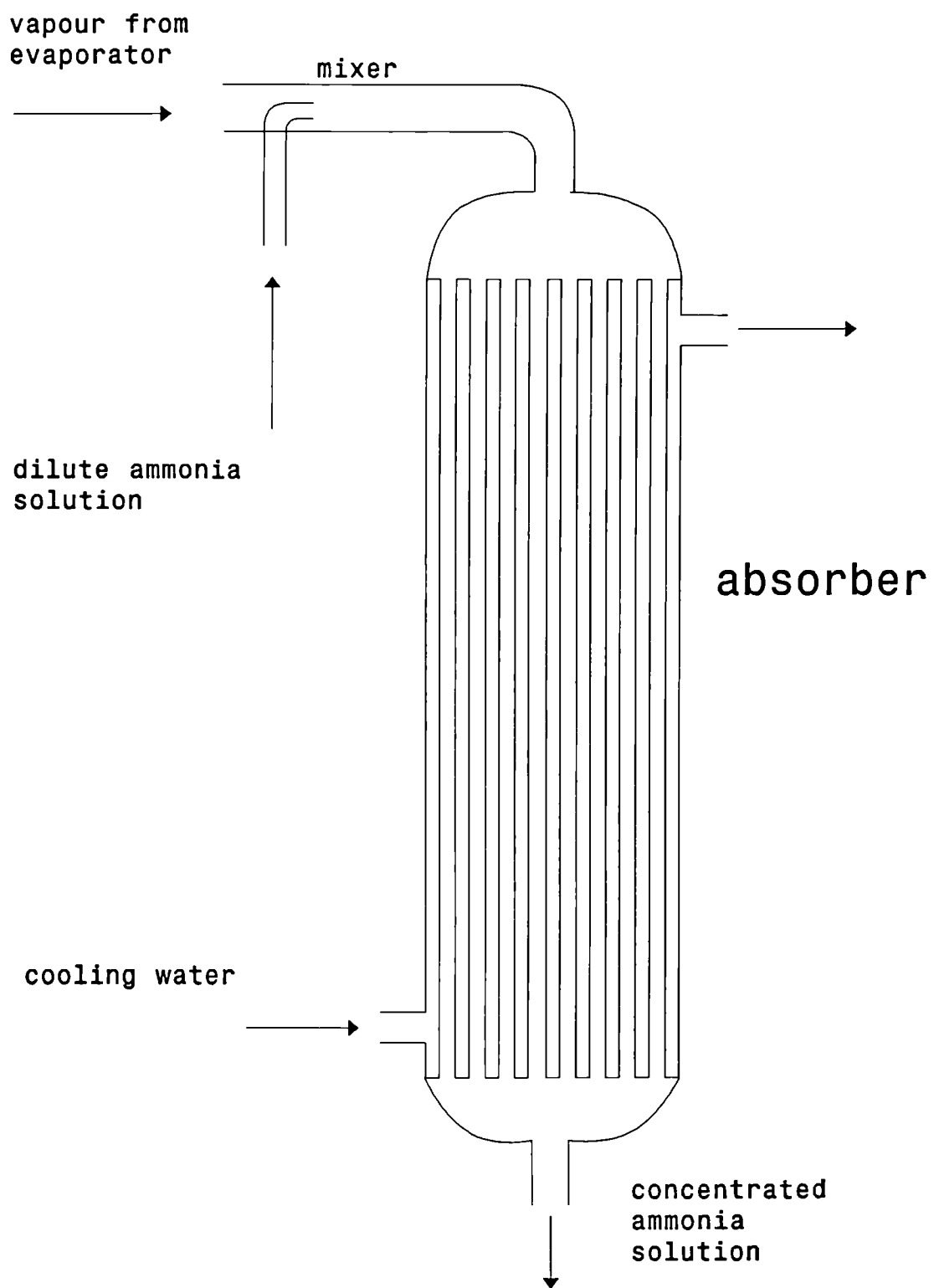


Fig. 4.2 Schematic diagram of the absorber

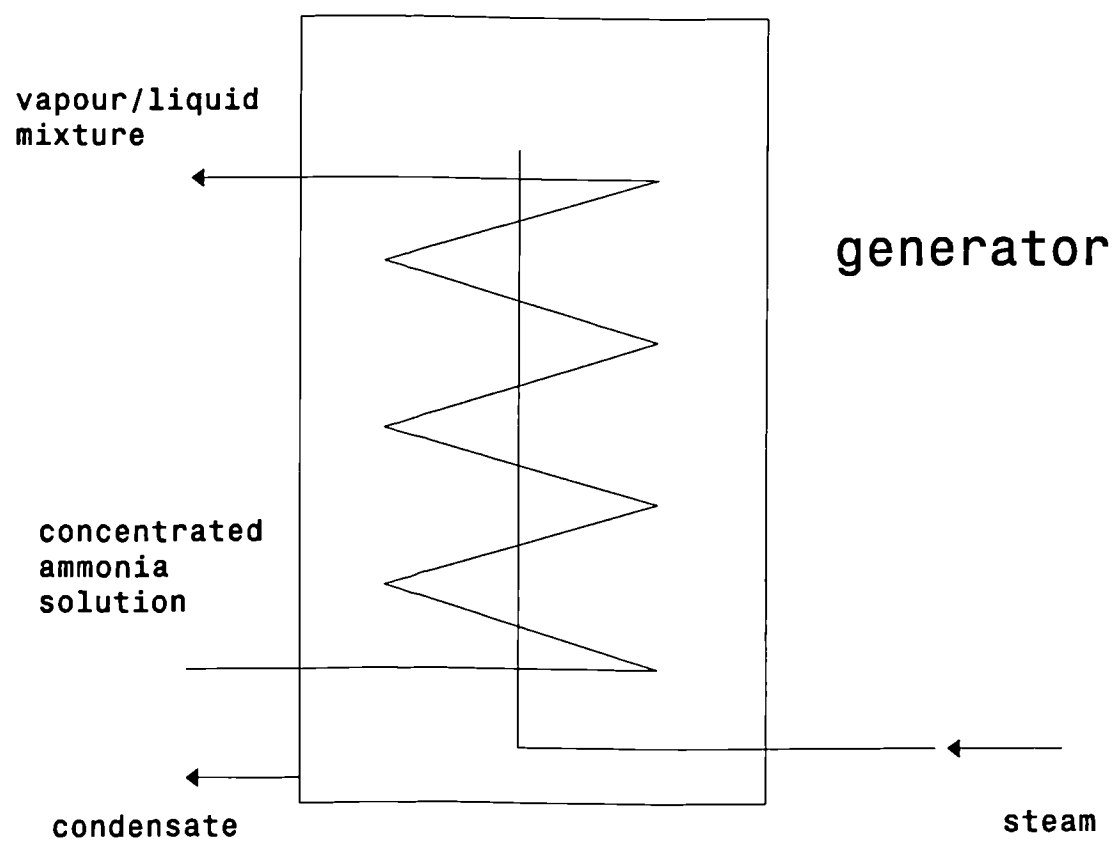


Fig. 4.3 Schematic diagram of the generator

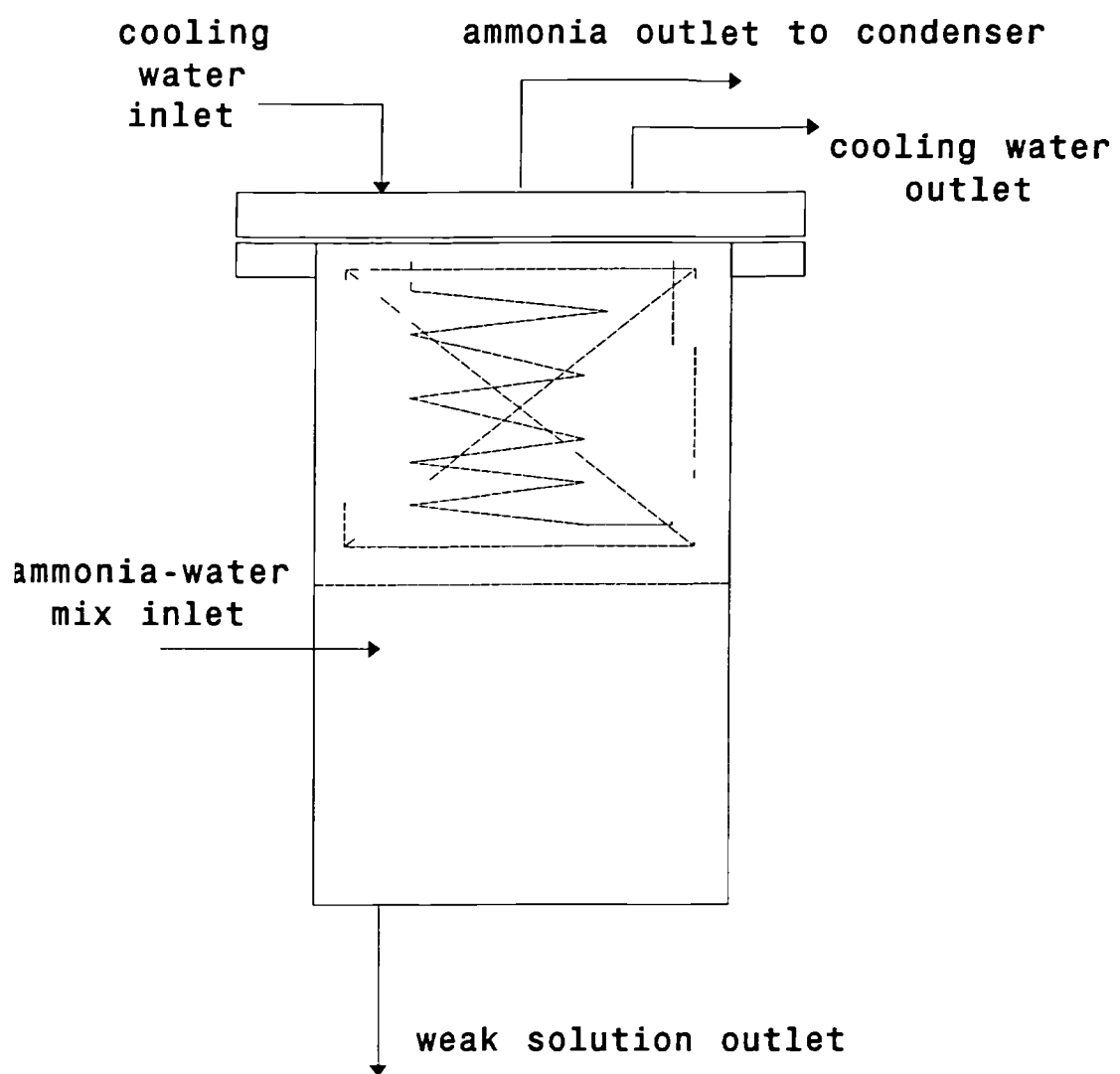


Fig. 4.4 Schematic of the new separator rectifier.

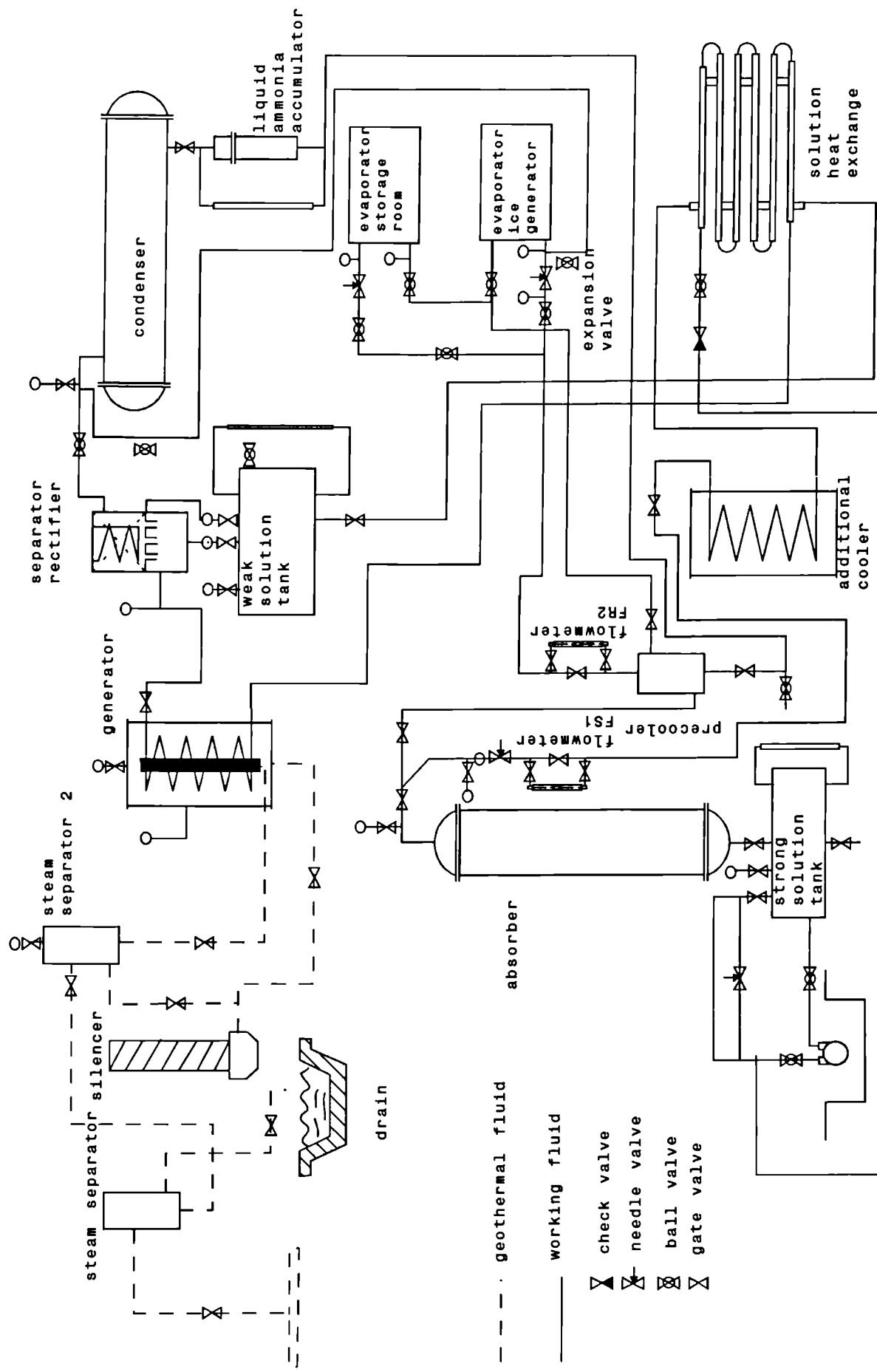


Fig. 4.5 Experimental water-ammonia absorption refrigeration

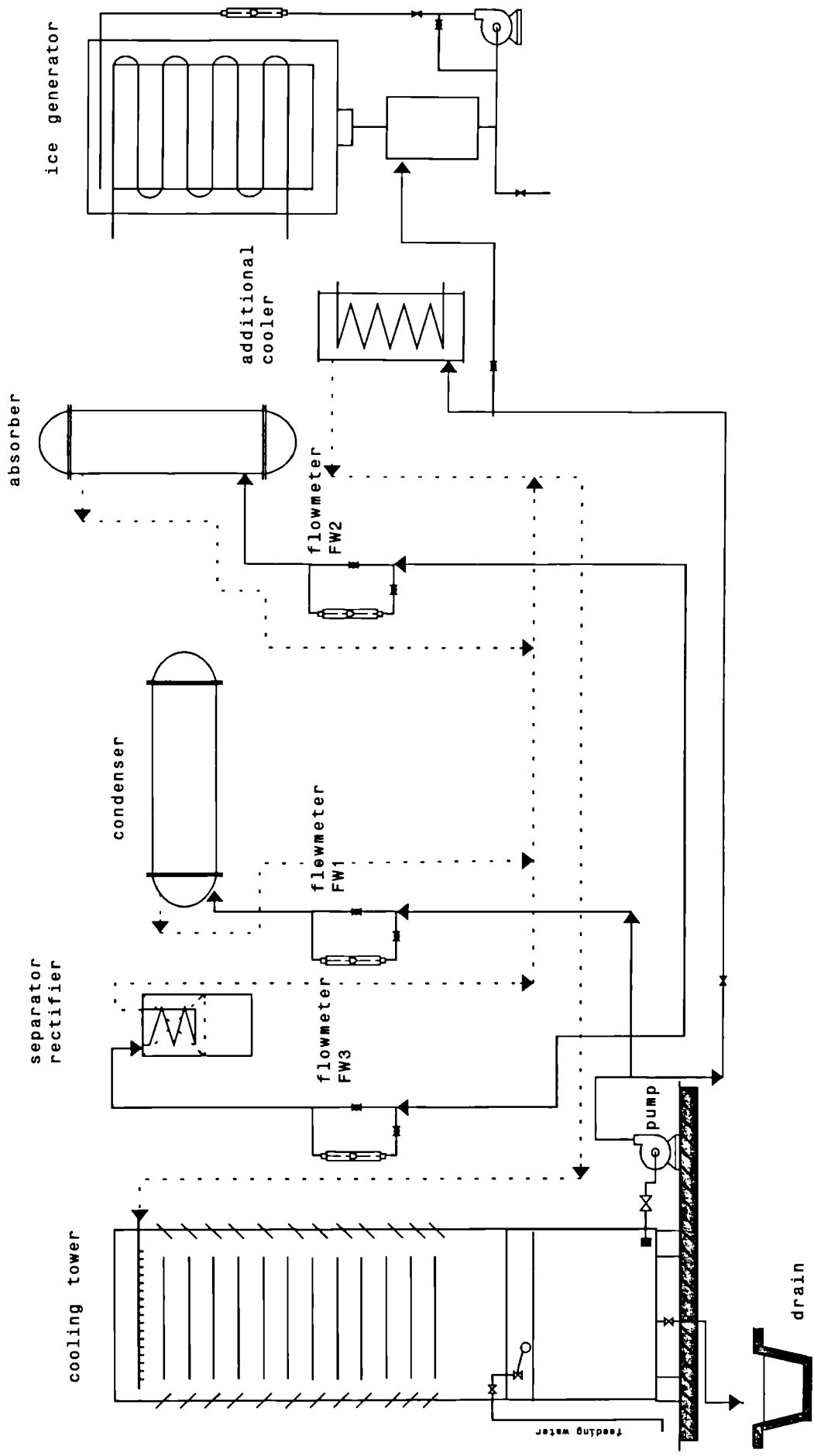


Fig 4.6 Cooling water system

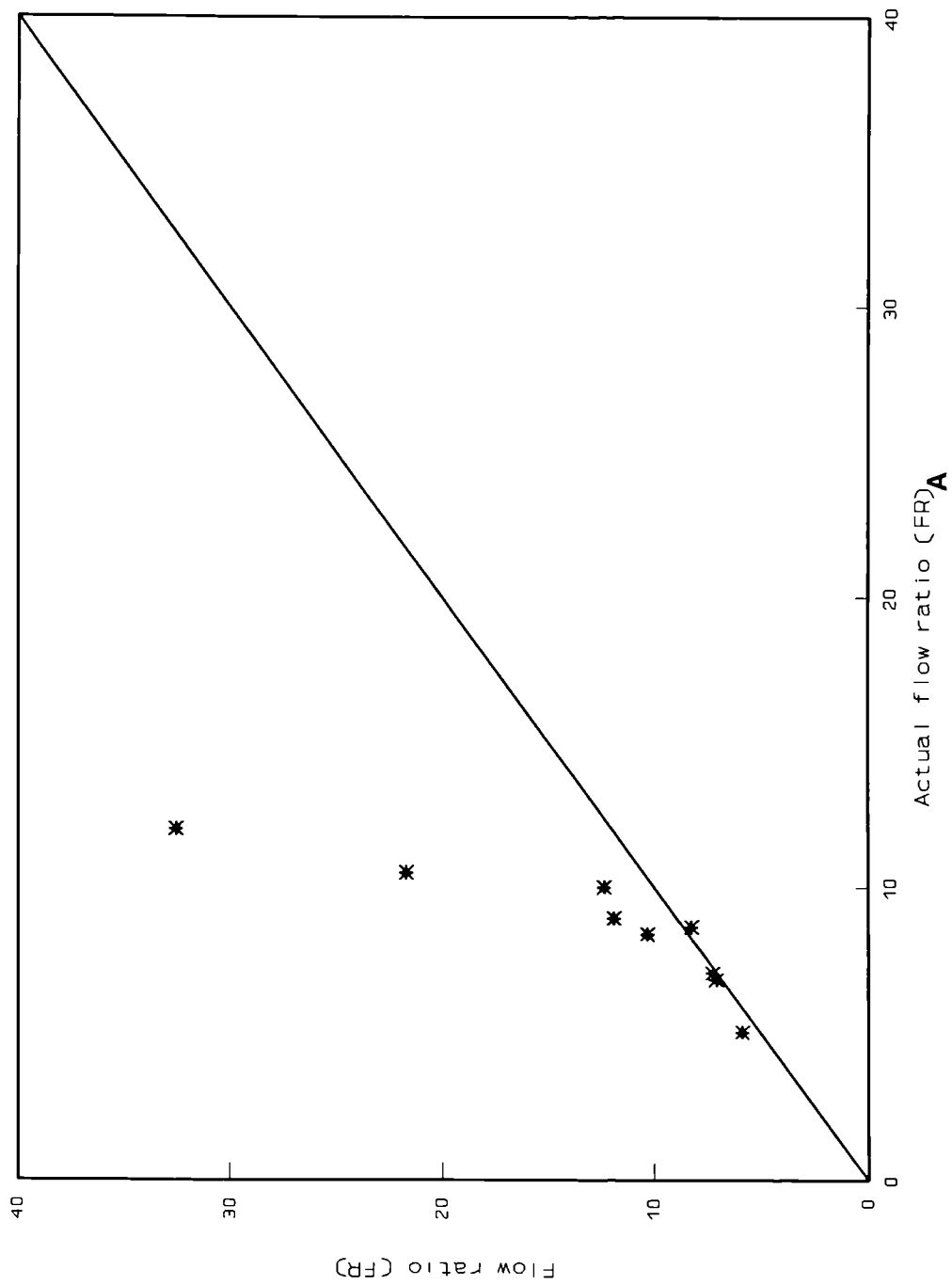


Fig. 4.7. Theoretical flow ratio against actual flow ratio.

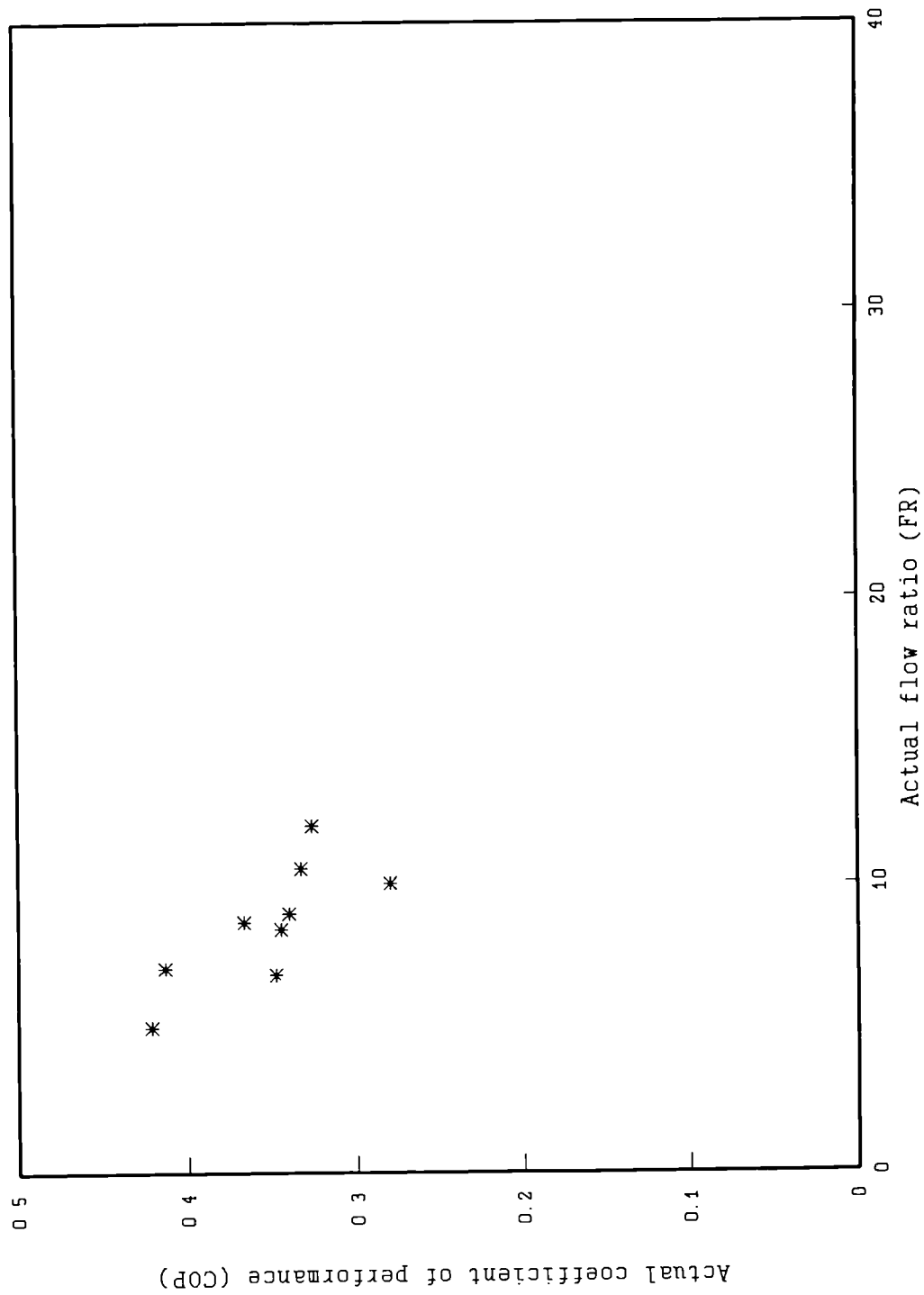


Fig. 4.8 Actual coefficient of performance against actual flow ratio.

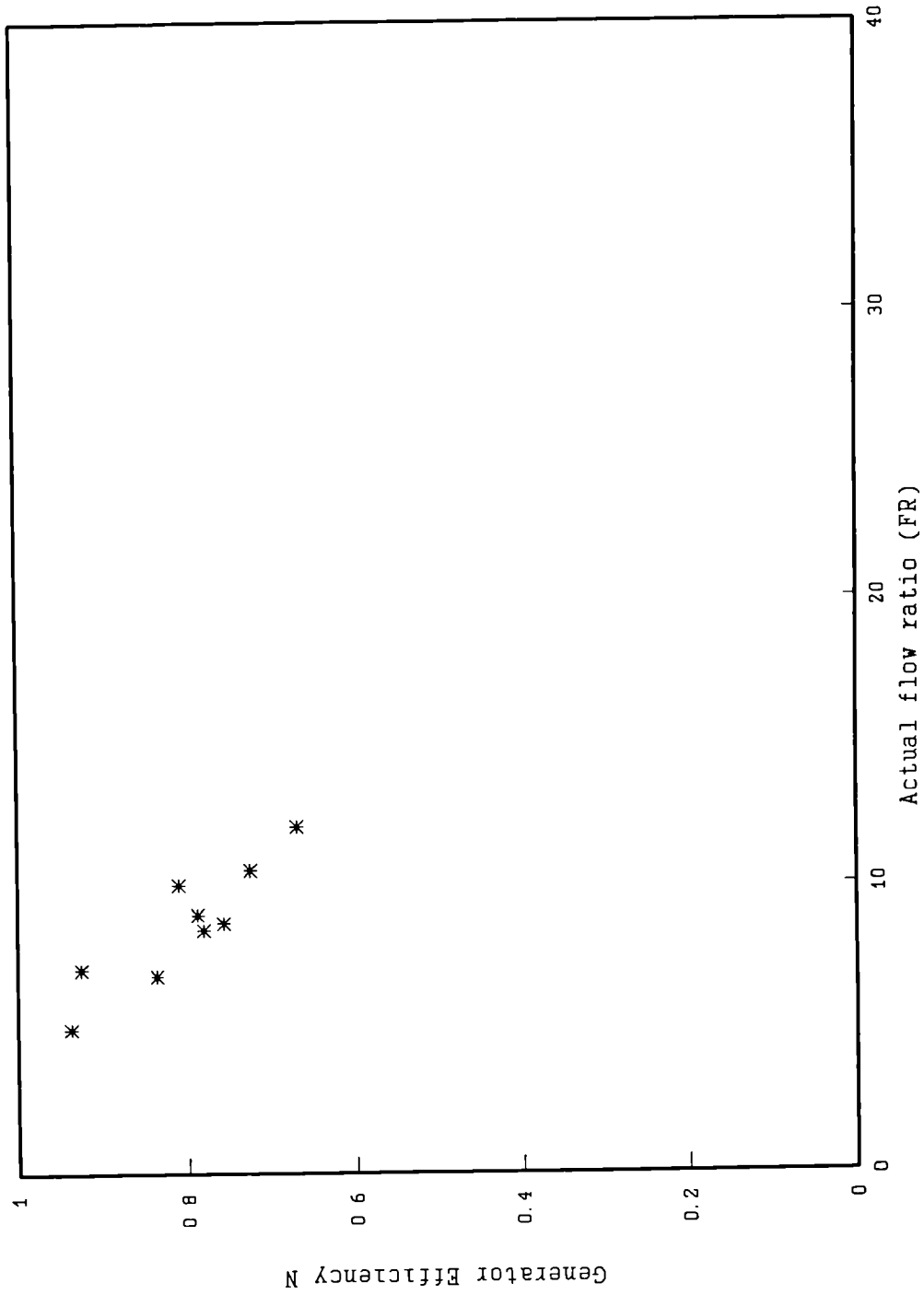


Fig. 4.9 Generator efficiency against actual flow ratio.

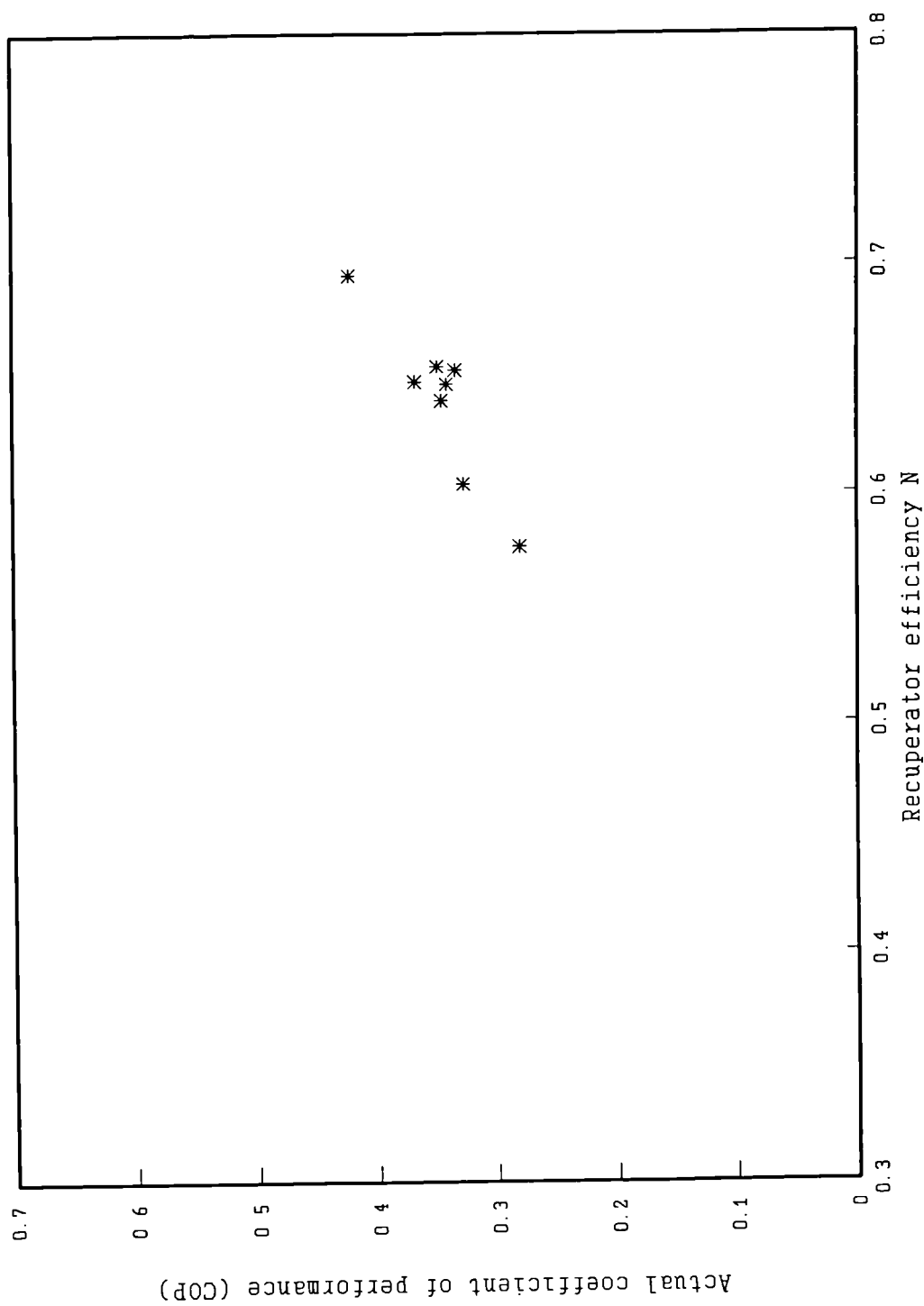


Fig. 4.10 Actual coefficient of performance against recuperator efficiency.

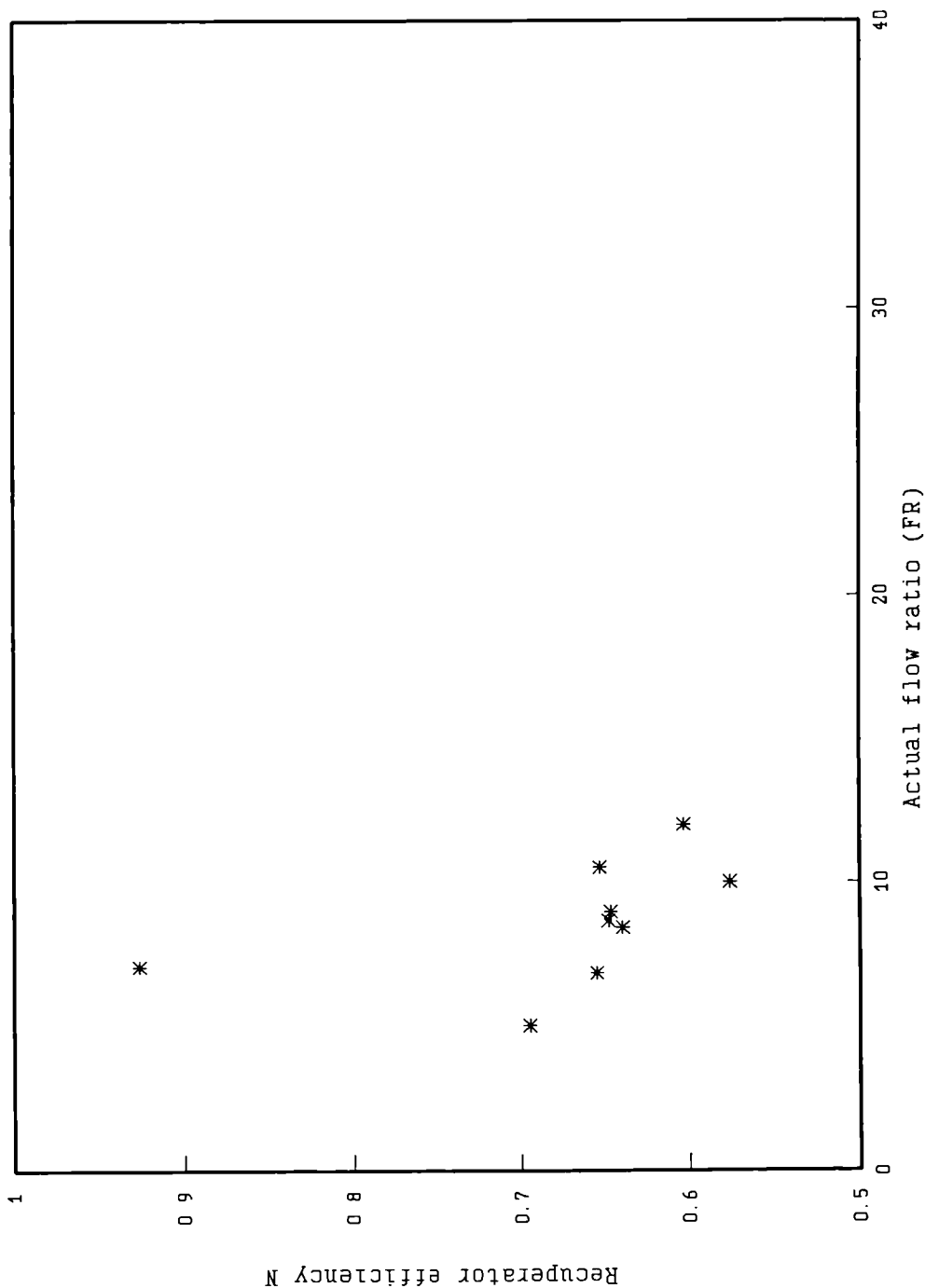


Fig. 4.11 Recuperator efficiency against actual flow ratio.

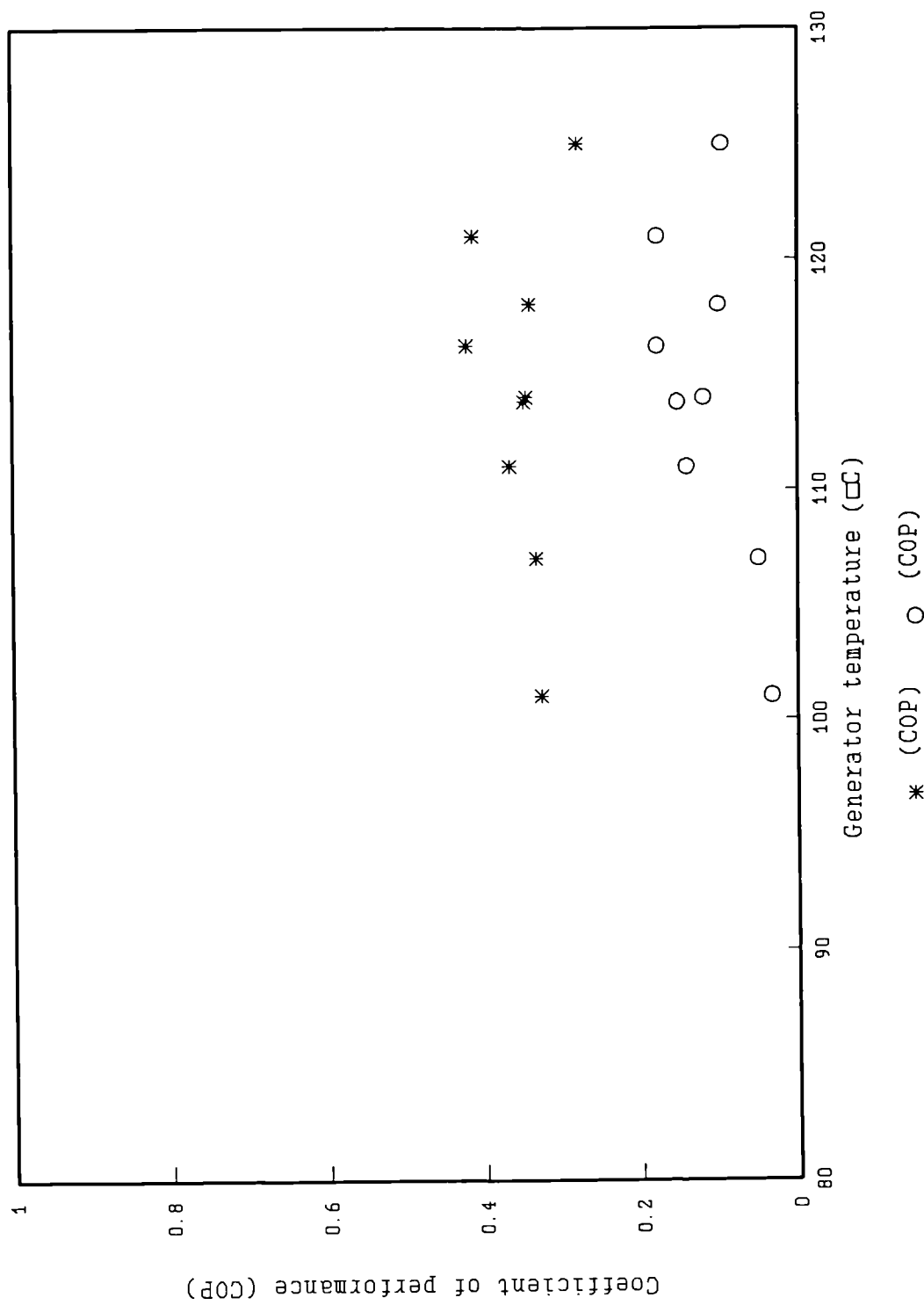


Fig. 4.12 Coefficient of performance against generator temperature.

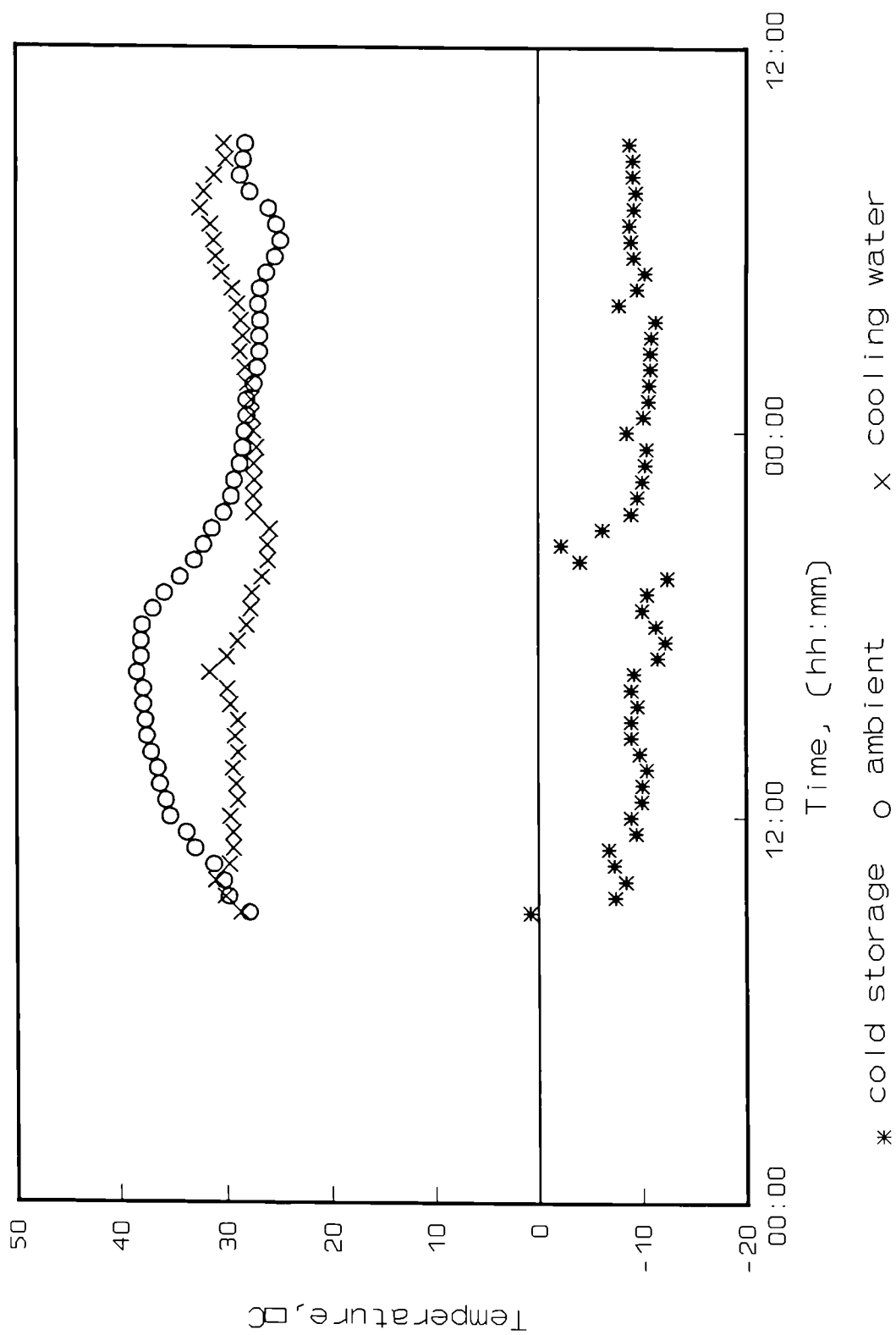


Fig. 4.13 Temperature against time, (August 17, 1990).

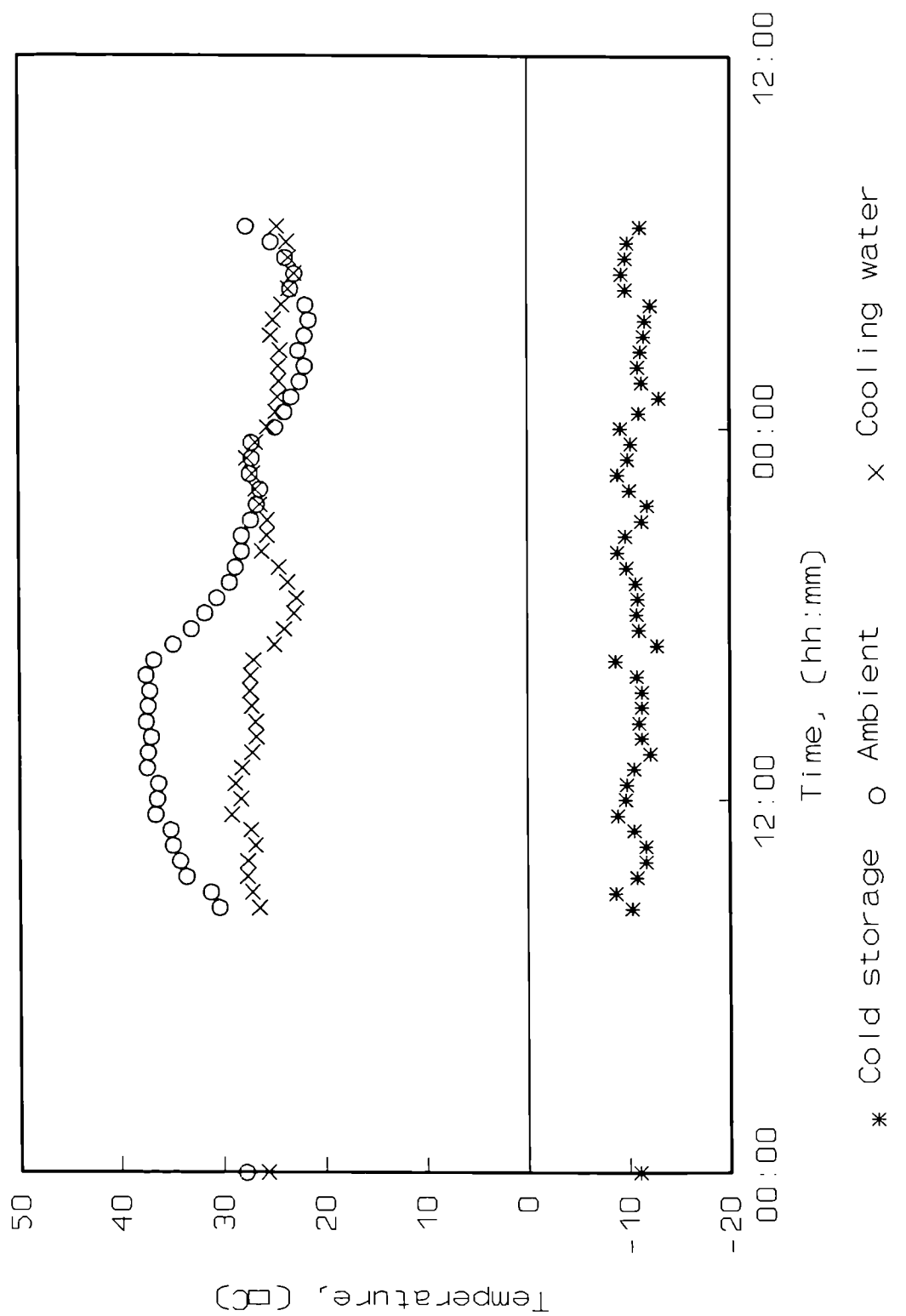


Fig. 4.14 Temperature against time, (August 21, 1990).

CHAPTER 5

EXPERIMENTAL STUDIES WITH AN ABSORPTION SYSTEM USED AS AN ICE MAKING MACHINE.

5.1 INTRODUCTION

Another potential application of the heat driven absorption cooling systems using the waste geothermal heat is to produce ice for perishable food during transportation and for other cooling uses.

The ice can be produced in these systems using the evaporator as the ice-generator in order to freeze water. The ice could be produced in blocks, cylinders, plates and more forms.

In this experimental study three ice-generator prototypes were constructed and connected to the experimental absorption cooling system and then were evaluated in order to find one that worked in the Cerro Prieto conditions. The three ice-generator prototypes studied were as follows;

- 1) Vertical Tubes
- 2) Inclined Plate with Tubing Coil
- 3) Vertical Tube Coil

In the next sections the three prototypes will be analyzed in detail.

5.2 VERTICAL TUBES ICE-GENERATOR

5.2.1 Introduction

In order to evaluate the ammonia-water absorption system as an ice-making machine, a vertical tubes ice-generator (VTIG), was designed and constructed [Peña P. (1988)]. This VTIG was incorporated in the experimental absorption unit. The VTIG was designed to substitute the evaporator diffuser and to produce ice in a batch process. The VTIG design takes into account an ice generator as a heat exchanger in the low pressure zone of ammonia/water absorption cooler.

Two stages in the batch process were considered. One is the freezing time and the other one is the melting time, this latter considers a certain defrost time to separate ice from the generator surface and some additional time for the necessary auxiliary operations to obtain the ice.

Thermodynamic considerations

The main considerations in the ice-making machine design were that [Best and al 1978]:

$$Q_{EV} = 6 \text{ kW}$$

$$COP_A = 0.3$$

The design conditions were:

refrigerant, ammonia R717	$T_f = 0 \text{ } ^\circ\text{C}$
$T_x = -10 \text{ } ^\circ\text{C}$	$T_{if} = -5 \text{ } ^\circ\text{C}$
$P_x = 290.83$	$c_w = 4.18$
$T_{wi} = 30 \text{ } ^\circ\text{C}$	$c_{if} = 2.094$
$T_k = 35 \text{ } ^\circ\text{C}$	$r_i = 335$
$P_k = 1351.0$	

where;

$$q_i = (T_{wi} - T_f)c_w + r_i + (T_f - T_{if})c_i \quad (5.1)$$

$$q_i = 471.08$$

Considering that the percent of freezing capacity is about 80 %, of the theoretical, the amount of ice obtained with the given evaporator capacity could be calculated as follows:

$$M_i = \frac{0.8 Q_{EV}}{q_i} \cdot 24 \cdot 3600 \quad (5.2)$$

$$M_i = 880.36 \text{ kg day}^{-1}$$

This consideration did not take account of losses in defrosting, which could be accepted as between 0.5 to 2 mm of defrosted ice thickness, between the ice and the generator surface.

Coefficient of performance

The main parameters that define the performance of an absorption refrigeration system are as follows.

From a thermodynamic analysis and from mass and heat balance considerations, using the above defined nomenclature for the process, illustrated in Fig. 5.3, the actual coefficient of performance is given by equation (5.3).

$$COP_A = \frac{Q_{EV}}{Q_{GE}} \quad (5.3)$$

The actual coefficient of performance already defined by equation (5.3) can also be rewritten as

$$COP_A = \frac{M_R (H_{17} - H_{15})}{M_{AB} (H_8 - H_7)} \quad (5.4)$$

where H_8 is the enthalpy of the vapour-liquid mixture leaving the generator.

The coefficient of performance in the ice generator can be written as

$$\text{COP}_{IG} = \frac{Q_{IG}}{Q_{EV}} \quad (5.5)$$

The ice-generator actual coefficient of performance already defined by equation (5.5) can also be rewritten as

$$\text{COP}_{IG} = \frac{M_w (H_I - H_W)}{M_R (H_{17} - H_{15})} \quad (5.6)$$

where M_w is the mass flow of ice generated in kg.s^{-1} .

5.2.2 Equipment

The physical model proposed is an evaporator with vertical tubes, where the generation surface is the tube exterior surface in contact with the water, see Fig 5.1.

The final design was performed with nominal 2 inches tubes and the final installation had to be modified in the field according with the space availability during the installation.

The VTIG is a recipient of approximate 500 l of volume for water, with 12 vertical tubes with a refrigerant header. The refrigerant is expanded in a receiver tank and then is pumped to the refrigerant header. The expansion point was located near to the ice-generator in the inlet to the refrigerant header. See Fig. 5.3. This header is a horizontal tube with two compartments. Liquid ammonia enters the header on the righthand side,

flows up inside the vertical tubes' righthand side compartment, then flows down inside the vertical tubes' lefthand side compartment to the lefthand compartment in the refrigerant header, and finally return to the absorber. The water in the recipient is cooled and the ice will be formed in the external surface of the vertical tubes.

The main modifications to the original flow diagram are that the refrigerant coming from the precooler is expanded in an accumulator, then is pumped to the ice generator and returned to the accumulator as a liquid/vapour mixture. At this point the liquid refrigerant goes down and the vapour goes to the precooler and absorber. See Fig. 5.2 and 5.3

5.2.3 Procedure

The refrigeration system was operated in the customary way. The refrigerant expansion point was located at the recirculation receiver tank and liquid refrigerant was accumulated. After the refrigerant level in the tank reached the level indicator, the recirculation pump was turned on. See Fig. 5.3.

At this point the pump outlet pressure did not increase. It is possible that the pump had cavitation problems due to refrigerant evaporation. During 2 hours the refrigeration system produced liquid refrigerant and it was accumulated in the recirculation tank and ammonia was fed to the unit. However the recirculation pump pressure never increased.

5.2.4 Results and Discussions

The system was operated at generation temperatures of 120 to 125 °C and a refrigerant expansion temperatures of -10 °C. The concentration of the strong solution was 45 % by weight. It has been shown that the problems that arose were located in the vertical tubes ice-generator, only.

Since the ice generator did not work as it was originally designed and installed, two modifications to the process had to be carried out.

- (a) In order to feed refrigerant directly to the ice-generator, a bypass line to the recirculation receiver tank was installed and two additional preliminary tests were performed. During these tests, the refrigerant did not enter the ice-generator because it was bypassed through the solenoid valves due to leaks in them and it returned to the absorber. See Fig. 5.4. This could be detected due to lower temperatures in the returning refrigerant line and some solenoid valves.
- (b) In order to approach the refrigerant expansion point to the vertical tubes ice-generator and to correct the leaks in some solenoid valves, a new arrangement with manual valves was installed on the refrigerant lines in the ice generator. See Fig. 5.5.

The two preliminary tests were carried out on the whole system to permit operation of the ice-making machine system with the new manual valves arrangement. The refrigeration system was operated in the customary way. The refrigerant expansion point was located near to the ice-generator in the inlet to the refrigerant header. See Fig. 5.5. This header is a horizontal tube with two compartments. Liquid ammonia enters the header on the righthand side, flows up inside the vertical tubes' righthand side compartment, then flows down inside the vertical tubes' lefthand side compartment to the lefthand compartment in the refrigerant header, and finally returns to the absorber. This would permit ice to be formed on the external surface of the vertical tubes. See Fig. 5.6.

During these tests the vertical tubes were cooled only about 10 cm above the refrigerant header. This could only happen due to an imperfect seal between the vertical tubes' compartments. See Fig. 5.6.

It was possible to observe that the internal plates in the ice-generator vertical tubes were loose, due to noises when the ice-generator tubes were manually beaten.

5.3 INCLINED PLATE WITH TUBING COIL ICE-GENERATOR

5.3.1 Introduction

In order to minimize the amount of water to be cooled the vertical tubes ice-generator is to be substituted by a inclined steel plate ice-generator, (IPIG), in which the water is sprayed over the inclined wall to produce the ice, the excess water is recirculated. See Fig. 5.7.

Two stages of a discontinuous process were considered. One is the freezing time and the other one is the fusion and recuperation time.

Thermodynamic considerations

The main considerations in the ice-making machine design were that [Best and al 1978], [Peña P. (1988)]:

$$Q_{EV} = 6 \text{ kW}$$

$$\text{COP}_A = 0.3$$

The design conditions were:

refrigerant, ammonia R717 $T_f = 0 \text{ } ^\circ\text{C}$

$T_x = -10 \text{ } ^\circ\text{C}$ $T_{if} = -5 \text{ } ^\circ\text{C}$

$P_x = 290.83$ $c_w = 4.18$

$T_{wl} = 37 \text{ } ^\circ\text{C}$ $c_i = 2.094$

$T_k = 35 \text{ } ^\circ\text{C}$ $r_i = 335$

$P_k = 1351.0$

Where;

$$q_i = (T_{wl} - T_f)c_w + r_i + (T_f - T_{if})c_i$$

$$q_i = 500.13$$

Also, considering that the percent of freezing capacity is about 80 %, the amount of ice obtained with the given evaporator capacity could be calculated as follows:

$$M_i = \frac{0.8 Q_{EV}}{q_i} \cdot 3600$$

$$M_i = 34.56 \text{ kg h}^{-1}$$

Considering that the plate has a surface of 1.77 m², it is possible to obtain ice with 1.92 cm of thickness every hour, this consideration did not take into account losses caused by defrosting. Between 0.5 to 2 mm of defrosted ice thickness between the ice and the generator surface would be acceptable.

Considering the specifications in the reference of TURBO ICE GENERATORS, [TURBO, 1988], where an ice-maker with a nominal ice capacity of 25 TON d⁻¹, requires a system

with 37.5 TON of refrigeration, (Standard Rating Conditions: 15 °C entering water, -18 °C liquid and 2.05 bar at evaporator). It is possible to obtain 15.16 kg h⁻¹ of ice, with the actual capacity of 6 kW.

5.3.2 Equipment

The old ice-generator recipient, without the bottom part was used in the construction of the new ice-generator. A new inclined bottom was installed with 3° of inclination to collect the water on one side. Then the inclined plate was constructed using steel of 0.0016m thickness, and the coil was built with 24m of stainless steel tubing with an internal diameter of 12.7mm. The recirculation water tank has a capacity of 30 litres and the recirculation pump is the same as previously used. See Fig. 5.7. and Fig. 5.9.

The plate has one refrigerant header at the inlet and another at the outlet. This permits the introduction of refrigerant at three points on the inclined plate. The separation between the tubes lines in the coil was about 6 cm due to the tube bends being manufactured with a tool that only allows 6 cm diameter bends. See Fig. 5.8.

5.3.3 Procedure

Figure 5.9 shows the IPIG flow diagram. The freezing surface is an inclined steel plate with a refrigerant stainless steel coil (back side). The water is pumped from the recirculation water tank and sprayed over the top of the plate (front side). Some water is frozen and the remainder flows down to the recirculation water tank. With this process, the amount of water to be cooled (about 30 litres) is lower than the amount in the old version (about 500 litres). Hot water is not fed until the next cycle. When the ice is formed, the hot vapours from the rectifier are used to separate the ice from the surface. And finally the ice is collected in the bottom part of the ice-generator. [Heard, 1991]

5.3.4 Results and Discussions

In order to prove the IPIG, three preliminary tests were carried out on the whole system. The refrigeration system was operated in the customary way. The refrigerant expansion point was located in the bottom part of the inclined plate (back side) and the outlet was connected to the absorber in the upper part. See Fig. 5.8. Liquid ammonia entered the tubing coil on the bottom part. It flowed upwards inside the coil and returned to the absorber through the upper part. The water flowed down over the inclined plate (front side), but the water temperature did not decrease.

During these tests the whole tubing coil quickly cooled due to the insulation on the back part of the inclined plate and to the poor heat transfer from the tubing coil to the inclined plate.

It was observed that the surface of the inclined plate was cooled only 1 cm above and below each tubing line, in such a way that approximately 4 cm, (the rest of the surface) were not cooled. Additionally, some lines of the tubing coil were separated from the inclined plate by about 1 to 2 mm due to an irregular plate surface, resulting in such parts of the plate not being cooled. It was also observed that the plate was cooled over a very small part of its surface and after one hour of operation, with a coil temperature (expansion temperature) of about - 7°C the water temperature increased from 28 to 33°C.

With such problems it was impossible to produce ice with this prototype.

5.4 VERTICAL TUBE COIL ICE-GENERATOR

5.4.1 Introduction

In order to increase contact surface between the liquid refrigerant and the water, a new vertical tube coil ice-generator, with horizontal spaced lines, (VTCIG), was designed.

This tube coil was designed to utilize all the external surface of the 1.22 cm (0.5 inches) of nominal steel tube diameter. This was connected by bends and separated by 2.5 cm (1 inch) with steel plate. See Fig. 5.10.

Two stages of a discontinuous process were considered, one is the freezing time stage and the other one is the fusion and recuperation time stage.

Thermodynamic considerations

Considering that the absorption system has a capacity of 6 kW of cooling and according to the thermodynamic considerations included in Section 5.3.1., 15.16 kg h^{-1} of ice could be produced.

5.4.2 Equipment

The vertical tube coil was constructed with 1.27 cm diameter steel tube and two 90° elbows connected with 3 cm closed couples to make the returns. The length of the horizontally spaced tubes was 1.12 m and the separation between the tubes was about 4.4 cm. This separation was filled with steel plate, welded to the tubes in three points and the complete seal was made with silicon paste. Eighteen 1.12 m length tubes were used to make the coil, giving a total surface of 0.39 m^2 . See Fig. 5.10.

The vertical tube coil was painted, with epoxy paint, and installed in the system. The vertical tube coil has the refrigerant inlet in the bottom part and the outlet in the top part. The refrigerant flows up inside the tubes. The water was sprayed over the top part through two tubes provided with small holes using a recirculation pump. The ice was formed on the external surface of the horizontally spaced tubes. The refrigerant expansion point was located at the refrigerant inlet, at the bottom. See Fig. 5.11.

5.4.3 Procedure

Figures 5.11 and 5.12 show the VTCIG flow diagram. The freezing surface is the external area of the tubes. The water is pumped from the recirculation water tank and sprayed over the top of the tube coil. Some water is frozen and the remainder flows down to the recirculation water tank. With this process, the amount of water to be cooled was 30 litres. Hot water is not fed until the next cycle. When the ice is formed, the hot vapour from the rectifier are used to separate the ice from the surface. Finally, the ice is collected in the bottom part of the ice-generator.

Next there is a experimental procedure description:

- | Step | Description |
|------|---|
| (a) | The absorption system is started up in the customary way. |
| (b) | When liquid ammonia is produced in the condenser, the valve at the inlet of the mixer is opened. This permits the ammonia to flow through the ice generator. The refrigerant valve at the evaporator inlet is normally open. The hot ammonia vapour valve is normally closed. |
| (c) | The recirculation water tank in the ice-generator is filled and the recirculation pump is started up. |

- (d) The parameters of the ice-generator are recorded every 5 minutes.
- (e) When the ice is formed in the ice-generator, the recirculation water pump is turned off (15 to 25 minutes)*, the refrigerant valve after the flowmeter is closed, and the hot ammonia vapour from the rectifier valve is opened. This permits the hot ammonia vapour to flow through the ice-generator coil and release the ice. The strainer in the recirculation water line is cleaned.
- (f) When the ice is released from the tube coil walls, the hot ammonia vapour valve is closed and the refrigerant valve is opened. The hot ammonia vapour flows for 1 to 2 minutes. The pressure in the evaporator increases to the pressure in the high pressure side of the absorption system and the evaporator inlet temperature increases to 110 °C. This value decreases when the hot ammonia vapour flow is suspended.
- (g) The ice is recovered and weighed. The time used in defrosting and recuperation is 5 minutes.
- (h) In order to start another cycle the procedure continues with step (c).
- (i) If the test is finished, the system is shut down in the customary way.
 - * During the last 2 experimental tests the cycle duration was increased to 30 minutes. With this time 2 periods per hour were obtained and 10 minutes of each hour are used for defrosting and recuperation. This was instead of 20 minute cycles, which have 15 minutes per hour of non-ice production.

5.4.4 Results and Discussions

During the first preliminary test, the water header consisted of two tubes of 1.27 cm diameter and 1.12 m length, with 43 holes per tube of 0.36 cm diameter spaced every 2.54 cm along the tube. However the water distribution was not uniform and the ice

production was only 4 kg h^{-1} . An additional water header was constructed using stainless steel tubing of 1.27 cm diameter and the same length. However the number of holes was increased to 86 per tubing spaced every 1.27 cm along the length. Using the tubing water header the water distribution was improved and the ice production was increased to 16.4 kg h^{-1} .

The system was operated at generation temperatures of 130 to 137°C . These tests were performed at the maximum generation temperatures in order to obtain the biggest ice-production. Also, the temperatures of the brine in the area that could be used for the industrial ice-plant are over 152°C .

The expansion temperature was -10°C . The concentration of the strong solution was 43% by weight. See Appendix 1 and Tables A1.11 to A1.16, for the raw experimental data, and the results of the programme REFRI, (Appendix 2), for the thermodynamic evaluation of the ammonia-water absorption system.

Tables 5.3 to 5.9, show the results of seven tests using the vertical tube coil as an ice-generator. It can be observed that the ice production increases at lower ambient temperatures.

Figures 5.13 to 5.19, are plots that show the temperature of the refrigerant (at the inlet and outlet), the temperature of the water recirculated and the temperature of the water in the recirculation tank, as a function of time for complete cycles of ice production.

5.5 ECONOMIC EVALUATION

Based on the intent of the company **Hielo Estrella, S.A.** to build a 400,000 kg day⁻¹ plant to produce ice using the geothermal brine from the Cerro Prieto Geothermal Field, an economic evaluation was prepared based on two kinds of equipment: an absorption system and a mechanical vapour compression.

Table 5.1, shows main data for the analyzed equipment [TURBO, 1988]

The main consideration for the economic evaluation are:

(costs are in U.S. Dollars).

- 6,000 hours (250 days) of operating per annum.
- Geothermal brine costs of \$0.0581 per TON (180 Mexican pesos) [A. Bacre, 1991]
- Electricity cost of \$0.0362 per kWh and \$7.23 per kW of maximum demand.
- Cost of the two plants at the present time are about 600,000 to 1000,000 however it can be assumed that the absorption plant cost is 2 times the mechanical compression system cost. [C. Heard, 1991].
- The labour and maintenance costs for the two systems are the same.

The payback period (PBP) for the absorption plant in comparison with the mechanical vapour compression plant would be the additional cost divided by the annual cost of the electricity saved.

Electricity costs absorption plant;

$$6000 * 0.1026 * 6 * 3 = 11,080.8 \text{ \$ per annum}$$

Geothermal energy cost, using geothermal brine at 13 bar.

$$6000 * 0.0581 * 202 = 70,417.2 \text{ \$ per annum}$$

$$\text{Total} = 81,498 \text{ \$ per annum}$$

Electricity costs compression plant

$$6000 * 0.0362 * 6 * 192 = 250,214 \text{ \$ per annum.}$$

The amount saved in the electricity is 172,714 US dollar per annum. Table 2 Shows the PBP for a series of electricity costs and plants costs.

5.6 CONCLUSIONS

It was observed that driving liquid refrigerant into the accumulator tank in the vertical tubes ice-generator involves many heat losses.

It was proved that the absorption system has a high coefficient of performance in the vertical tube ice-generator.

It is necessary to test a commercial ice-generator in order to test the absorption system. The actual prototype has many limitations in the amount of labour necessary to produce the ice.

The operation of a plant with an average PBP of 3 year for the additional investment to install a absorption plant would be highly profitable, considering the high demand of ice and the low supply of electricity during summer in Mexicali.

5.7 REFERENCES

- 5.1 P. Peña, Refrigeración por absorción amoníaco agua para la producción de hielo, Reporte sobre adiestramiento técnico, Instituto de Investigaciones Eléctricas, (1988).
- 5.2 R. Best, C. L. Heard, H. Fernandez and J. Siqueiros, Developments in geothermal energy in Mexico-Part five: The commissioning of an ammonia/water absorption cooler operating on low enthalpy geothermal energy, *J. Heat Recovery Systems* 6(3), 209-216 (1986).
- 5.3 R. Best, C. L. Heard, P. Peña, H. Fernandez and F. A. Holland, Developments in geothermal energy in Mexico-Part twenty six: Experimental assessment of an ammonia/water absorption cooler operating on low enthalpy geothermal energy, *J. Heat Recovery Systems* 10(1), 61-70 (1990).
- 5.4 Turbo Refrigerating Company, 1815 Shady Oaks Drive, Denton, Texas 76202, (1988).
- 5.5 A. Bacre, Personnel communication, Industrias Textiles de B.C. (1991).
- 5.6 C. L. Heard, Economic and technical justification for the continuation into the phase III of the three projects in module I of the IIE/SALFORD/ODA Programme, Cuernavaca, Mor, (1991).

Table 5.1
Characteristics of the equipment analyzed for economic analysis

MODEL	Nominal Ice Capacity kg day ⁻¹	Model Number	Compressor Motor kW	Water Pump kW	Feed Water l min ⁻¹	Units required	Total Ice Production kg day ⁻¹
Mechanical compression	72,640	TIG-080-OSC	2 @ 93.2	3 @ 2	49	6	435,840
Absorption	68,100	TICAR-75-0	-	3 @ 1	49	6	408,600

Table 5.2
PBP for a series of electricity costs

Electricity Cost USD per kWh	Total Cost Saved USD per annum	Additional cost for the absorption plant	PBP years
0.0362	175,714	600,000	3.41
0.0362	175,714	900,000	5.12
0.0362	175,714	1,200,000	6.83
0.1	609,809	600,000	0.98
0.1	609,809	900,000	1.48
0.1	609,809	1,200,000	1.97
0.2	1,290,209	600,000	0.47
0.2	1,290,209	900,000	0.70
0.2	1,290,209	1,200,000	0.93

Table 5.3 Ice-generator experimental data.
September 10/91

Time hh:mm	T _i °C	T _o °C	T _w °C	T _{rt} °C	W _c kg	W kg h ⁻¹
08:50 AM	16.8	23.4	28.8	27.3		
08:55 AM	-8.8	21.2	17	25.1		
09:00 AM	-9.2	12.8	8.4	22.6		
09:05 AM	-4.9	16.3	7.9	19.9		
09:10 AM	-6.3	-1.6	4.7	18.2		
09:15 AM	-6.3	-1.6	4.7	18.2	3.5	8.4
09:20 AM	-6.1	14.5	15.7	28.4		
09:25 AM	-10.8	15.9	13.3	24		
09:30 AM	-11.9	8.9	5.6	19.7		
09:35 AM	-12.3	11.2	4.3	18.1		
09:40 AM	-11.8	3.7	4.3	17.9		
09:45 AM	-12.2	0	4.4	17.7		
09:50 AM	-12.3	-5.3	5.4	17.4	8.2	16.4
09:55 AM	-5.4	16.8	12.6	32.9		
10:00 AM	-8.8	9.8	5.8	23.7		
10:05 AM	-8.6	6.9	4.7	20.1		
10:10 AM	-8.6	6.6	4.7	18.9		
10:15 AM	-8.2	3.1	5.4	18.8		
10:20 AM	-7.7	2	5.4	18.6	8.2	19.68
10:25 AM	-6.1	17.7	20.8	39		
10:30 AM	-10.2	19.2	16.1	28.9		
10:35 AM	-8	9.8	7.2	23.5		
10:40 AM	-9.2	6.6	5.3	20.8		
10:45 AM	-9.3	-1.6	5.5	20		
10:50 AM	1	19.2	19.5	35.8	8.1	19.44
Average					7.0	15.9
Complete cycle average					13.3	

Note:

Ti : refrigerant inlet temperature
 To : refrigerant outlet temperature
 Tv : vapour from rectifier temperature
 Tw : water temperature after recirculation pump
 Trt: recirculation tank water temperature
 Pin: evaporator inlet pressure
 Pout : evaporator outlet pressure
 tf : fusion time
 tr : defrosting and recuperation time
 tc : cycle time
 Wc : cycle ice production
 W : ice production per hour

Table 5.4 Ice-generator experimental data.
September 11/91

Time hh:mm	T _i °C	T _o °C	T _w °C	T _{rt} °C	W _c kg	W kg h ⁻¹
07:45 AM	-11.6	14.9	13.2	17.3		
07:50 AM	-11.75	9.7	6.2	15.3		
07:55 AM	-11.3	4.9	2.2	13.6		
08:00 AM	-11.3	0	2.1	13	4.2	16.8
08:05 AM	-5.6	10.6	8.7	18.7		
08:10 AM	-10.4	8.3	5.6	16.4		
08:15 AM	-11.2	16.3	19.9	7.9		
08:20 AM	-11.6	-3.7	3.6	14.4		
08:25 AM	-12.1	-5.6	4.5	14.2	7.7	23.1
08:30 AM	-7.2	14.8	15.1	25.2		
08:35 AM	-9.1	12.1	9.3	21.2		
08:40 AM	-12.6	6.7	4.6	17		
08:45 AM	-14.7	4.8	3.2	15.4		
08:50 AM	-15.1	3.3	2.8	14.9	6.8	20.4
08:55 AM	-16.6	2.7	2.4	14.3		
09:00 AM	-1.4	11.8	14.2	23.9		
09:05 AM	-17.8	14.2	11.1	20.3		
09:10 AM	-18.4	8.2	4.2	17.2		
09:15 AM	-16.6	3.8	2.2	15.4	7.4	22.2
09:20 AM	-17.6	2.2	2.1	14.9		
09:25 AM	-10.5	12.1	10.6	26.6		
09:30 AM	-14.3	2.9	2.7	18.3		
09:35 AM	-17.3	-17.3	8.2	16.1	8.6	34.4
Average				6.94	23.38	
Complete cycle average						19.5

Table 5.5 Ice-generator experimental data.
October 31/91

Time hh:mm	T _i °C	T _o °C	T _v °C	T _w °C	T _{rt} °C	P _{in} bar	P _{out} bar	F _{w4} kg s ⁻¹	t _f min	t _d min	t _c min	W _c kg	W kg h ⁻¹
08:05	-2.3	15.0	57.1	9.1	18.4	1.8	1.8	0.5					
08:10	-8.4	10.7	27.2	10.2	18.1	1.4	1.3	0.6					
08:15	-12.9	8.9	18.9	7.8	18.2	1.4	1.3	0.6					
08:20	-8.4	3.3	13.7	4.1	18.3	1.8	1.2	0.6					
08:25	-8.6	1.9	9.9	3.6	18.3	1.8	1.3	0.6	20	5	25	5.0	12.0
08:30	19.1	12.0	58.7	9.6	19.6	2.1	1.2	0.6					
08:35	-6.2	3.4	35.5	4.7	19.3	2.0	1.3	0.6					
08:40	-7.2	-7.3	20.3	4.0	19.3	2.0	1.4	0.6					
08:45	-6.5	13.9	14.5	4.2	19.5	1.9	1.6	0.6	15	5	20	11.0	33.0
08:50	14.9	15.3	55.8	13.8	20.4	2.3	1.4	0.6					
08:55	-8.4	4.4	25.1	4.9	20.3	1.8	1.5	0.6					
09:00	-7.8	3.7	21.2	4.6	20.2	1.8	1.5	0.6					
09:05	-8.6	3.1	15.3	4.6	20.7	1.8	1.5	0.6	15	5	20	6.5	19.5
09:10	-4.7	10.4	60.5	9.8	21.5	2.2	1.5	0.6					
09:15	-6.2	4.2	32.2	5.2	21.1	2.0	1.4	0.6					
09:20	-6.7	-2.3	20.0	5.4	21.1	1.9	1.4	0.6					
09:25	-5.4	-2.1	15.9	5.7	21.2	1.8	1.4	0.6	15	5	20	11.8	35.3
09:30	-1.5	13.1	63.2	11.1	22.8	2.1	1.5	0.6					
09:35	-6.3	5.2	38.8	5.8	22.4	1.8	1.4	0.6					
09:40	-5.7	5.1	25.1	6.0	22.3	1.7	1.3	0.6					
09:45	-5.9	2.8	19.4	6.0	22.3	1.8	1.5	0.6	15	5	20	9.3	27.8
09:50	-3.3	19.6	63.2	17.1	23.8	1.8	1.6	0.6					
09:55	-0.6	13.2	29.4	12.8	23.7	2.5	2.0	0.6					
10:00	-1.3	10.0	27.2	10.1	23.7	2.3	1.8	0.6					
10:05	-3.0	5.8	21.6	6.9	23.4	2.2	1.8	0.6					
10:10	-3.9	5.7	18.6	7.3	23.3	2.0	2.0	0.6	20	5	25	4.5	10.8

Average 23.0

Table 5.6 Ice-generator experimental data.
November 1/91

Time hh:mm	T _i °C	T _o °C	T _v °C	T _w °C	Trt °C	Pin bar	Pout bar	Fw4 kg s ⁻¹	tf min	td min	tc min	Wc kg	W kg h ⁻¹
08:30	-11.6	4.6	59.5	10.1	21.2	1.8	1.2	0.3					
08:35													
08:40	-17.2	3.8	35.2	4.8	21.6	1.7	1.2	0.3					
08:45	-18.5	4.3	27.6	5.3	22.0	1.5	1.2	0.3					
08:50	-15.5	2.9	24.6	5.4	22.4	1.5	1.2	0.3					
08:55	-19.5	11.8	68.7	9.7	22.4	1.7	1.4	0.3	25	5	30	10	20
09:00	-13.8	5.1	50.2	5.9	22.6	1.7	1.4	0.3					
09:05	-17.0	5.2	36.8	5.8	23.2	1.7	1.2	0.3					
09:10	-17.8	4.7	29.7	5.8	23.7	1.6	1.2	0.3					
09:15	-14.3	3.3	26.2	6.7	23.7	1.6	1.2	0.3	20	5	25	11.1	26.6
09:20	-15.0	16.4	65.3	15.4	23.3	1.3	1.2	0.3					
09:25	-12.5	8.7	46.4	8.9	23.6	1.7	1.2	0.3					
09:30	-15.0	5.8	35.3	6.7	23.7	1.8	1.3	0.4					
09:35	-12.5	1.6	28.3	6.7	23.9	1.8	1.3	0.4					
09:40	-13.8	-3.3	25.1	6.7	24.1	1.8	1.2	0.4	20	5	25	10.9	26.2
09:45	5.8	8.0	69.4	13.3	23.7	1.7	1.2	0.4					
09:50	-10.7	7.7	52.3	8.6	23.9	1.7	1.2	0.4					
09:55	-13.2	4.9	40.2	6.9	24.3	1.8	1.3	0.4					
10:00	-12.4	0.9	33.2	6.4	24.4	1.9	1.4	0.4	15	5	20	7	21
10:05	-10.7	12.5	63.2	12.6	24.4	2.0	1.4	0.4					
10:10	-10.3	5.1	45.2	7.3	24.4	2.0	1.4	0.4					
10:15	-12.5	0.3	33.8	7.0	24.6	1.9	1.4	0.4					
10:20	-14.4	0.6	28.2	6.9	24.9	1.7	1.2	0.4	15	5	20	11.1	33.3
10:25	-12.9	13.0	75.8	14.0	25.2	2.0	1.3	0.4					
10:30	-15.6	7.4	50.1	7.6	25.4	1.7	1.2	0.4					
10:35	-11.8	5.8	37.7	7.3	25.6	2.0	1.4	0.4					
10:40	-10.7	4.0	31.3	7.4	25.9	2.0	1.6	0.4					
10:45	-12.3	0.8	28.1	7.1	26.0	2.0	1.6	0.4	20	5	25	10	24
Average										25.2			

Table 5.7 Ice-generator experimental data.
November 12/91

Time hh:mm	T _i °C	T _o °C	T _v °C	T _w °C	T _{rt} °C	P _{in} bar	P _{out} bar	F _{w4} kg s ⁻¹	t _f min	t _d min	t _c min	W _c kg	W kg h ⁻¹	
07:55	7.2	20.6	68.1	19.2	32.9	2.0	1.6	0.4						
08:00	-6.1	2.4	54.3	12.7	32.9	2.0	1.6	0.4						
08:05	-9.3	9.6	41.4	10.2	31.4	2.0	1.6	0.4						
08:10	-9.9	6.7	32.8	9.5	30.6	2.0	1.6	0.3	15	5	20		5.2 15.6	
08:15														
08:20	-6.8	13.4	56.8	13.1	28.3	2.3	1.7	0.3						
08:25	-9.7	6.7	41.3	8.2	28.1	2.0	1.6	0.3						
08:30	-10.8	4.3	34.0	7.6	27.9	2.0	1.6	0.3						
08:35	-11.2	2.8	30.5	7.7	27.9	2.0	1.6	0.3	15	5	20		7.4 22.2	
08:40	-8.9	9.8	76.3	8.8	28.1	2.3	1.7	0.3						
08:45	-10.9	4.7	53.4	6.6	28.2	2.0	1.6	0.3						
08:50	-11.3	3.0	39.8	6.6	28.4	2.0	1.6	0.3						
08:55	-13.1	2.4	32.8	6.3	28.4	2.0	1.6	0.3	15	5	20		8.5 25.5	
09:00	-9.8	16.1	72.1	16.9	28.2	2.1	1.7	0.3						
09:05	-10.6	9.8	52.1	9.4	28.1	2.3	1.7	0.3						
09:10	-12.1	3.7	37.1	6.3	28.1	2.3	1.7	0.3						
09:15	-11.1	-1.7	30.4	6.4	28.1	2.0	1.9	0.3	15	5	20		5.7 17.1	
									Average				20.1	

Table 5.8 Ice-generator experimental data.
November 19/91

Time hh:mm	T _i °C	T _o °C	T _v °C	T _w °C	T _{rt} °C	P _{in} bar	P _{out} bar	F _{w4} kg s ⁻¹	t _f min	t _d min	t _c min	W _c kg	W kg h ⁻¹	
08:30	-11.6	4.6	59.5	10.1	21.2	1.8	1.2	0.3						
08:35														
08:40	-17.2	3.8	35.2	4.8	21.6	1.7	1.2	0.3						
08:45	-18.5	4.3	27.6	5.3	22.0	1.5	1.2	0.3						
08:50	-15.5	2.9	24.6	5.4	22.4	1.5	1.2	0.3						
08:55	-19.5	11.8	68.7	9.7	22.4	1.7	1.4	0.3	25	5	30		10 20	
09:00	-13.8	5.1	50.2	5.9	22.6	1.7	1.4	0.3						
09:05	-17.0	5.2	36.8	5.8	23.2	1.7	1.2	0.3						
09:10	-17.8	4.7	29.7	5.8	23.7	1.6	1.2	0.3						
09:15	-14.3	3.3	26.2	6.7	23.7	1.6	1.2	0.3	20	5	25		11.1 26.6	
09:20	-15.0	16.4	65.3	15.4	23.3	1.3	1.2	0.3						
09:25	-12.5	8.7	46.4	8.9	23.6	1.7	1.2	0.3						
09:30	-15.0	5.8	35.3	6.7	23.7	1.8	1.3	0.4						
09:35	-12.5	1.6	28.3	6.7	23.9	1.8	1.3	0.4						
09:40	-13.8	-3.3	25.1	6.7	24.1	1.8	1.2	0.4	20	5	25		10.9 26.2	
09:45	5.8	8.0	69.4	13.3	23.7	1.7	1.2	0.4						
09:50	-10.7	7.7	52.3	8.6	23.9	1.7	1.2	0.4						
09:55	-13.2	4.9	40.2	6.9	24.3	1.8	1.3	0.4						
10:00	-12.4	0.9	33.2	6.4	24.4	1.9	1.4	0.4	15	5	20		7 21	
10:05	-10.7	12.5	63.2	12.6	24.4	2.0	1.4	0.4						
10:10	-10.3	5.1	45.2	7.3	24.4	2.0	1.4	0.4						
10:15	-12.5	0.3	33.8	7.0	24.6	1.9	1.4	0.4						
10:20	-14.4	0.6	28.2	6.9	24.9	1.7	1.2	0.4	15	5	20		11.1 33.3	
10:25	-12.9	13.0	75.8	14.0	25.2	2.0	1.3	0.4						
10:30	-15.6	7.4	50.1	7.6	25.4	1.7	1.2	0.4						
10:35	-11.8	5.8	37.7	7.3	25.6	2.0	1.4	0.4						
10:40	-10.7	4.0	31.3	7.4	25.9	2.0	1.6	0.4						
10:45	-12.3	0.8	28.1	7.1	26.0	2.0	1.6	0.4	20	5	25		10 24	
									Average				25.2	

Table 5.9 Ice-generator experimental data.
November 20/91

Time hh:mm	T _i °C	T _o °C	T _w °C	T _{rt} °C	t _f min	t _r min	t _c min	w _c kg	w kg h ⁻¹
08:40 AM	-5.3	8.8	14.7	19.8					
08:45 AM	-13.3	5.0	6.1	20.6					
08:50 AM	-15.7	2.6	3.9	20.6					
08:55 AM	-17.8	3.1	4.1	20.8					
09:00 AM	-14.6	0.6	4.2	21.2					
09:05 AM	-16.3	1.7	4.2	21.7	25	5	30	12	24.0
09:10 AM	-13.1	11.7	12.8	22.2					
09:15 AM	-8.2	2.7	5.2	22.4					
09:20 AM	-12.0	0.2	5.1	22.3					
09:25 AM	-3.1	-6.1	5.2	22.4					
09:30 AM	-14.2	-7.8	5.2	22.6					
09:35 AM	-14.7	-7.6	5.8	22.8	25	5	30	17.8	35.6
09:40 AM	-7.6	15.7	14.9	23.4					
09:45 AM	-11.6	6.0	6.9	23.4					
09:50 AM	-13.2	3.1	5.5	23.2					
09:55 AM	-13.8	1.5	5.6	23.2					
10:00 AM	-14.6	0.4	5.6	23.4					
10:05 AM	-11.1	-2.4	5.8	27.7	25	5	30	16.7	33.4
10:10 AM	-5.8	18.7	17.9	24.7					
10:15 AM	-10.2	9.4	9.7	24.7					
10:20 AM	-10.8	4.8	6.6	24.6					
10:25 AM	-11.9	1.2	6.6	24.7					
10:30 AM	-11.8	3.2	6.9	24.7					
10:35 AM	-12.4	0.2	7.0	24.9	25	5	30	13.2	26.4
10:40 AM	-8.4	21.9	18.6	26.4					
10:45 AM	-9.6	8.6	9.1	26.7					
10:50 AM	-11.6	6.2	7.4	26.7					
10:55 AM	-10.4	6.2	7.8	26.9					
11:00 AM	-11.4	3.4	7.8	27.2					
11:05 AM	-11.9	-0.4	8.0	27.4	25	5	30	14.4	28.8
11:10 AM	-5.0	19.6	17.3	28.3					
11:15 AM	-8.8	7.1	8.6	28.2					
11:20 AM	-7.2	6.6	8.3	28.3					
11:25 AM	-8.9	3.3	8.6	28.3					
11:30 AM	-8.8	-3.9	8.2	28.3					
11:35 AM	-9.9	-6.3	8.7	28.4	25	5	30	15.2	30.4
11:40 AM	-7.7	31.2	14.6	29.3					
11:45 AM	-8.3	15.9	15.4	29.4					
11:50 AM	-7.1	8.2	9.4	29.4					
11:55 AM	-8.8	6.3	9.6	29.4					
12:00 PM	-9.4	3.0	9.7	30.1					
12:05 PM	-10.3	0.5	9.2	29.9	25	5	30	13.6	27.2
12:10 PM	-8.5	17.0	19.3	30.6					
12:15 PM	-8.4	10.7	11.4	30.3					
12:20 PM	-11.6	8.4	9.1	30.1					
12:25 PM	-7.8	5.8	9.3	29.9					
12:30 PM	-8.9	2.2	9.3	29.9					
12:35 PM	-10.2	0.2	9.2	29.9	25	5	30	14.2	28.4
12:40 PM	-8.9	24.1	25.9	31.0					
12:45 PM	-8.6	10.7	10.9	30.4					
12:50 PM	-9.4	8.8	9.6	30.2					
12:55 PM	-7.8	7.6	9.4	29.8					
01:00 PM	-8.8	6.6	9.1	30.0					
01:05 PM	-10.5	1.2	9.2	30.0	25	5	30	13	26.0

Table 5.9 Ice-generator experimental data.
November 20/91 (Continued)

Time hh:mm	T _i °C	T _o °C	T _w °C	T _{rt} °C	t _f min	t _r min	t _c min	w _c kg	w kg h ⁻¹
01:10 PM	-8.4	18.6	14.5	31.2					
01:15 PM	-6.9	12.7	12.7	30.9					
01:20 PM	-6.9	8.2	9.7	30.4					
01:25 PM	-8.1	5.2	9.6	30.2					
01:30 PM	-9.1	0.8	9.6	30.2					
01:35 PM	-10.9	0.1	9.2	30.2	25	5	30	14.8	29.6
01:40 PM	-9.5	30.2	15.4	31.0					
01:45 PM	-9.3	11.2	10.6	30.7					
01:50 PM	-1.1	8.8	9.5	30.5					
01:55 PM	-9.1	9.0	8.7	30.4					
02:00 PM	-10.9	7.8	9.0	30.4					
02:05 PM	-9.8	2.6	9.4	30.5	25	5	30	11.4	22.8
02:10 PM	-3.0	22.8	21.8	31.6					
02:15 PM	-6.8	10.9	11.2	31.2					
02:20 PM	-9.3	8.1	8.6	30.7					
02:25 PM	-7.6	4.1	8.7	30.4					
02:30 PM	-8.1	2.3	8.6	30.6					
02:35 PM	-8.9	-1.1	9.2	30.8	25	5	30	14.8	29.6
02:40 PM	-5.3	17.1	16.8	32.5					
02:45 PM	-7.2	8.8	9.8	32.5					
02:50 PM	-5.7	6.8	9.9	32.6					
02:55 PM	-6.6	2.8	11.2	32.4					
03:00 PM	-7.2	1.4	10.7	33.7					
03:05 PM	-8.0	0.6	11.1	33.7	25	5	30	15.4	30.8
03:10 PM	-3.4	19.1	17.7	34.2					
03:15 PM	-3.6	13.2	13.5	34.1					
03:20 PM	-3.0	9.8	11.2	33.4					
03:25 PM	-4.8	6.8	10.9	33.3					
03:30 PM	1.1	3.9	11.5	33.4					
03:35 PM	-4.0	0.2	11.4	33.6	25	5	30	12.4	24.8
03:40 PM	-5.1	15.3	22.3	35.4					
03:45 PM	1.1	11.7	12.8	34.6					
03:50 PM	0.8	6.7	10.9	33.7					
03:55 PM	-3.2	6.7	10.6	33.1					
04:00 PM	-3.7	5.6	10.3	32.7					
04:05 PM	-5.4	-1.0	10.2	32.4	25	5	30	11	22
04:10 PM	-1.9	16.0	15.1	34.0					
04:15 PM	-4.8	8.7	10.2	32.9					
04:20 PM	-0.4	7.4	10.2	32.3					
04:25 PM	-5.9	-0.3	10.2	32.3					
04:30 PM	-6.2	-1.4	10.9	32.3					
04:35 PM	-5.2	-2.0	10.4	32.4	25	5	30	17	34
04:40 PM	-1.6	21.6	23.2	34.7					
04:45 PM	2.6	14.3	14.6	34.1					
04:50 PM	-1.0	7.4	11.3	33.5					
04:55 PM	-0.3	3.2	11.3	33.2					
05:00 PM	-2.0	1.9	11.5	33.1					
05:05 PM	-2.4	0.7	11.7	32.9	25	5	30	12.2	24.4
05:10 PM	2.1	25.2	25.4	35.3					
05:15 PM	-2.8	18.2	17.6	34.8					
05:20 PM	-1.5	11.8	13.2	34.3					
05:25 PM	-2.2	6.2	13.1	33.9					
05:30 PM	-1.4	2.0	12.9	33.7					
05:35 PM	-1.8	2.3	13.5	33.7	25	5	30	13.8	27.6

Table 5.9 Ice-generator experimental data.
November 20/91 (Continued)

Time hh:mm	T _i °C	T _o °C	T _W °C	T _r t °C	t _f min	t _r min	t _c min	w _c kg	w kg h ⁻¹
05:40 PM	3.9	13.6	19.6	35.8					
05:45 PM	0.4	11.3	14.1	34.9					
05:50 PM	-0.7	7.4	13.6	34.1					
05:55 PM	-1.9	6.8	13.4	33.3					
06:00 PM	-2.7	6.0	12.9	32.5					
06:05 PM	-4.3	4.3	12.6	31.8	25	5	30	16.8	33.6
06:10 PM	-4.8	15.9	17.9	31.8					
06:15 PM	-3.1	8.2	11.7	30.6					
06:20 PM	-3.7	6.0	11.4	30.1					
06:25 PM	-5.0	3.9	10.9	29.3					
06:30 PM	-6.3	2.4	10.4	28.7					
06:35 PM	-7.1	1.3	10.1	28.3	25	5	30	16.6	33.2
06:40 PM	-5.8	16.7	15.9	27.7					
06:45 PM	-4.7	8.9	10.1	26.9					
06:50 PM	-6.0	6.1	9.0	26.3					
06:55 PM	-6.7	2.2	8.9	26.0					
07:00 PM	-7.2	-0.4	8.4	25.9					
07:05 PM	-7.6	-2.7	8.3	26.9	25	5	30	12.2	24.4
07:10 PM	-2.2	12.1	12.1	26.5					
07:15 PM	-4.4	6.7	8.1	26.2					
07:20 PM	-7.0	3.1	7.8	26.2					
07:25 PM	-8.4	-2.9	7.8	26.3					
07:30 PM	-8.6	-4.2	7.9	26.3					
07:35 PM	-8.7	-4.4	8.3	26.3	25	5	30	18	36
07:40 PM	-6.1	18.2	18.2	27.1					
07:45 PM	-5.5	9.4	10.1	26.8					
07:50 PM	-6.1	4.7	9.0	26.5					
07:55 PM	-7.3	-1.9	9.0	26.5					
08:00 PM	-7.8	-4.1	9.1	26.7					
08:05 PM	-8.8	-6.4	9.6	26.6	25	5	30	18.2	36.4
08:10 PM	-0.8	13.7	14.9	27.6					
08:15 PM	-5.5	7.8	9.8	27.2					
08:20 PM	-7.2	5.0	10.0	26.8					
08:25 PM	-3.9	3.4	10.2	26.8					
08:30 PM	-5.9	0.6	10.3	27.2					
08:35 PM	-6.2	-2.6	11.1	27.2	25	5	30	18.2	36.4
08:40 PM	-0.4	17.9	17.1	28.4					
08:45 PM	-2.9	10.6	11.3	27.8					
08:50 PM	-5.6	9.5	11.0	27.7					
08:55 PM	-3.5	9.6	11.3	27.6					
09:00 PM	-3.6	4.1	11.3	27.4					
09:05 PM	-3.7	0.3	11.3	27.3	25	5	30	14.4	28.8
								Average	29.4

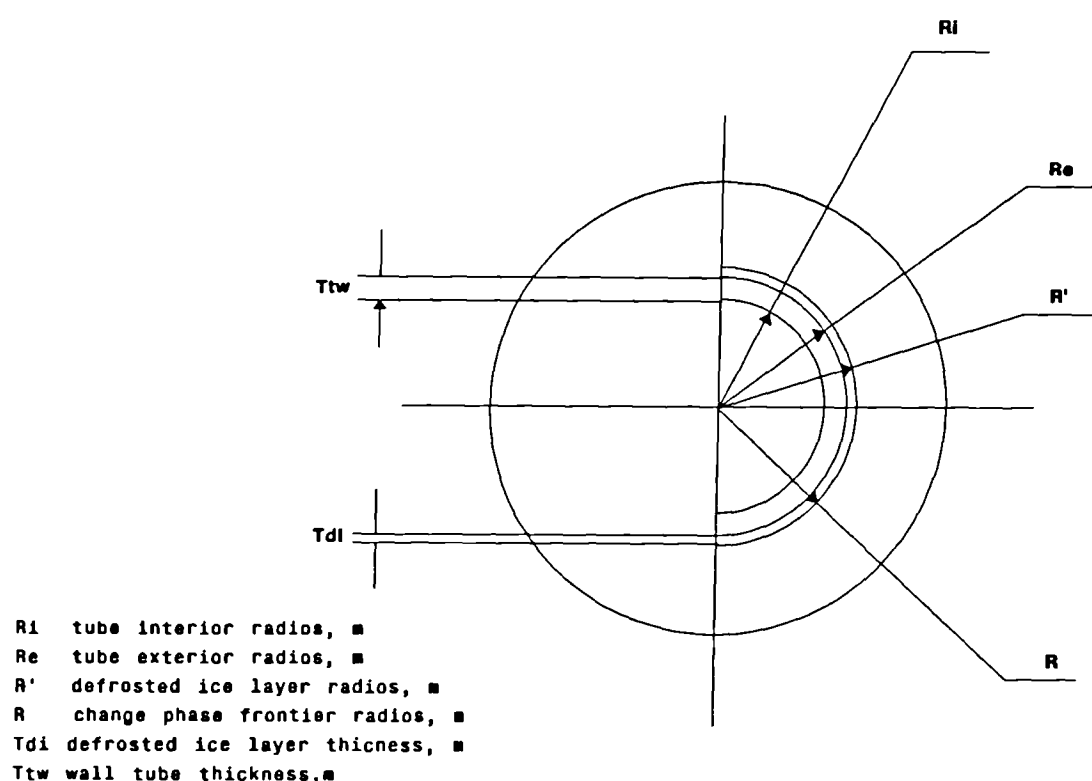


Fig. 5.1 Physical geometrical characteristics

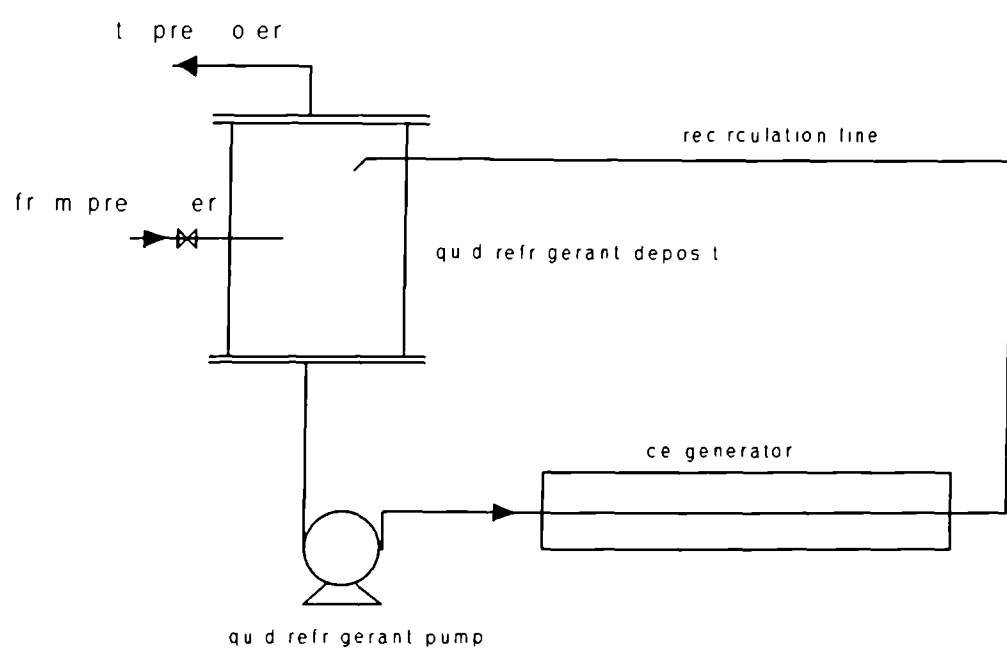


Fig. 5.2 Schematic of vertical tubes ice-generator system

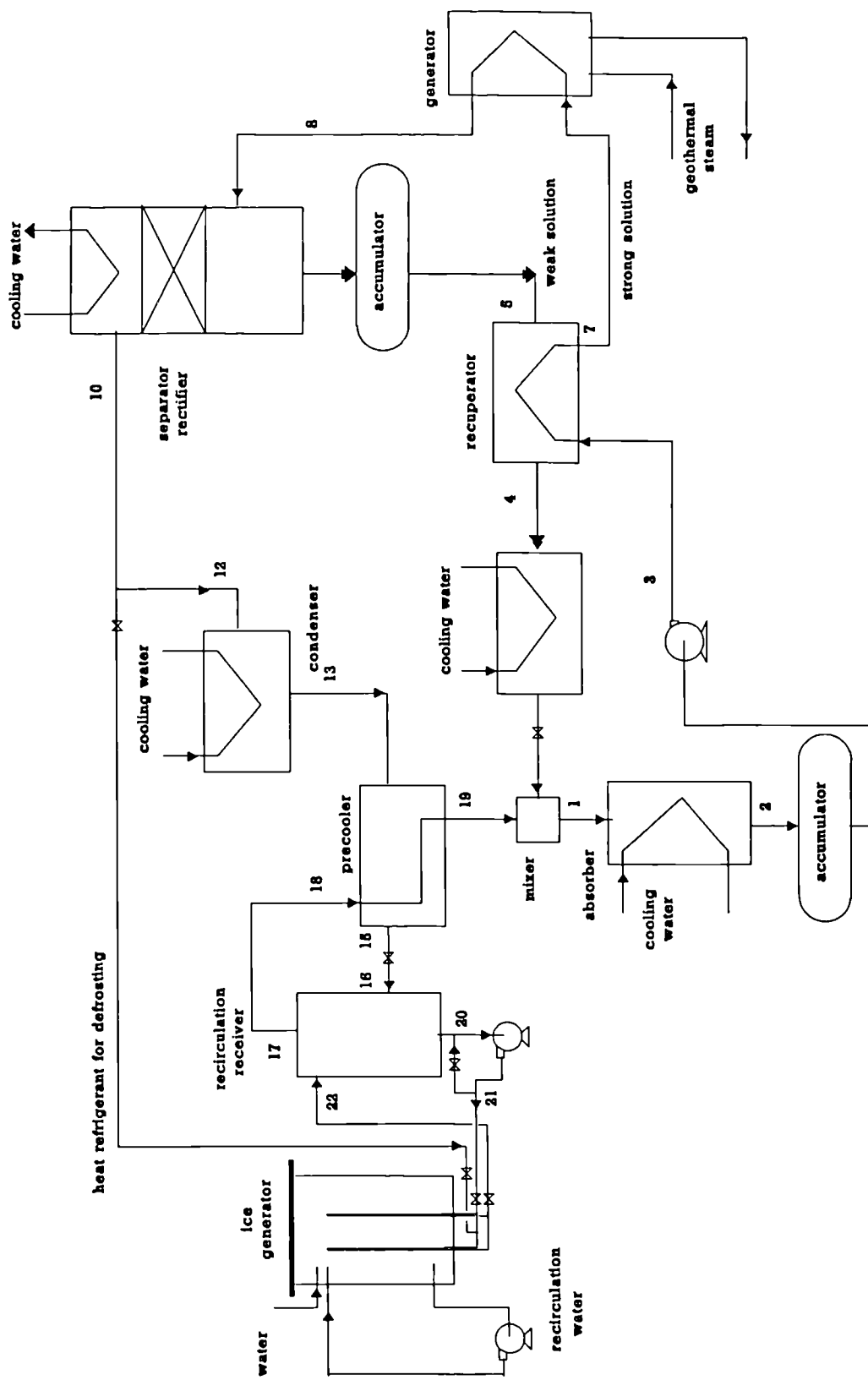


Fig. 5.3 Schematic diagram of the ammonia-water absorption vertical tube prototype

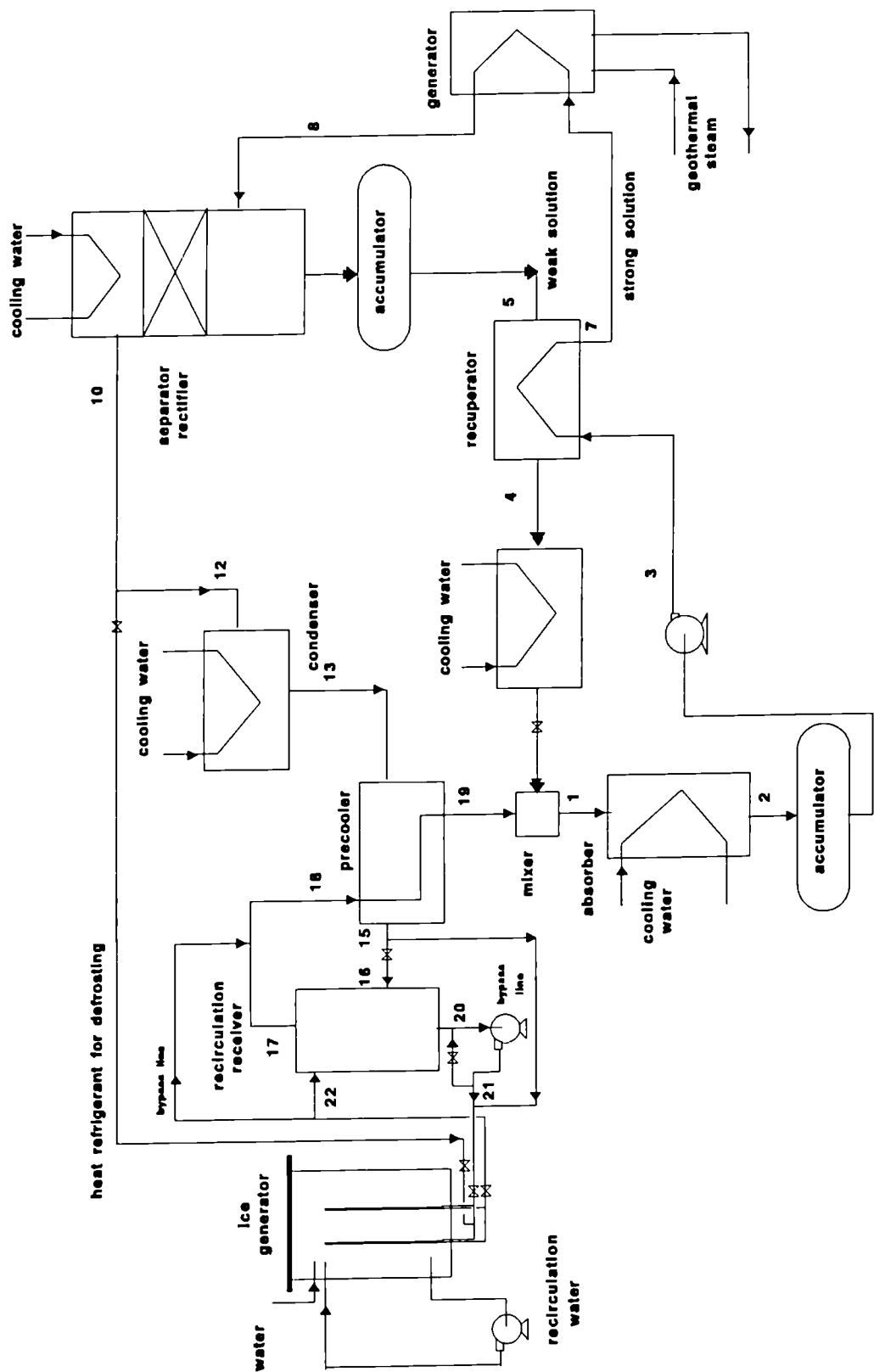


Fig. 5.4 Schematic diagram of the ammonia-water absorption vertical tube prototype with recirculation

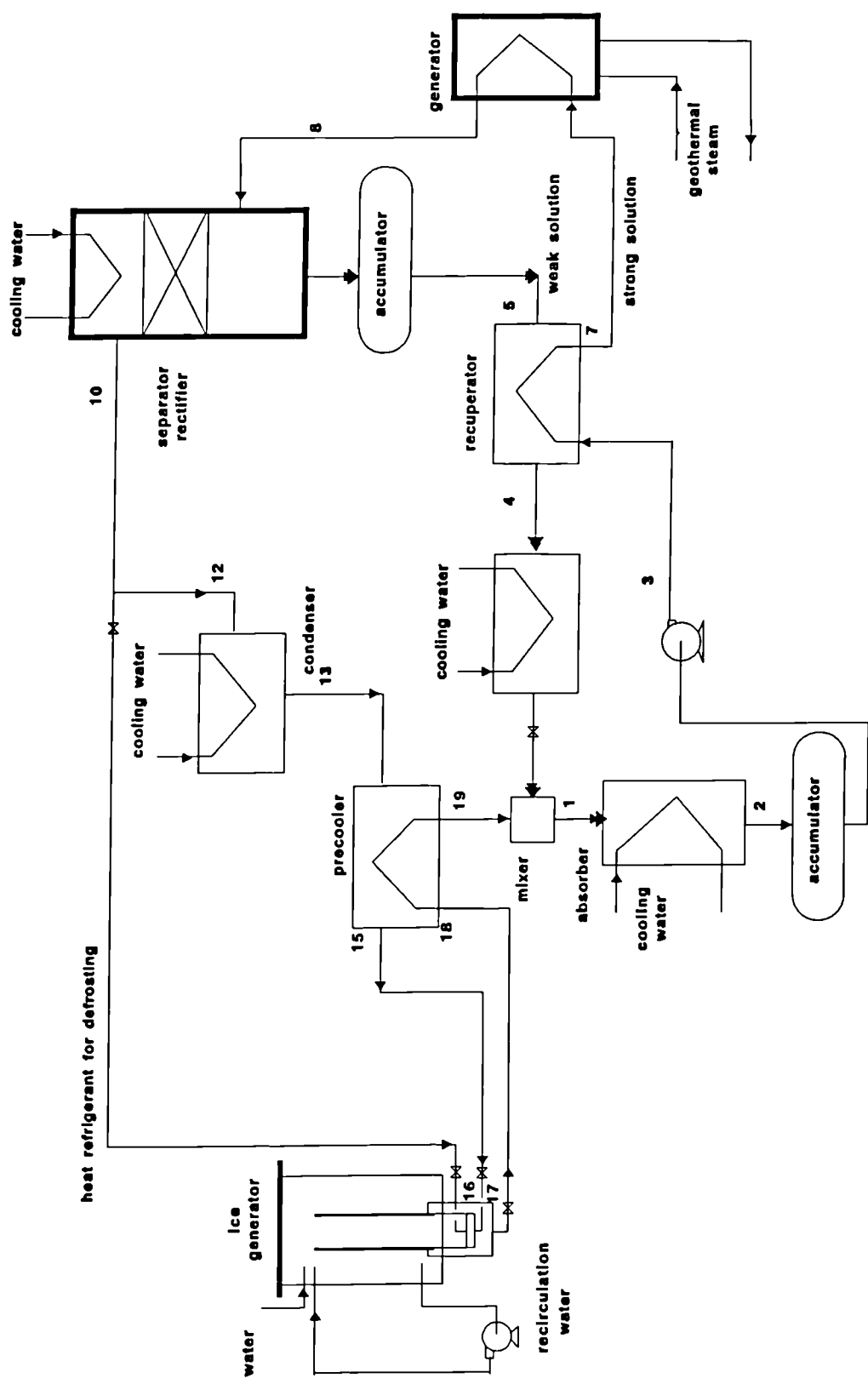


Fig. 5.5 Schematic diagram of the ammonia-water absorption vertical tube prototype with manual valves

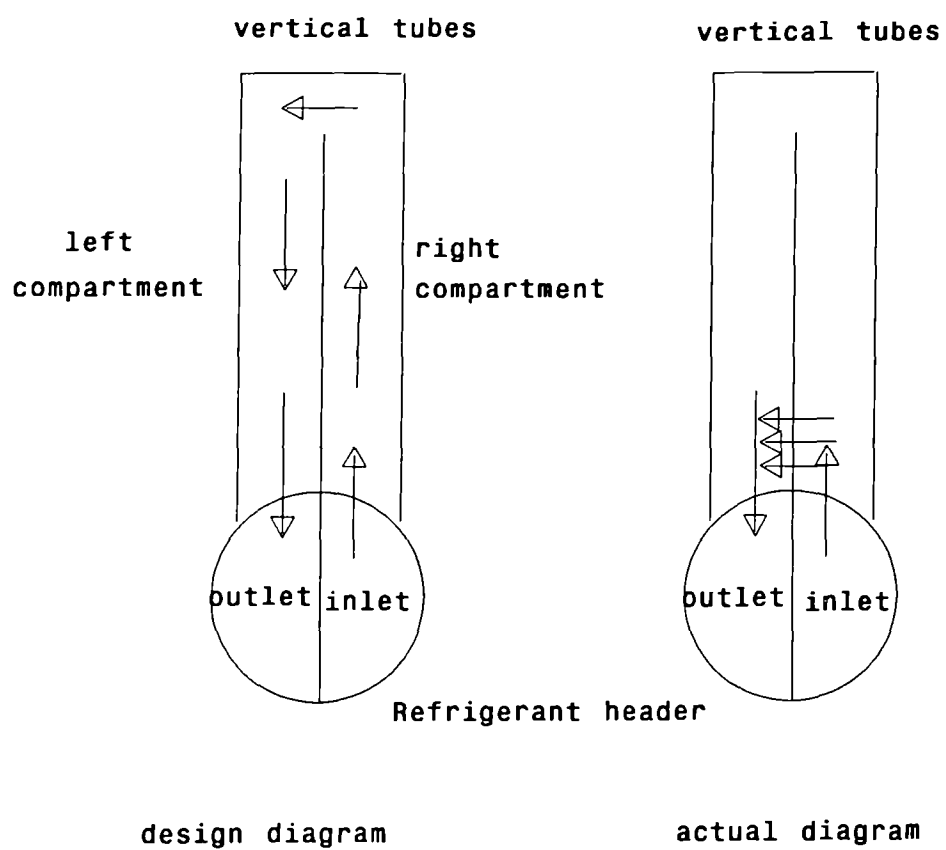


Fig. 5.6 Vertical tubes refrigerant flow diagram

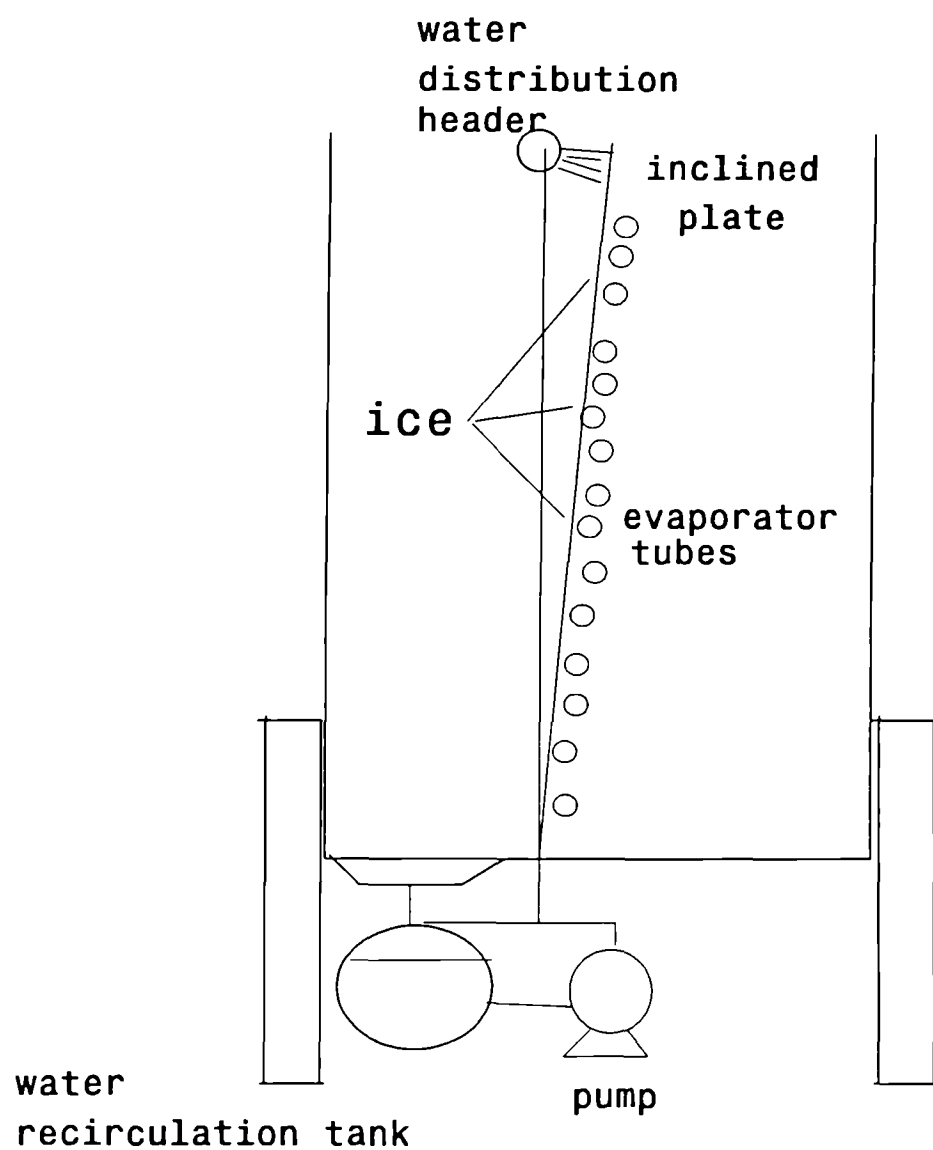


Fig. 5.7 Schematic diagram of the inclined plate ice generator

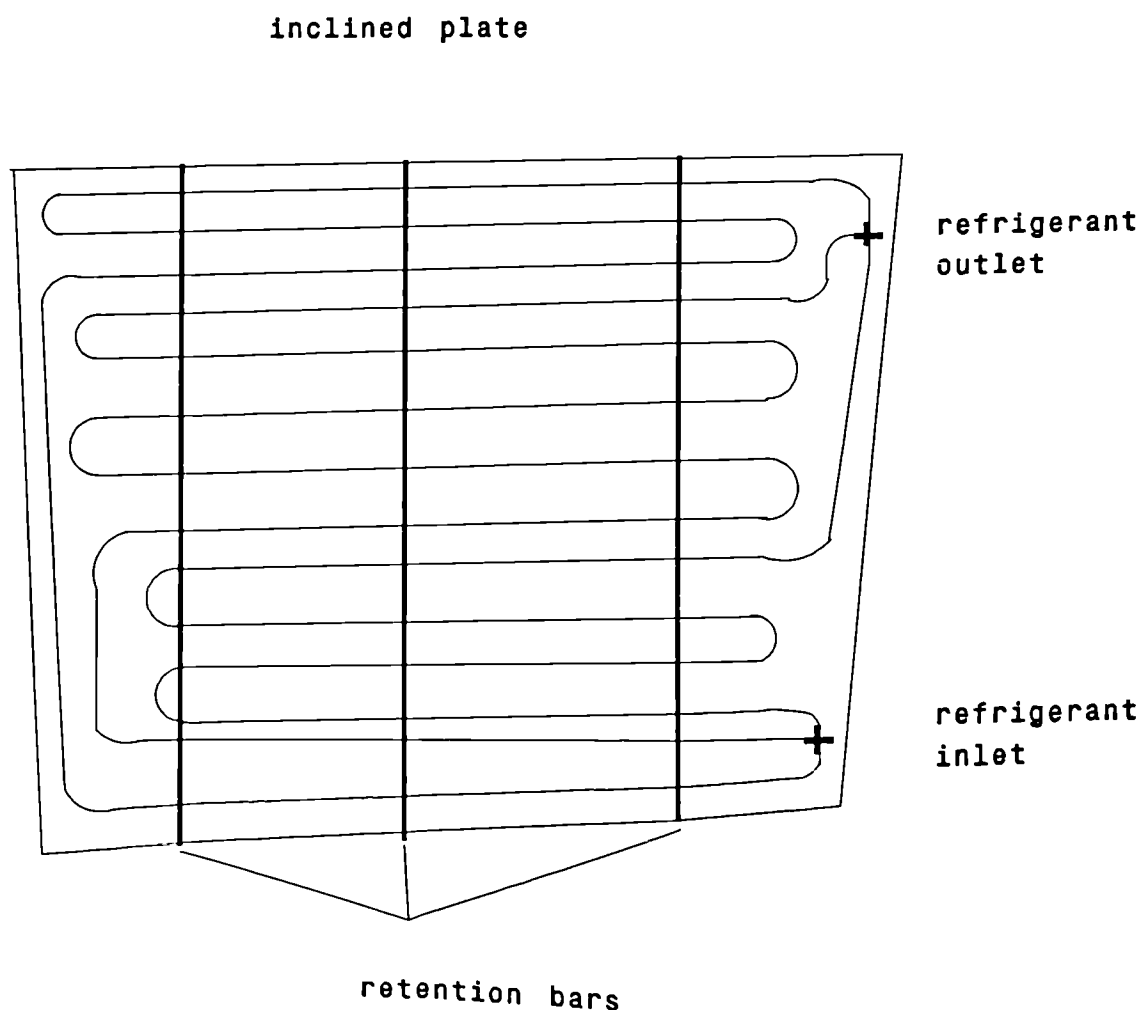


Fig. 5.8 Stainless steel tubing coil distribution on the inclined plate ice generator.

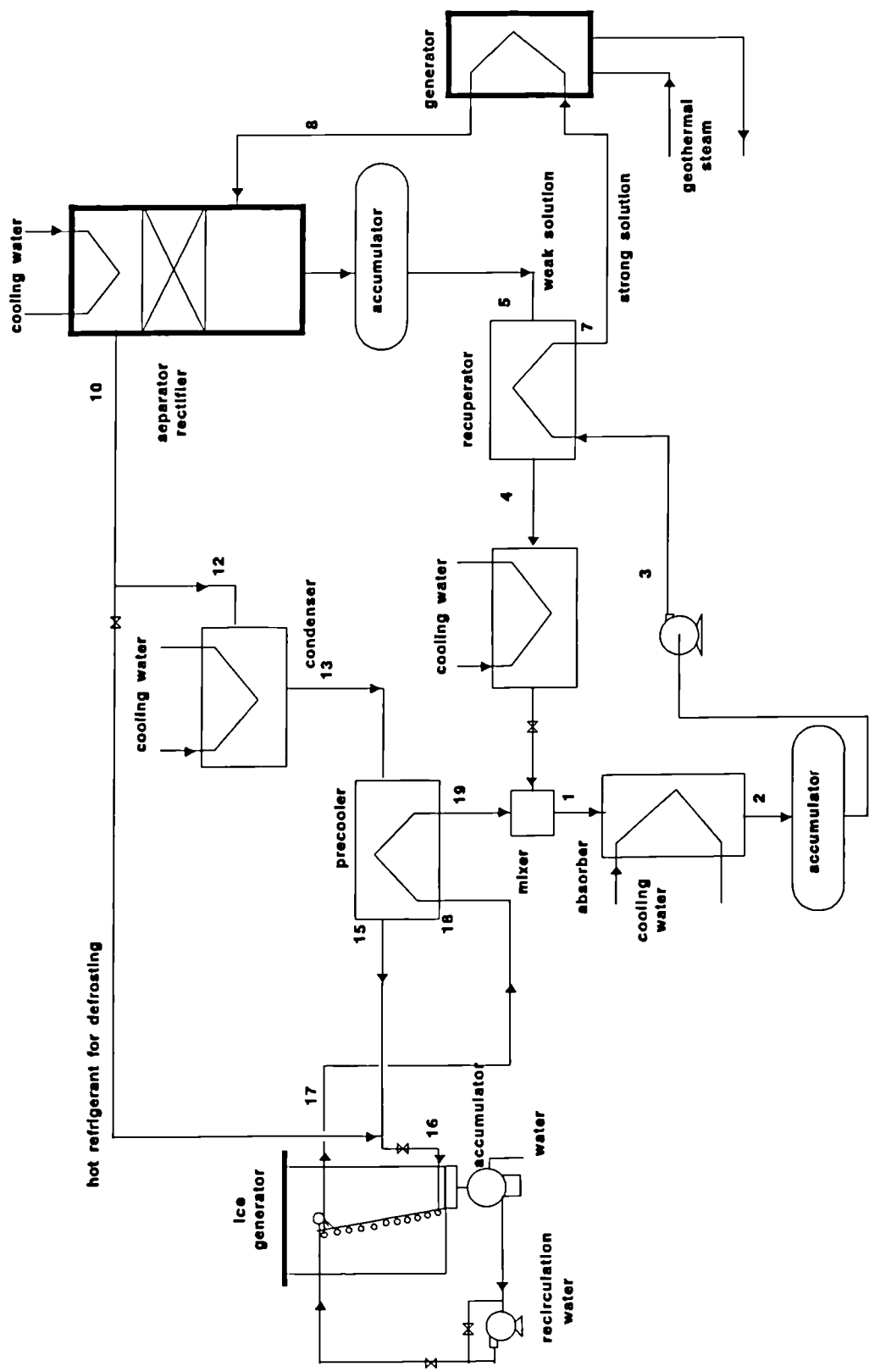


Fig. 5.9 Schematic diagram of the ammonia-water absorption unit with the inclined plate ice generator

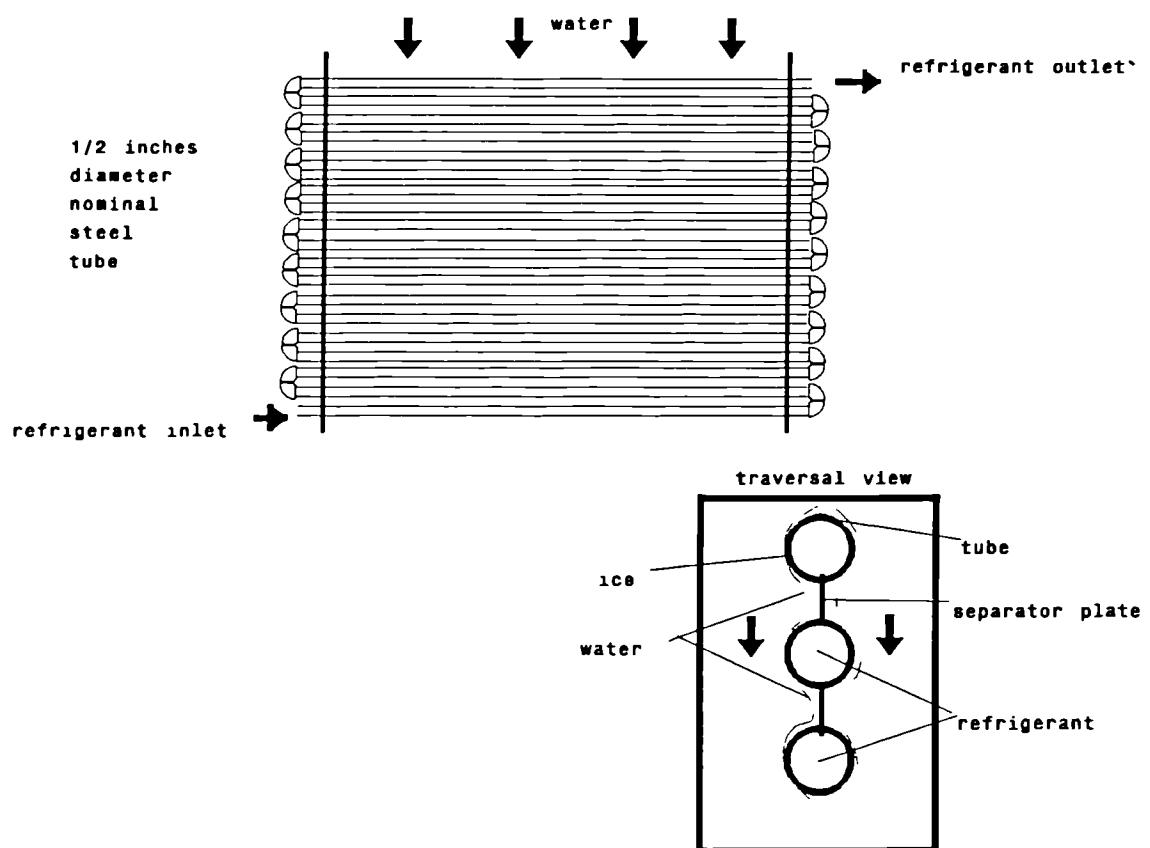
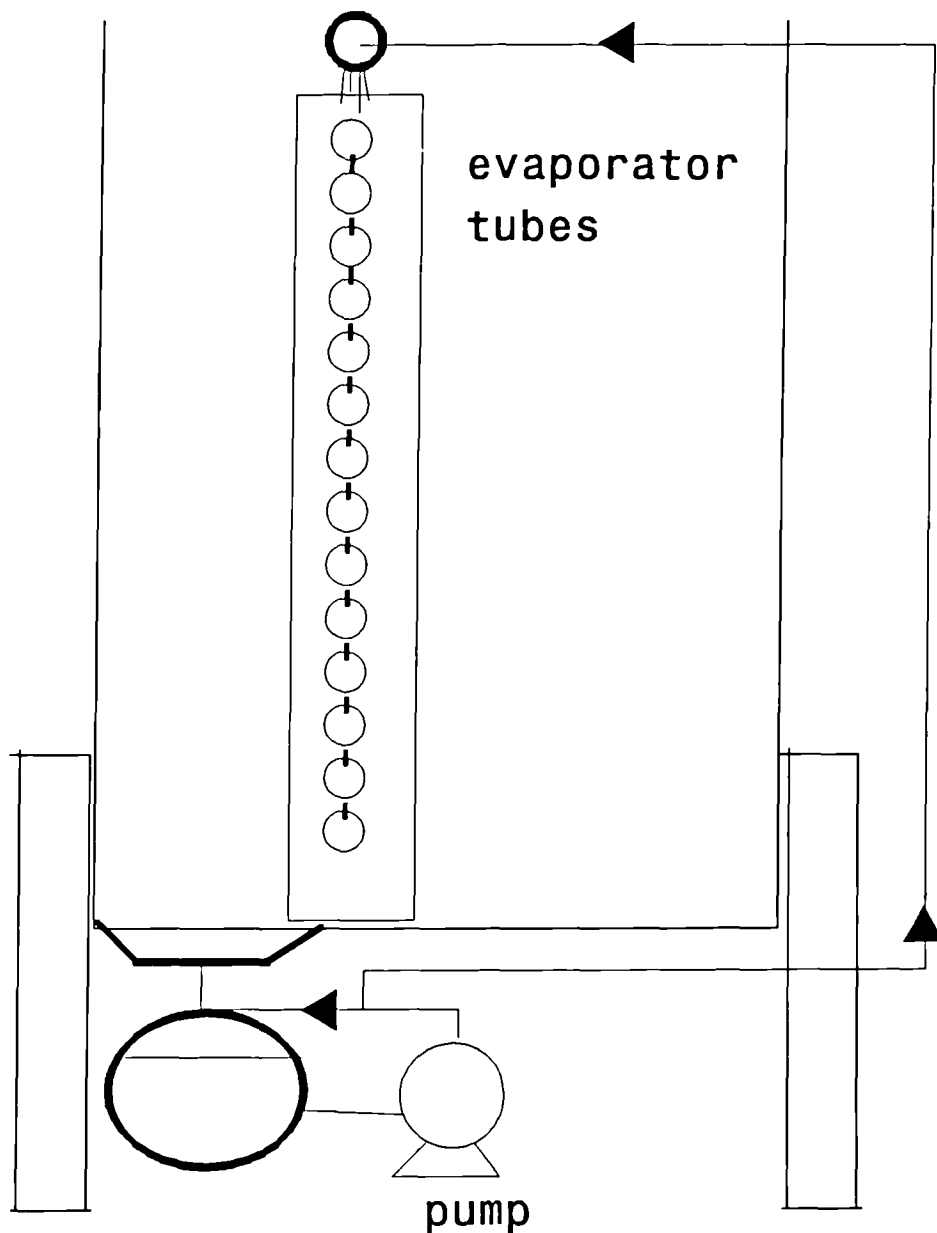


Fig. 5.10 Vertical tube coil diagram

water distribution header



water
recirculation
tank

Fig. 5.11 Vertical tube coil ice generator flow diagram

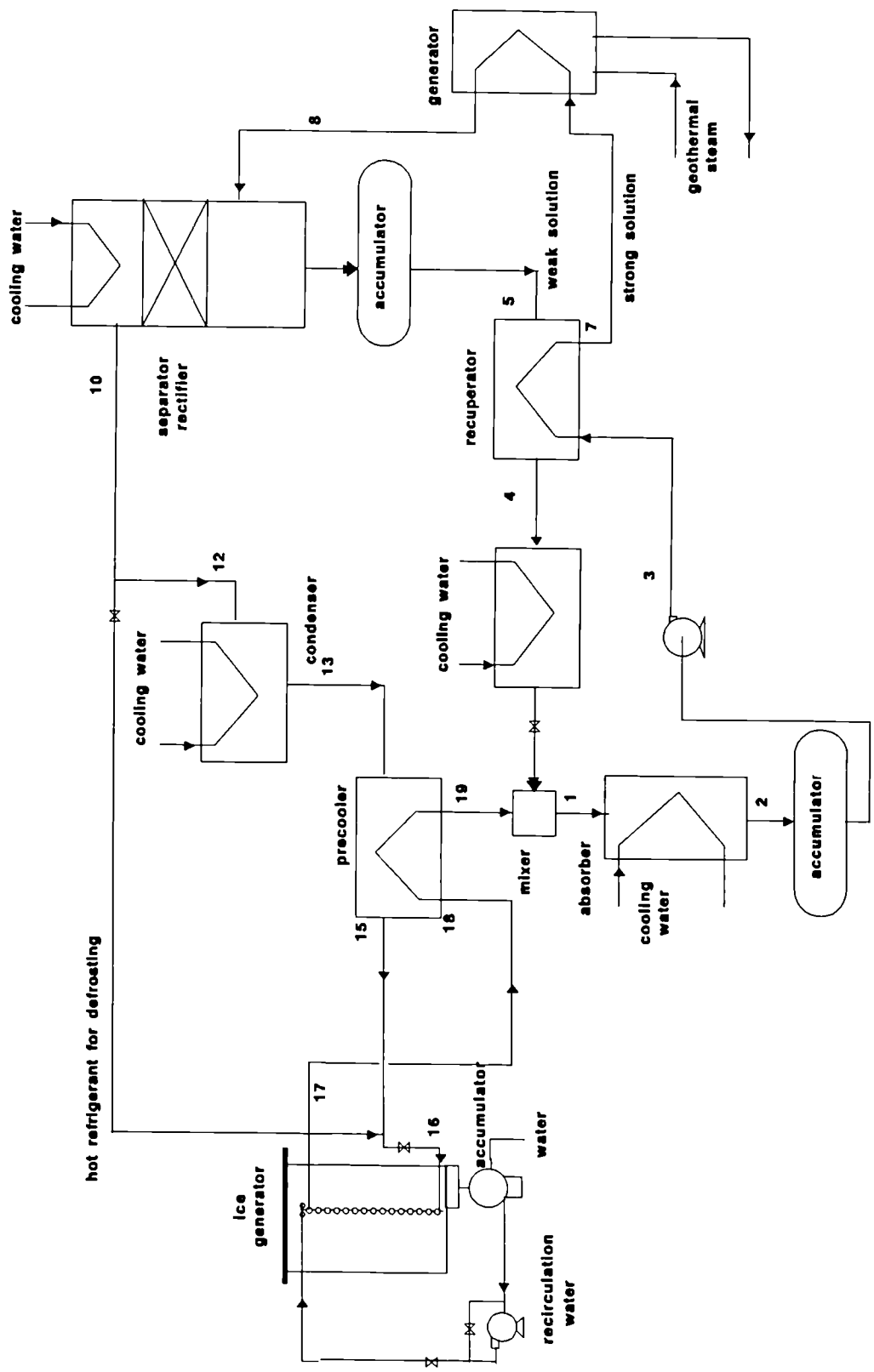


Fig. 5.12 Ammonia-water absorption system with the vertical tube coil ice generator

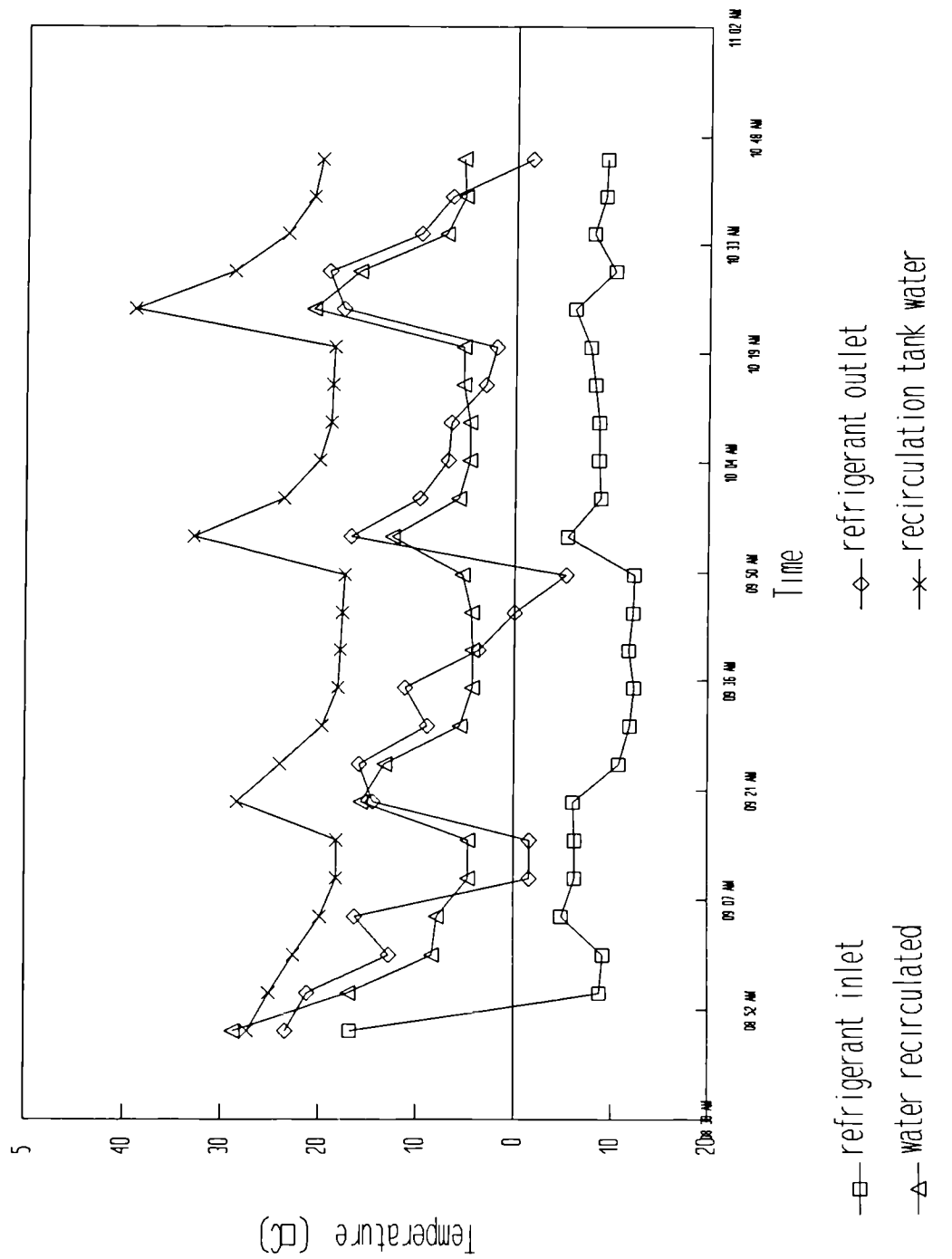


Fig. 5.13 Vertical tube coil ice-generator preliminary test (September 10, 1991)

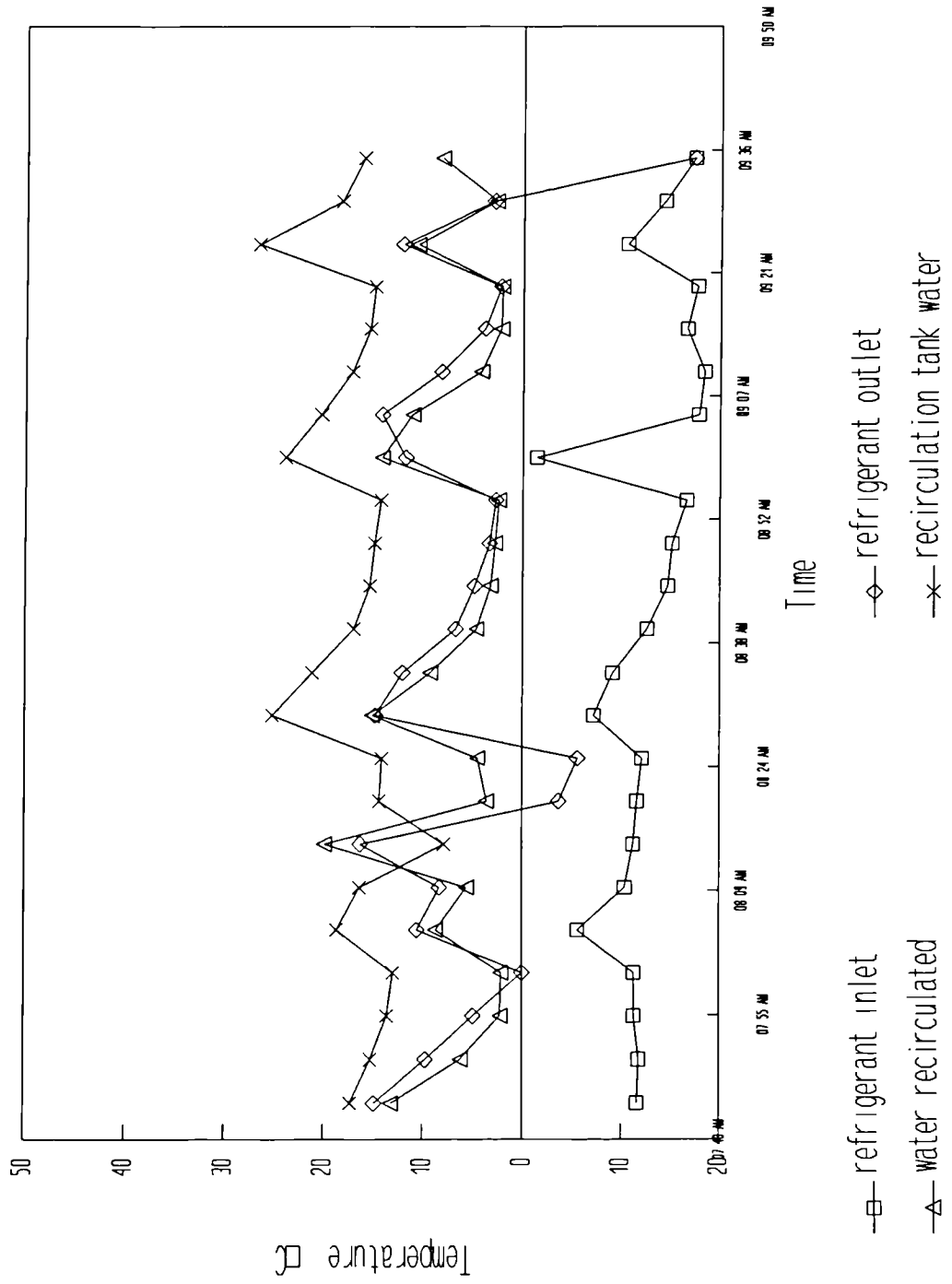


Fig. 5.14 Vertical tube coil ice-generator preliminary test (September 11, 1991)

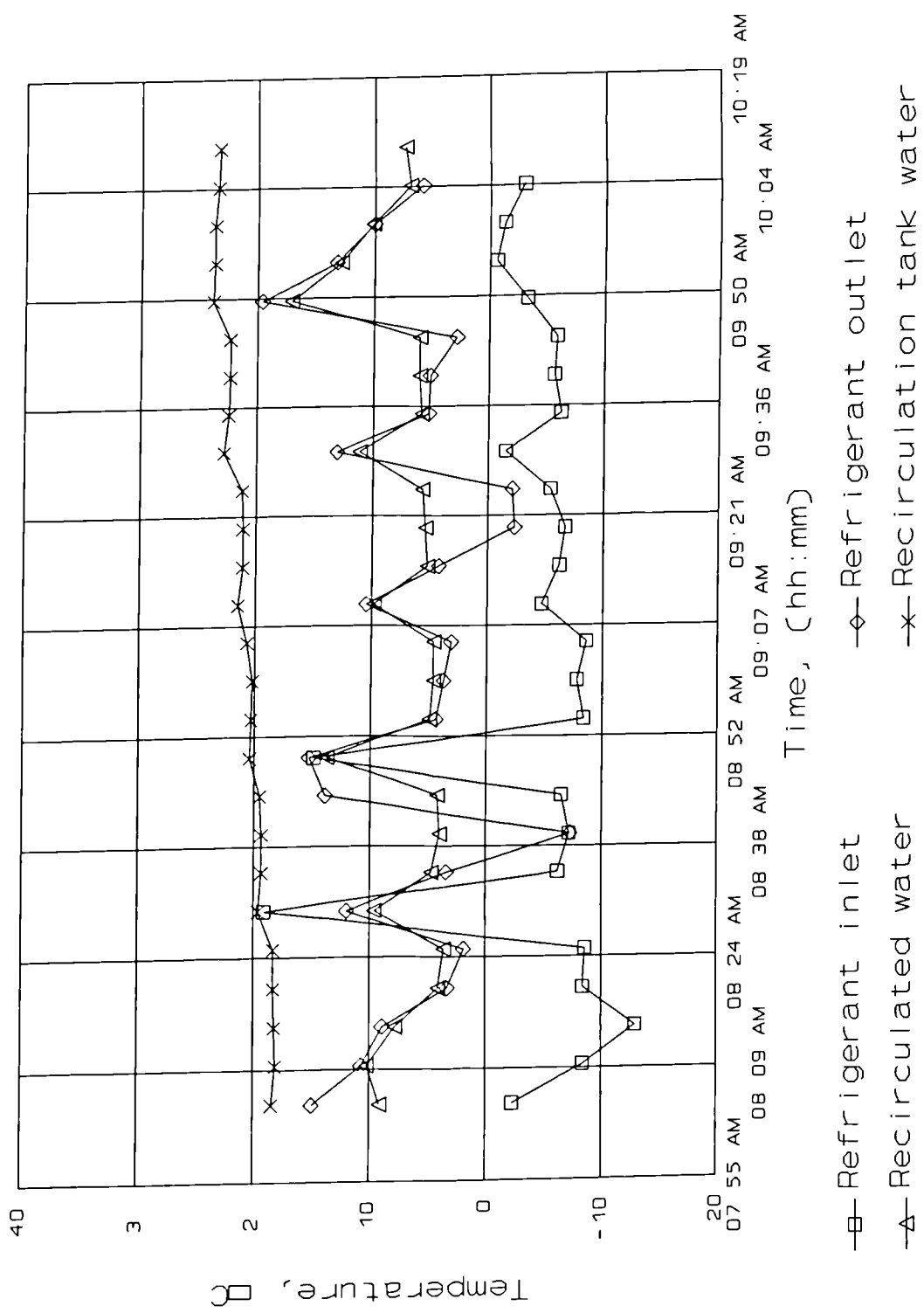


Fig. 5.15 Ice-generator evaluation test (October 31, 1991)

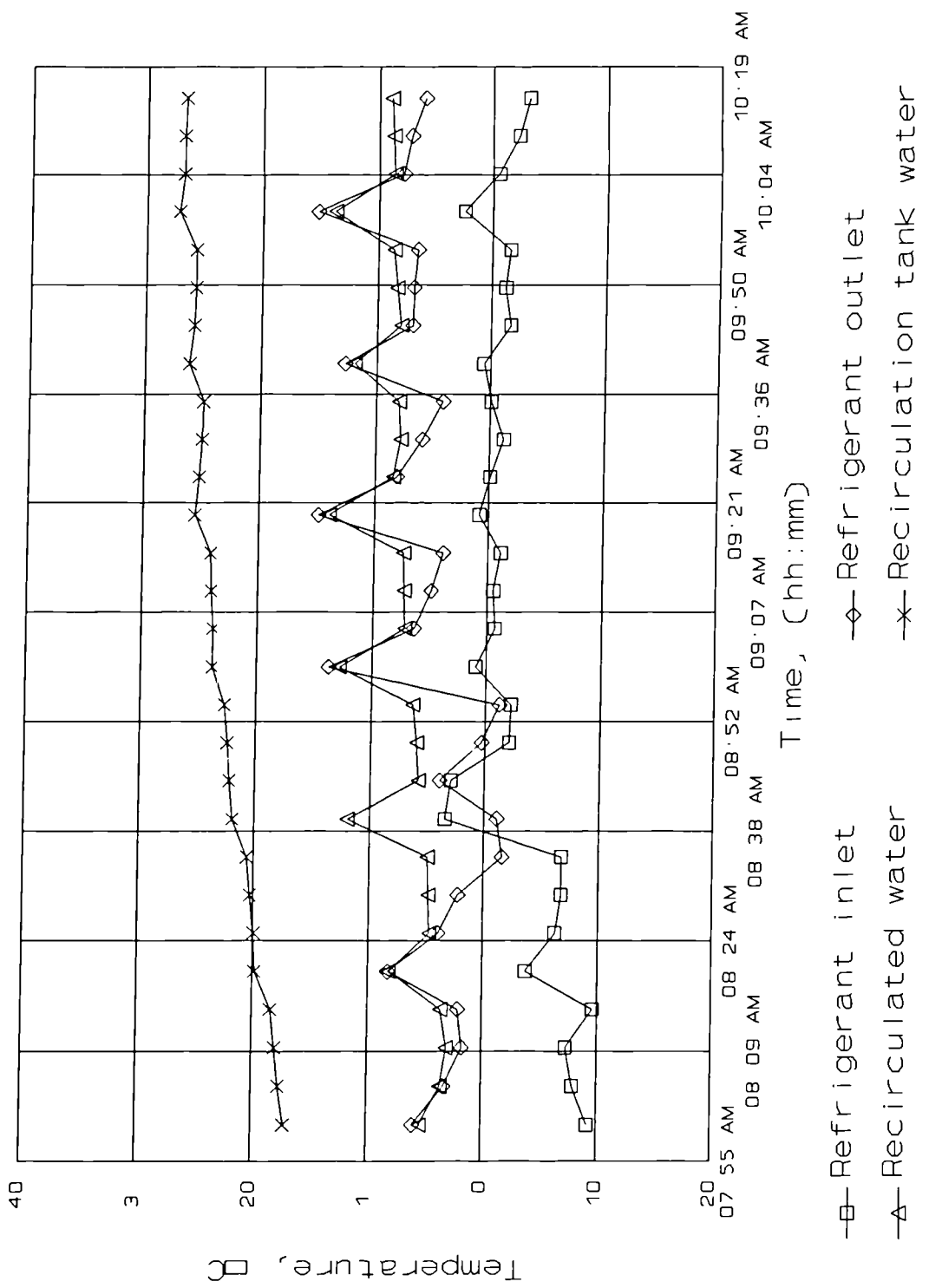


Fig. 5.16 Ice-generator evaluation test (November 1, 1991)

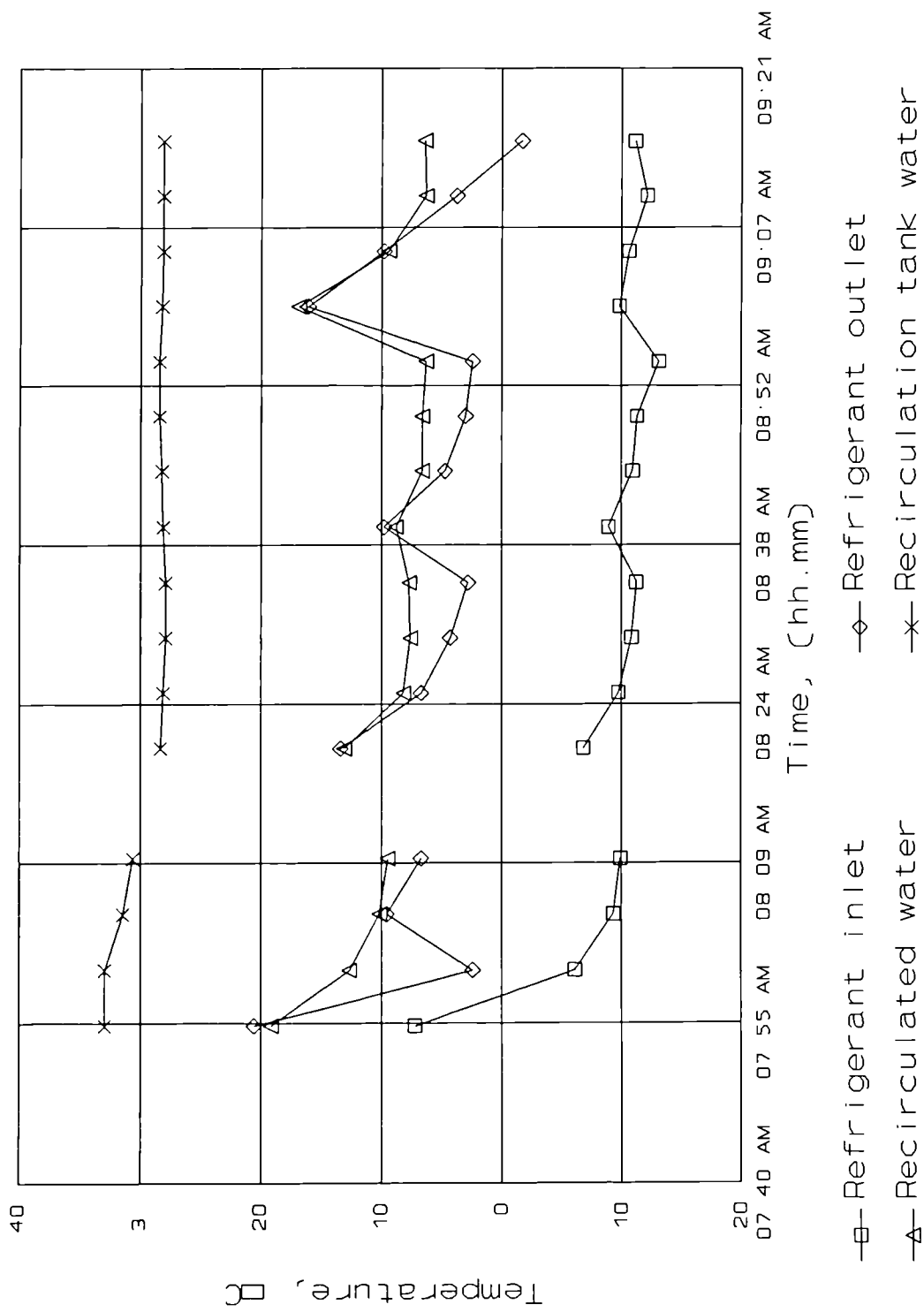


Fig. 5.17 Ice-generator evaluation test (November 12, 1991)

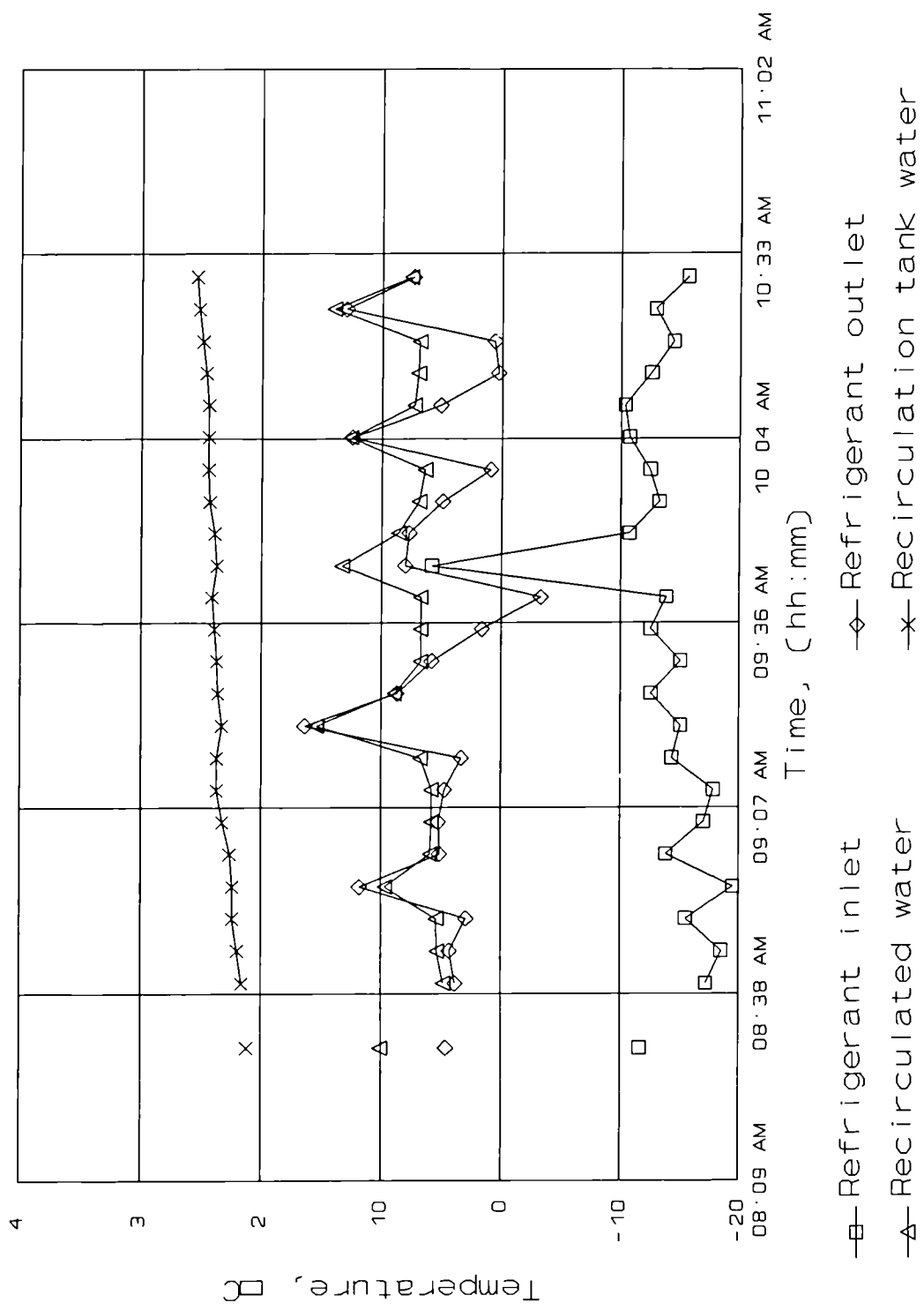


Fig. 5.18 Ice-generator evaluation test (November 19, 1991)

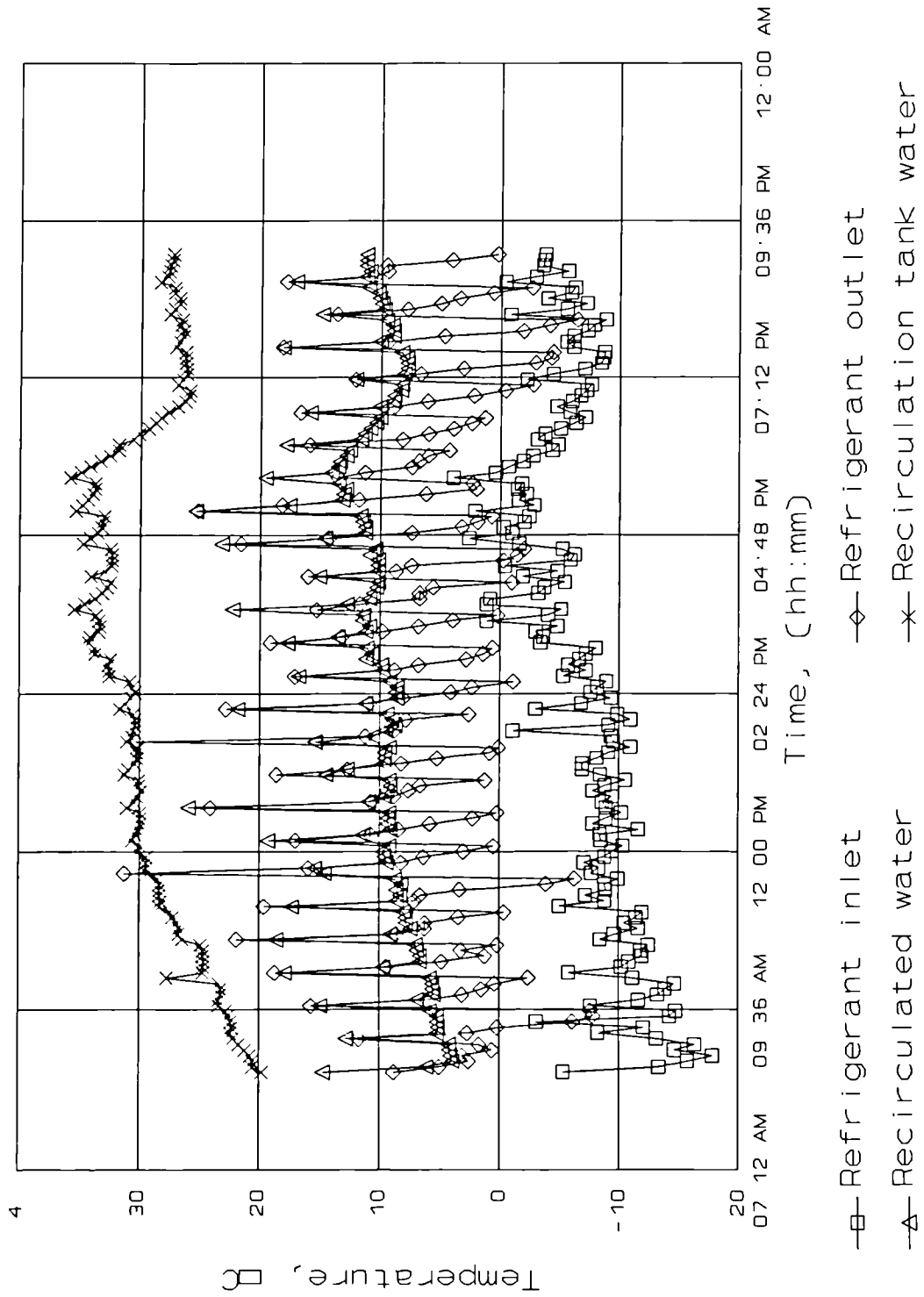


Fig. 5.19 Ice-generator evaluation test (November 20, 1991)

CHAPTER 6

EXPERIMENTAL STUDIES WITH AN ABSORPTION SYSTEM USING A FLUIDISED BED HEAT EXCHANGER.

6.1 INTRODUCTION

In order to prove the ammonia-water absorption system using the geothermal brine as a heat resource, a liquid fluidised bed heat exchanger, (LFBHE) was tested. The LFBHE was used to avoid the fouling properties of the brine in Cerro Prieto Geothermal field. This brine might cause very severe fouling of the heat transfer surfaces in conventional heat exchangers.

The material to be used in the bed was sand particles in order to evaluate an economic material and to prove the sand's growing tendency in the geothermal brine medium.

6.2 EQUIPMENT

Brine separation system

Figure 6.1 shows the brine separation system, it consists of one separator of the shell and tube type connected to the 302 well brine pipeline with one water tank and a silencer.

This system transmits brine from the 55.88 cm (22 inches) diameter pipeline at 8.1 bar pressure, to the LFBHE through a 5.08 cm (2 inches) nominal diameter carbon steel tube. As well as carrying the brine the separation system is used to; eliminate the steam formed and throw away the excess brine.

The separation system could work at a pressure below that of the pressure of the pipeline and the outlet pressure of the brine could be regulated. This permitted the LFBHE to operate at various pressures.

Liquid fluidised bed heat exchanger

The LFBHE is of the shell and tube type, see Fig 6.1 and Fig. 6.2. The carbon steel shell has a nominal diameter of 7.62 cm, (3 inches) and a height of 6 m. Inside the shell there is a single carbon steel tube of nominal diameter 5.08 cm (2 inches). The geothermal brine circulates on the tube side. The secondary flow (ammonia-water, strong solution) circulates through the shell. [C. Heard, 1989]

Bed particle classification

The bed (sand particles) material used was classified and homogenized. In order to homogenize the bed material, a small tube with a recirculation pump was constructed.

The bed in the LFBHE was formed with sand particles of 3-4 mm diameter. The classification was carried out with two wire cloths one with 4.5 X 4.5 mm mesh and the second with 3.4 X 3.4 mm mesh. Then a homogenizing process was performed, water flowing up through a particle bed, in a PVC tube with 7.62 cm nominal diameter and 1.2 m height see Fig. 6.3 for details. The water flow cleaned the particles of dust and removed the lighter particles from the bed.

Table 6.1, shows the characteristics of the particles of the sand used in the LFBHE tests.

This kind of bed was used in a LFBHE and proved in the Los Azufres geothermal field, [J. Siqueiros, 1990] and it was observed that the particles had the property of growing with the silica removed from the brine.

6.3 PROCEDURE

The start up procedure for the LFBHE was developed during a series of preliminary tests in order to test the LFBHE performance itself. For this purpose geothermal brine was fed in the tube side and cool water from the cooling tower in the shell side. It was observed that silica precipitated in the first stage of the start up procedure, so the first step was to warm up the feed pipeline and the LFBHE with small quantities of geothermal steam. During this step it was very important to feed the steam slowly to avoid the steam carrying away the sand particles.

With the above procedure, during the test period of the LFBHE connected to the absorption system it was necessary to start the absorption system with the steam based generator in order to warm the working fluid and the LFBHE was also warmed with steam.

Next there is an experimental procedure description.

Step	Description
(a)	The LFBHE is fed with the amount required of sand particles.
(b)	The absorption system is started up in the customary way using the steam based generator.
(c)	The LFBHE is warmed up.
(d)	With the LFBHE warm the geothermal brine is fed on the tube side and the ammonia solution is fed on the shell side. Closing the corresponding valves, the steam based generator is bypassed. At this moment the absorption system is operating using brine to heat the strong solution in the LFBHE.

- (e) The temperature, pressure and flow data are recorded manually, the absorption system data are recorded every 30 minutes and the LFBHE data every 10 minutes. Two samples of brine are taken at the inlet and outlet of the brine in order to analyse the amount of silica deposited on the sand surface.
- (f) In order to measure the amount of brine passed through the LFBHE an indirect method was prepared, this method consisted in introducing a receiver with a known volume (186 litres) and measuring the time necessary to reach that level.
- (g) In order to finish the test it is necessary to shutdown the absorption system in the customary way and wait for the LFBHE to purge all the brine and extract the sand to evaluate the amount of silica deposited.

6.4 RESULTS AND DISCUSSIONS

Six preliminary tests were carried out in order to evaluate the performance of the LFBHE without using the absorption system. The fluid heated was water from the cooling tower and this test helped to develop the start up procedure and to set the necessary points to control the LFBHE. See tables A1.23 to A1.27.

During these tests the LFBHE efficiency was about 80 to 85%, and it was observed that pressure drop between the inlet and outlet in the LFBHE (1 bar), increased with time because of the growth of the sand particles, and during two tests of 24 hours it was observed that the LFBHE was plugged because of the sand and silica agglomeration. Table 6.1 show the chemical data of the brine and the silica removal efficiency.

The LFBHE was tested connected to the absorption system during three tests and only in one test the experimental data was recorded, see tables A1.22 and A1.28. During this test it was observed that the LFBHE efficiency decreased to 40 to 50 % because the sand did

not prevent the silica scaling. With this problem it was impossible to reach high generation temperatures to operate the absorption system.

During the experimental work the following problems were observed and these could help in future work to design another system to use the brine efficiently to operate an absorption system.

- (a) There was a high pressure drop between the separation system and the inlet of the LFBHE, (2.5 bar).
- (b) The heat losses were very high because this pipeline was not insulated. The length of the pipeline was 45 meters and the diameter was 5.08 cm (2 inches).
- (c) The material for the bed (sand particles) behaved as attraction nuclei for the silica dissolved in the brine, reducing the fluidised state, and turbulence, thus silica precipitation was permitted over the heat transfer wall, reducing the heat transfer rate. The pressure drop in the LFBHE increased with the silica precipitation on the sand particles.
- (d) The LFBHE was constructed with scrap nominal tube and this kind of tube has an irregular surface that permits the silica precipitation.

6.5 CONCLUSIONS

It is necessary to have a sufficiently big pipeline diameter to minimize the pressure drop between the separation system and the heat exchanger, it is also necessary to have a good insulated pipeline.

It is necessary to modify the LFBHE design in order to recirculate particles inside the tube.

It is necessary to evaluate the LFBHE using particles that do not grow in the brine.

6.6 REFERENCES

- 6.1 C. L. Heard, personal design of the LFBHE for the ammonia-water absorption system, (1990).
- 6.2 J. Siqueiros, H. Fernandez, H. Gamiño, D. Barragan, J.L. Frías and J. Peralta, Developments in geothermal energy in Mexico- part Thirty nine: Extraction of useful heat and silica removal from geothermal brine utilizing liquid fluidized bed heat exchangers. *J. Heat Recovery Systems, and CHP* 12(2) 169-179 (1992).
- 6.3 D. G. Klaren, Fluid bed heat exchanger - A solution for heat transfer involving severe fouling liquids, CPP Edition Europe, 1987.

Table 6.1

Properties of sand particles

Average diameter	4 to 5 mm
Density of particles	1372 kg m ⁻³
Quiescent porosity	.441

Table 6.2

Brine chemical data in the LFBHE

Date	Point	SiO ₂ mg l ⁻¹	D.T.S. mg l ⁻¹	Silica Removal Efficiency
March 10, 1992	Inlet	823.2		
		811.2		
March 26, 1992	Outlet	787.3		
		790.7		3.55 %
March 26, 1992	Inlet	753.9	24190	
		759.0	24190	
		757.3	24020	
		755.6	23793	
	Outlet	654.6	23800	
		652.9	23770	
		675.2	23987	
		660.6	23830	12.7%

D.T.S. Dissolved total solids

$$\text{Silica Removal Efficiency} = \frac{\text{Inlet concentration} - \text{outlet concentration}}{\text{Inlet concentration}} * 100$$

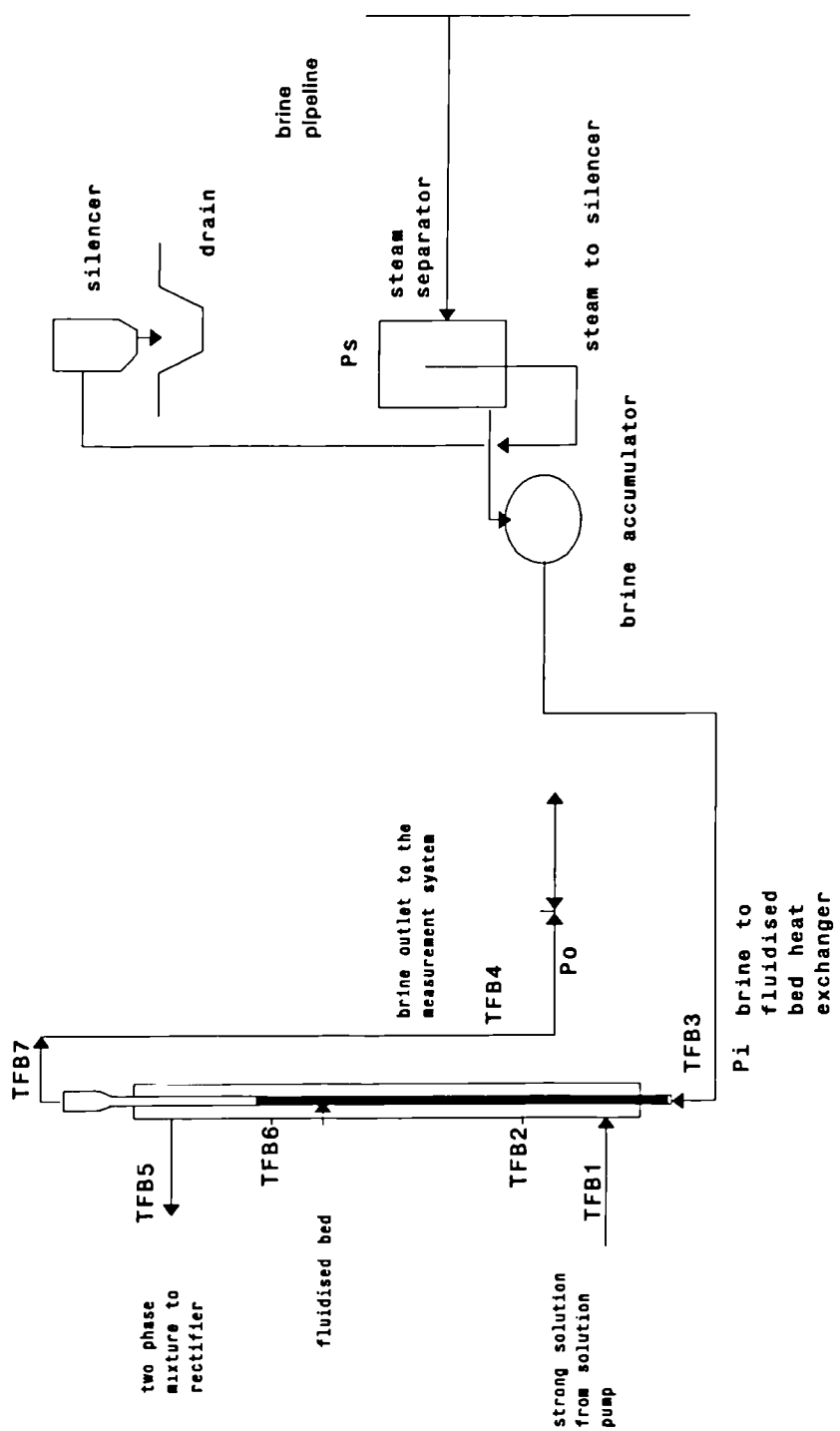


Fig. 6.1 Brine separation system and LFBHEx

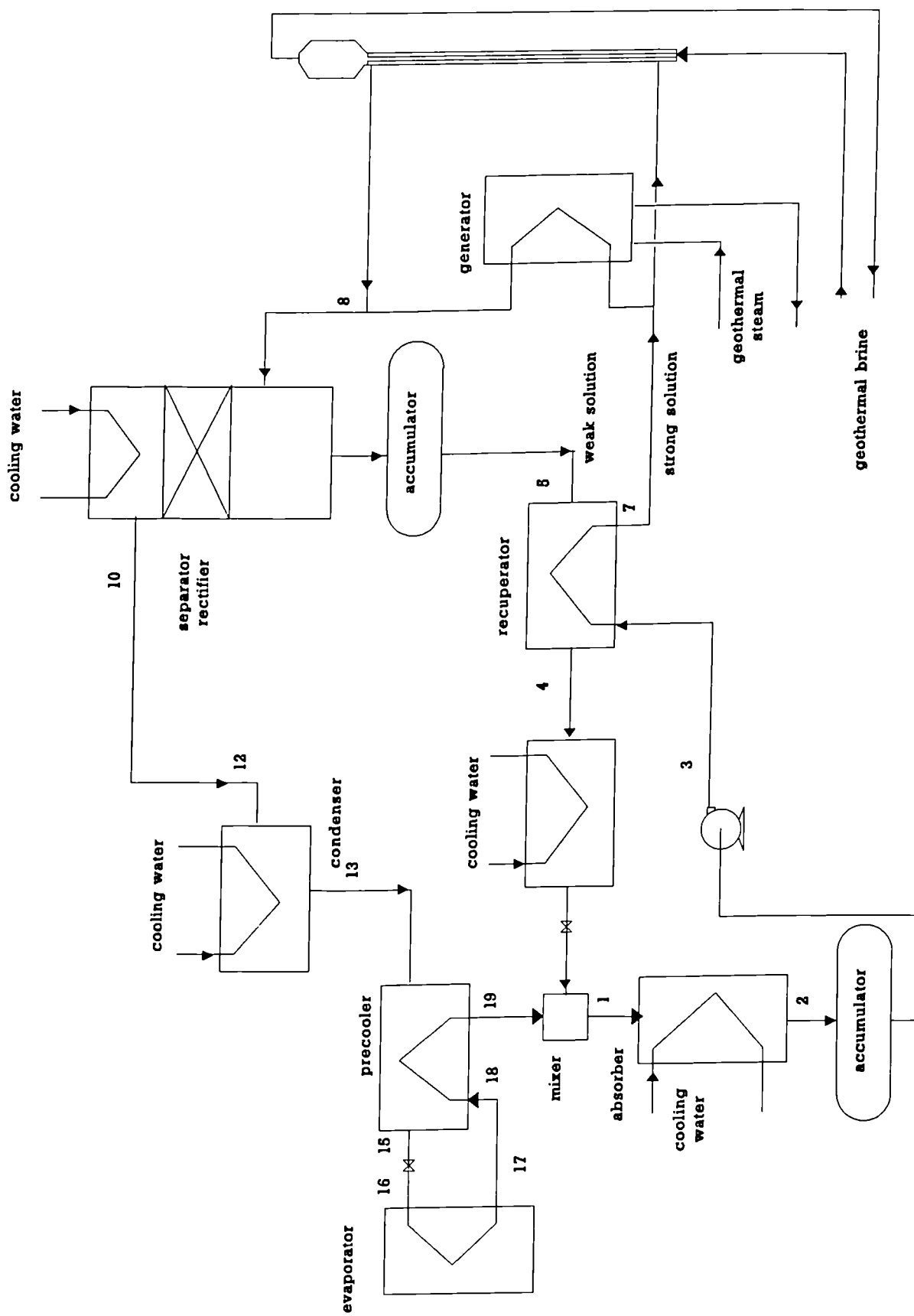


Fig. 6.2 Schematic diagram of the absorption system and the LFBHE

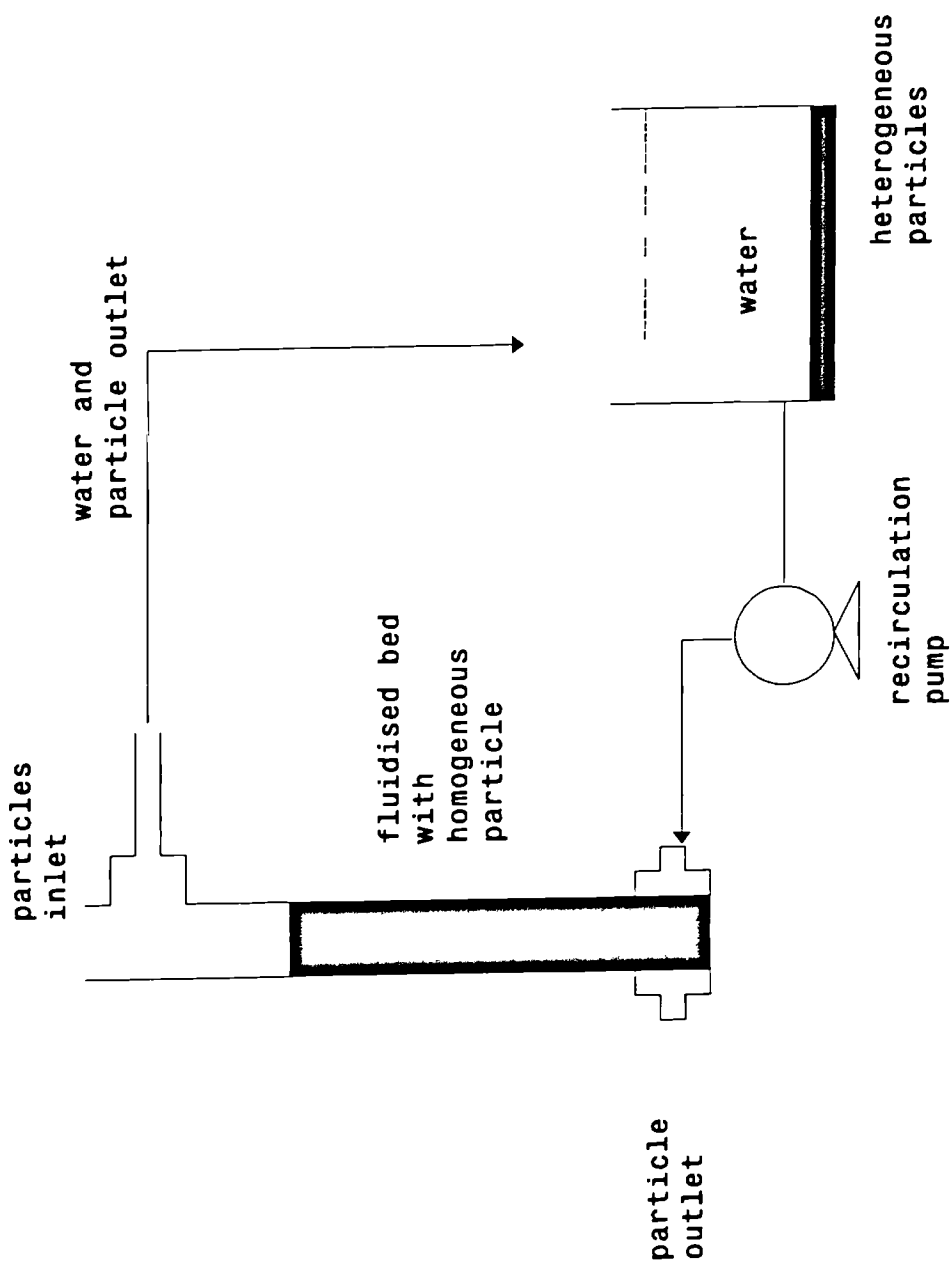


Fig. 6.3 Particles classification system

CHAPTER 7

CONCLUSIONS AND RECOMMENDATIONS

7.1 CONCLUSIONS

Experimental studies with an absorption system for cold storage.

The experimental work performed with the ammonia-water absorption prototype installed at the Cerro Prieto geothermal field for cold storage has shown that the ammonia-water absorption refrigerant system has a good performance for long periods. It can operate with a minimum of control, under very high ambient temperatures.

The use of ammonia-water absorption refrigeration based on low grade geothermal heat is highly attractive both from the economic and technical point of view for the enormous quantity of unused geothermal resources in Mexico. The technical and economic advantages of the absorption system are as follows.

Technical

- (a) This system can be designed and constructed in countries like Mexico and others in Central America because of its relatively simple technology.
- (b) Absorption systems are highly reliable and simple to maintain. Ammonia-water systems use carbon steel as the main construction material. As has been shown in the experimental equipment, agricultural grade ammonia with sodium dichromate corrosion inhibitor is a satisfactory working fluid when used with distilled water. attention should be given to purging air from the system to avoid the formation of solid corrosion products.

- (c) These systems use a working fluid that can be released to the atmosphere without causing damage to the ozone layer unlike CFC's.

Economic

- (a) The cost of the low grade geothermal energy is negligible when used in absorption systems.
- (b) The large amounts of geothermal fields in Mexico and Central America near important agricultural areas make these systems very promising and potentially profitable.

The experimental data obtained will be added to the data base and will be used to improve the design and operation of the system and will provide an excellent basis for the design of large scale heat driven absorption refrigeration systems. These data will be particularly useful in regions with high ambient temperatures (40 to 50 °C) and low grade heat sources.

Experimental studies with an absorption system for an ice making machine

Ammonia-water absorption systems behave very well when coupled to intermittent ice production units. The absorption process recovers very quickly from the upset caused by the admission of the hot vapour to the evaporator directly from the rectifier.

During the experimental work with the ice-generator prototypes, it was observed that driving liquid refrigerant into the accumulator tank involves many heat losses. It was also proved that the absorption system has a high coefficient of performance with the vertical tube ice-generator.

An economic evaluation was based on two kinds of equipment: an absorption system and a mechanical vapour compression system. The operation of an absorption plant *with an* average pay back period of three years for the additional investment would be highly profitable, considering the high demand for ice and the scarce supply of electricity during the summer in Mexicali.

Experimental studies with an absorption system using a fluidised bed heat exchanger.

The use of liquid fluidised bed heat exchangers with waste geothermal brine, supersaturated in silica, needs further development. At present it has been shown that with the degree of supersaturation in the Cerro Prieto brine, the use of small silica particles as a bed material is not feasible.

7.2 RECOMMENDATIONS

The ammonia-water absorption system is highly reliable and not subject to the danger of crystallization as are those which use lithium bromide as an absorbent. However the ammonia-water system uses a rectifier and rectification column, *making the system more* complicated than water-lithium bromide systems. Additives to the absorption solution or an alternative absorbent would make it possible to dispense with the rectification system. Future work will be necessary in the development of the absorption system controls and to reduce the amount of equipment in order to minimize the costs in operation and investment.

It is necessary to test a commercial ice-generator with the absorption system. The present prototype has many limitations in the amount of labour necessary to produce the ice.

In future work it will be necessary to have a sufficiently big pipeline diameter to minimize the pressure drop between the separation system and the heat exchanger. It is also necessary to have a well insulated pipeline.

It is necessary to modify the liquid fluidised bed heat exchanger design in order to recirculate particles inside the tube.

It is necessary to evaluate the liquid fluidised bed heat exchanger using particles that do not grow in the brine.

APPENDIX 1

Nomenclature for Tables A1.1 TO A1.10 AND A1.18 TO A1.22

T1	geothermal fluid entering generator	[°C]
T2	geothermal fluid leaving generator	[°C]
T3	strong refrigerant solution entering generator	[°C]
T4	two-phase mixture leaving generator	[°C]
T5	solution-vapor mixture entering absorber (after mixer)	[°C]
T6	solution leaving absorber	[°C]
T7	refrigerant vapor entering condenser	[°C]
T8	refrigerant leaving condenser	[°C]
T9	refrigerant entering evaporator	[°C]
T10	refrigerant leaving evaporator	[°C]
T11	rold storage	[°C]
T12	rmbient	[°C]
T13	refrigerant vapor entering mixer	[°C]
T14	weak refrigerant solution entering mixer	[°C]
T15	weak refrigerant solution leaving economizer	[°C]
T16	weak refrigerant solution entering economizer	[°C]
T17	strong refrigerant solution entering economizer	[°C]
T18	strong refrigerant solution entering economizer	[°C]
T19	liquid refrigerant entering precooler	[°C]
T20	liquid refrigerant leaving precooler	[°C]
T21	refrigerant vapor entering precooler	[°C]
T22	refrigerant vapor leaving precooler	[°C]
T23	two-phase mixture entering separator-rectifier	[°C]
T24	refrigerant vapor leaving separator-rectifier	[°C]
T25	weak refrigerant solution leaving separator-rectifier	[°C]
T26	cooling water entering separator-rectifier	[°C]
T27	cooling water leaving separator-rectifier	[°C]
T28	cooling water entering condenser	[°C]
T29	cooling water leaving condenser	[°C]
T30	cooling water entering absorber	[°C]
T31	cooling water leaving absorber	[°C]
T32	cooling Water	[°C]
Pv1	geothermal steam pressure	[bar]
Pv2	generator pressure, shell side	[bar]
P1	rectifier pressure	[bar]
P2	weak solution accumulator pressure	[bar]
P3	condenser pressure	[bar]
P4	refrigerant leaving condenser pressure	[bar]
P5	weak solution entering to mixer pressure	[bar]
P6	strong solution pressure	[bar]
P7	refrigerant entering evaporator pressure	[bar]
P8	refrigerant leaving evaporator pressure	[bar]
Fs1	weak refrigerant solution flow rate	[m ³ s ⁻¹ (10 ⁻³)]
Fr1	liquid refrigerant flow rate	[m ³ s ⁻¹ (10 ⁻³)]
Fw2	cooling water flow rate to rectifier	[m ³ s ⁻¹ (10 ⁻³)]
Fw3	cooling water flow rate to condenser	[m ³ s ⁻¹ (10 ⁻³)]
Fw1	cooling water flow rate to absorber	[m ³ s ⁻¹ (10 ⁻³)]

Table A1.4 Raw experimental data.
August 30, 1990

Time	T1	T2	T3	T4	T5	T6	T7	T8	T9	T10	T11	T12	T13	T14	T15	T16
08:30	141.1	125.0	88.6	119.5	50.2	42.5	111.2	30.2	-11.3	12.9	11.9	31.4	21.8	42.2	70.4	122.8
09:00	140.2	123.8	89.3	118.8	49.6	41.9	110.3	31.2	-12.2	4.8	4.3	32.6	15.6	43.4	71.4	121.4
09:30	140.4	123.0	87.6	118.6	49.7	42.5	83.3	31.4	-12.9	0.4	-0.3	34.4	11.3	43.7	71.0	120.4
10:00	139.4	122.3	87.4	117.8	50.4	42.9	80.3	31.6	-13.3	-4.6	-5.0	33.0	11.6	44.1	71.1	117.8
10:30	14.6	123.2	87.5	118.4	50.4	42.8	79.9	32.2	-13.3	-9.5	-8.7	36.1	5.8	44.1	70.9	117.8
11:00	141.1	123.4	88.0	119.0	51.0	43.8	82.2	33.4	-12.3	-10.8	-8.9	36.9	-6.2	45.6	71.7	119.1
11:30	140.6	122.8	88.7	118.0	50.0	44.3	82.7	35.4	-8.5	-8.1	-6.3	38.3	-6.4	46.7	71.2	117.6
12:00	140.3	123.7	87.5	118.6	51.4	44.1	83.6	35.2	-10.0	-8.6	-6.8	38.7	-4.0	46.3	74.6	117.6
Avg.	124.7	123.4	88.1	118.6	50.3	43.1	89.2	32.6	-11.7	-2.9	-2.5	35.2	6.2	44.5	71.5	119.3
Std.	41.6	0.8	0.7	0.5	0.6	0.8	12.5	1.8	1.6	7.8	6.9	2.6	10.0	1.4	1.2	1.9

Table A1.4 (continued)

Time	T17	T18	T19	T20	T21	T22	T23	T24	T25	T26	T27	T28	T29	T30	T31	T32
08:30	41.8	90.4	30.6	24.0	16.1	20.6	123.8	115.6	125.1	33.2	33.6	30.2	35.1	29.8	31.4	31.1
09:00	42.4	89.9	31.1	21.8	7.9	13.3	121.8	111.9	124.9	33.6	35.2	30.2	35.2	29.7	31.2	31.2
09:30	42.6	88.8	31.4	20.1	3.6	9.4	122.8	89.2	121.7	31.3	35.4	30.9	34.8	30.5	31.9	30.9
10:00	43.3	87.8	31.6	20.1	-0.4	7.7	121.1	83.7	120.8	31.2	35.4	30.9	34.9	30.5	32.2	30.9
10:30	43.0	87.2	31.8	18.0	7.2	0.9	121.6	84.3	120.6	31.5	35.7	31.1	35.6	30.8	32.6	31.1
11:00	43.8	88.5	33.3	9.5	-9.9	-6.8	122.7	90.2	121.2	33.1	37.5	32.9	37.5	32.9	34.5	33.0
11:30	44.0	87.1	35.2	3.6	-8.0	-6.5	120.0	87.1	119.1	34.3	38.8	34.2	39.6	33.9	35.6	34.1
12:00	44.3	95.3	35.1	18.2	-8.3	-7.7	126.0	132.0	124.0	34.3	38.4	34.1	38.9	34.0	35.5	34.1
Avg.	43.1	89.4	32.5	16.9	1.0	3.9	122.5	99.3	122.2	32.8	36.3	31.8	36.5	31.5	33.1	32.0
Std.	0.8	2.5	1.7	6.4	8.7	9.9	1.7	16.9	2.1	1.2	1.7	1.6	1.8	1.7	1.7	1.4

Table A1.4 (continued)

Time	PV1	PV2	P1	P2	P3	P4	P5	P6	P7	P8	Fr1	Fs1	Fw1	Fw2	Fw3
08:30	7.372	2.986	14.8	14.8	14.8	14.8	5.129	2.274	2.274	2.274	0.013	0.095	1.041	0.126	1.041
09:00	7.372	2.986	15.3	15.3	15.3	15.3	5.537	2.274	2.274	2.274	0.013	0.095	1.041	0.126	1.041
09:30	7.372	2.914	15.3	15.3	15.3	15.3	5.639	2.478	2.478	2.478	0.009	0.095	1.041	0.221	0.946
10:00	7.372	2.914	15.3	15.3	15.3	15.3	5.843	2.682	2.682	2.682	0.009	0.095	0.978	0.284	0.946
10:30	7.372	2.914	15.3	15.3	15.3	15.3	5.843	2.682	2.682	2.682	0.009	0.095	0.946	0.315	0.946
11:00	7.576	2.914	15.6	15.6	15.6	15.6	6.047	2.886	2.886	2.886	0.011	0.095	1.009	0.284	0.915
11:30	7.576	2.771	16.7	16.7	16.7	16.7	6.557	3.294	3.294	3.294	0.014	0.095	1.009	0.284	0.915
12:00	7.576	2.843	16.7	16.7	16.7	16.7	6.557	3.090	3.090	3.090	0.006	0.095	1.009	0.284	0.915
Avg.	7.449	2.905	15.6	15.6	15.6	15.6	5.894	2.707	2.707	2.707	0.011	0.095	1.009	0.241	0.958
Std.	0.099	0.066	0.6	0.6	0.6	0.6	0.459	0.345	0.345	0.345	0.002	0.000	0.032	0.070	0.050

Table A1.11 Experimental data and result of REFRI programme
September 10, 1991

Test Date	-	09/10/91	
Experimental data:		Thermodynamic results:	
absorption temperature (°C)	35.1	actual Coefficient of Performance (COP)	0.29
absorption pressure (bar)	3.1	Carnot for cooling (COP)	-0.18
strong solution concentration	43.16%	enthalpy based for cooling (COP)	9.28
weak solution concentration	30.53%		
solution flow (m ³ s ⁻¹)	6.94E-05	flow ratio (FR)	10.78
refrigerant flow (m ³ s ⁻¹)	8.83E-06	actual flow ratio (FRA)	3.98
evaporation temperature (°C)	-8.7		
evaporation pressure (bar)	3.1	recuperator efficiency (NREC)	0.69
evaporator liq. conc.	94.65%	generator efficiency (NGE)	1.10
evaporator vap. conc.	99.83%		
condenser temperature (°C)	25.0	heat balances	
condenser pressure (bar)	12.7	evaporator duty (kW)	8.01
rectification temperature (°C)	110.0		
generation temperature (°C)	119.1	generator exit quality	0.08

Table A1.12 Experimental data and result of REFRI programme
September 11, 1991

Test Date	-	09/11/91	
Experimental data:		Thermodynamic results:	
absorption temperature (°C)	30.6	actual Coefficient of Performance (COP)	0.30
absorption pressure (bar)	2.6	Carnot for cooling (COP)	-3.98
strong solution concentration	42.88%	enthalpy based for cooling (COP)	1.95
weak solution concentration	24.51%		
solution flow (m ³ /s)	1.07E-04	flow ratio (FR)	12.66
refrigerant flow (m ³ /s)	8.83E-06	actual flow ratio (FRA)	1.12
evaporation temperature (°C)	26.8		
evaporation pressure (bar)	2.6	recuperator efficiency (NREC)	0.68
evaporator liq. conc.	45.06%	generator efficiency (NGE)	0.97
evaporator vap. conc.	43.10%		
condenser temperature (°C)	21.8	heat balances	
condenser pressure (bar)	11.9	evaporator duty (kW)	11.97
rectification temperature (°C)	123.5		
generation temperature (°C)	118.6	generator exit quality	0.07

Table A1.13 Experimental data and result of REFRI programme
October 31, 1991

Test Date	10/31/91		
Experimental data:	Thermodynamic results:		
absorption temperature (°C)	32.3	actual Coefficient of Performance (COP)	0.66
absorption pressure (bar)	2.6	Carnot for cooling (COP)	-11.99
strong solution concentration	41.91%	enthalpy based for cooling (COP)	1.35
weak solution concentration	34.73%		
solution flow (m³/s)	1.28E-04	flow ratio (FR)	13.14
refrigerant flow (m³/s)	9.88E-06	actual flow ratio (FRA)	1.37
evaporation temperature (°C)	17.4		
evaporation pressure (bar)	2.6	recuperator efficiency (NREC)	0.67
evaporator liq. conc.	50.86%	generator efficiency (NGE)	0.46
evaporator vap. conc.	80.85%		
condenser temperature (°C)	16.3	heat balances	
condenser pressure (bar)	10.7	evaporator duty (kW)	13.16
rectification temperature (°C)	130.4		
generation temperature (°C)	132.7	generator exit quality	0.07

Table A1.14 Experimental data and result of REFRI programme
November 1, 1991

Test Date	11/01/91		
Experimental data:	Thermodynamic results:		
absorption temperature (°C)	29.9	actual Coefficient of Performance (COP)	0.36
absorption pressure (bar)	2.5	Carnot for cooling (COP)	8.68
strong solution concentration	42.73%	enthalpy based for cooling (COP)	1.90
weak solution concentration	22.45%		
solution flow (m³/s)	1.26E-04	flow ratio (FR)	13.03
refrigerant flow (m³/s)	1.04E-05	actual flow ratio (FRA)	1.29
evaporation temperature (°C)	17.0		
evaporation pressure (bar)	2.5	recuperator efficiency (NREC)	0.69
evaporator liq. conc.	50.49%	generator efficiency (NGE)	0.78
evaporator vap. conc.	80.84%		
condenser temperature (°C)	18.6	heat balances	
condenser pressure (bar)	10.2	evaporator duty (kW)	13.79
rectification temperature (°C)	134.9		
generation temperature (°C)	134.8	generator exit quality	0.07

Table A1.15 Experimental data and result of REFRI programme
November 19, 1991

Test Date	11/19/91		
Experimental data:		Thermodynamic results:	
absorption temperature (°C)	28.7	actual Coefficient of Performance (COP)	0.46
absorption pressure (bar)	2.2	Carnot for cooling (COP)	-8.32
strong solution concentration	41.32%	enthalpy based for cooling (COP)	2.64
weak solution concentration	15.47%		
solution flow (m³/s)	6.31E-05	flow ratio (FR)	5.43
refrigerant flow (m³/s)	1.26E-05	actual flow ratio (FRA)	1.21
evaporation temperature (°C)	19.7		
evaporation pressure (bar)	2.2	recuperator efficiency (NREC)	0.71
evaporator liq. conc.	46.67%	generator efficiency (NGE)	0.98
evaporator vap. conc.	63.03%	heat balances	
condenser temperature (°C)	17.8	evaporator duty (kW)	17.01
condenser pressure (bar)	9.8		
rectification temperature (°C)	129.5	generator exit quality	0.16
generation temperature (°C)	132.7		

Table A1.16 Experimental data and result of REFRI programme
November 20, 1991

Test Date	11/20/91		
Experimental data:		Thermodynamic results:	
absorption temperature (°C)	37.2	actual Coefficient of Performance (COP)	0.48
absorption pressure (bar)	2.0	Carnot for cooling (COP)	4.55
strong solution concentration	39.76%	enthalpy based for cooling (COP)	2.94
weak solution concentration	18.01%		
solution flow (m³/s)	6.26E-05	flow ratio (FR)	5.40
refrigerant flow (m³/s)	1.26E-05	actual flow ratio (FRA)	1.42
evaporation temperature (°C)	21.8	recuperator efficiency (NREC)	0.74
evaporation pressure (bar)	2.0	generator efficiency (NGE)	0.96
evaporator liq. conc.	48.66%	heat balances	
evaporator vap. conc.	69.50%	evaporator duty (kW)	16.77
condenser temperature (°C)	25.3		
condenser pressure (bar)	12.5	Generator exit quality	0.16
rectification temperature (°C)	140.3		
generation temperature (°C)	137.3		

Table A1.17 Experimental data and result of REFRI programme
March 26, 1992

Test Date	03/26/92		
Experimental data:		Thermodynamic results:	
absorption temperature (°C)	30.1	actual Coefficient of Performance (COP)	0.20
absorption pressure (bar)	2.3	Carnot for cooling (COP)	-0.09
strong solution concentration	41.11%	enthalpy based for cooling (COP)	1.07
weak solution concentration	30.36%		
solution flow (m ³ /s)	1.26E-04	flow ratio (FR)	23.26
refrigerant flow (m ³ /s)	6.31E-06	actual flow ratio (FRA)	-1.03
evaporation temperature (°C)	-6.0	recuperator efficiency (NREC)	0.57
evaporation pressure (bar)	2.3	generator efficiency (NGE)	3.00
evaporator liq. conc.	71.25%	heat balances	
evaporator vap. conc.	98.48%	evaporator duty (kW)	7.52
condenser temperature (°C)	22.7		
condenser pressure (bar)	9.5	generator exit quality	0.04
rectification temperature (°C)	59.8		
generation temperature (°C)	51.5		

Table A1.18 Raw experimental data
October 31, 1991

Time	8:55	09:20	09:40	AVG.	STD.
T1	146.0	146.4	148.2	146.9	1.0
T2	135.4	132.4	135.4	134.4	1.4
T3	85.5	82.6	91.0	86.4	3.5
T4	132.6	132.1	133.5	132.7	0.6
T5	48.1	55.5	48.8	50.8	3.3
T6	31.8	33.0	32.1	32.3	0.5
T7	95.6	95.6	98.1	96.4	1.2
T8	15.8	16.3	16.9	16.3	0.4
T9	17.2	17.4	17.7	17.4	0.2
T10	17.4	17.6	18.0	17.7	0.2
T11	19.6	19.3	19.2	19.4	0.2
T12	16.4	17.1	17.4	17.0	0.4
T13	0.2	3.8	6.2	3.4	2.5
T14	34.6	33.6	35.8	34.7	0.9
T15	64.7	62.1	67.1	64.6	2.0
T16	126.2	121.8	128.2	125.4	2.7
T17	31.4	33.7	32.3	32.5	0.9
T18	87.3	82.8	91.3	87.1	3.5
T19	15.7	16.3	16.9	16.3	0.5
T20	7.0	8.8	6.7	7.5	0.9
T21	5.8	4.3	1.6	3.9	1.7
T22	0.9	5.7	5.1	3.9	2.1
T23	131.4	131.3	133.6	132.1	1.1
T24	129.0	129.1	133.0	130.4	1.9
T25	129.9	15.2	132.1	92.4	54.6
T26	16.3	32.1	17.2	21.9	7.2
T27	31.4	16.4	33.0	26.9	7.5
T28	16.9	16.4	16.8	16.7	0.2
T29	21.8	22.2	22.7	22.2	0.4
T30	18.0	16.4	16.8	17.1	0.7
T31	18.0	18.6	18.9	18.5	0.4
T32	31.0	22.3	22.7	25.3	4.0
PV1	6.0	6.0	6.0	6.0	0.0
PV2	4.4	4.4	4.5	4.4	0.0
P1	10.5	10.7	10.7	10.6	0.1
P2	10.5	10.7	10.8	10.6	0.1
P3	10.5	10.8	10.8	10.7	0.1
P4	10.5	10.7	10.8	10.6	0.1
P5	2.6	2.6	2.6	2.6	0.0
P6	2.6	2.6	2.6	2.6	0.0
P7	1.9	2.3	2.4	2.2	0.2
P8	2.1	2.1	2.2	2.2	0.0
FR1	9.5E-06	1.1E-05	9.5E-06	9.9E-06	5.9E-07
FS1	1.3E-04	1.3E-04	1.3E-04	1.3E-04	3.0E-06
FW1	6.9E-04	6.9E-04	6.9E-04	6.9E-04	0.0E+00
FW2	1.3E-03	1.3E-03	1.3E-03	1.3E-03	0.0E+00
FW3	2.5E-04	2.5E-04	2.5E-04	2.5E-04	0.0E+00

Table A1.19 Raw experimental data
November 1, 1991

Time	08:10	08:30	08:50	09:10	09:30	09:50	10:10	Avg.	Std.
T1	144.5	148.8	152.2	149.3	150.3	149.9	149.8	149.3	2.2
T2	127.9	137.8	145.5	139.2	140.6	139.8	139.2	138.6	4.9
T3	90.4	92.4	109.3	94.5	97.3	95.9	92.9	96.1	5.8
T4	129.9	134.5	137.6	135.4	136.0	134.5	135.4	134.8	2.2
T5	44.3	48.6	55.4	55.6	57.2	55.1	53.4	52.8	4.3
T6	25.9	31.3	28.5	29.9	32.2	30.3	31.1	29.9	2.0
T7	93.4	102.8	116.4	105.4	106.4	105.9	103.8	104.9	6.3
T8	16.0	16.7	18.6	19.2	19.4	19.9	20.2	18.6	1.5
T9	15.4	16.1	16.7	17.2	17.5	18.0	18.4	17.0	1.0
T10	15.7	16.0	16.4	16.9	17.3	17.6	17.8	16.8	0.7
T11	18.4	19.1	19.2	19.0	19.1	19.2	19.2	19.0	0.3
T12	15.9	16.4	17.0	17.6	18.1	18.6	19.4	17.6	1.1
T13	0.1	3.9	0.8	4.2	4.8	4.6	5.4	3.4	1.9
T14	29.0	33.3	35.4	35.1	36.5	36.6	21.9	32.5	5.0
T15	53.6	66.2	76.7	66.1	67.8	67.0	64.8	66.0	6.3
T16	123.1	127.9	133.6	134.1	134.6	134.3	133.3	131.6	4.1
T17	26.2	31.1	32.6	30.4	31.9	30.9	32.9	30.9	2.1
T18	70.2	93.4	111.2	98.6	100.3	97.1	93.8	94.9	11.5
T19	15.6	16.6	18.3	19.9	19.3	19.9	20.4	18.6	1.7
T20	7.9	7.6	6.5	9.7	10.2	11.5	11.1	9.2	1.8
T21	0.3	-2.1	-5.6	-0.6	-0.4	9.2	1.2	0.3	4.2
T22	0.8	3.1	5.5	3.3	3.9	4.9	4.8	3.8	1.5
T23	124.6	135.3	143.4	136.0	138.0	137.7	136.9	136.0	5.2
T24	123.0	134.0	141.0	136.0	137.0	137.0	136.0	134.9	5.2
T25	123.8	133.6	140.6	136.0	19.6	136.4	135.6	117.9	40.4
T26	15.5	16.8	18.6	19.3	28.0	20.0	20.1	19.8	3.7
T27	28.0	28.0	28.1	27.3	19.3	27.1	26.9	26.4	2.9
T28	15.3	16.6	19.4	19.2	25.3	19.8	19.9	19.4	2.9
T29	21.7	23.5	24.8	25.1	19.2	25.7	25.8	23.7	2.3
T30	15.3	16.6	18.3	19.1	21.2	19.6	19.8	18.6	1.9
T31	16.8	18.7	20.4	20.9	21.2	21.7	21.7	20.2	1.7
T32	22.0	25.6	25.1	25.1	25.4	25.7	25.8	25.0	1.2
PV1	6.0	6.6	6.3	6.3	6.3	6.3	6.3	6.3	0.2
PV2	4.3	4.9	4.7	4.6	4.4	4.4	4.4	4.5	0.2
P1	9.9	10.5	9.8	10.3	10.3	10.3	10.3	10.2	0.2
P2	9.9	10.5	9.8	10.3	10.3	10.3	10.3	10.2	0.2
P3	9.9	10.5	9.8	10.3	10.3	10.3	10.3	10.2	0.2
P4	9.9	10.5	9.8	10.3	10.3	10.3	10.3	10.2	0.2
P5	2.2	2.4	2.6	2.6	2.6	2.6	2.6	2.5	0.1
P6	2.2	2.4	2.6	2.6	2.6	2.6	2.6	2.5	0.1
P7	2.0	2.7	1.9	2.0	1.7	1.5	1.4	1.9	0.4
P8	1.9	2.4	1.9	1.9	1.7	1.5	1.4	1.8	0.3
FR1	1.3E-05	1.3E-05	9.5E-06	9.5E-06	9.5E-06	9.5E-06	9.5E-06	1.0E-05	1.4E-06
FS1	1.3E-04	0.0E+00							
FW1	6.9E-04	1.3E-03	1.3E-03	1.3E-03	1.3E-03	1.3E-03	1.3E-03	1.2E-03	2.2E-04
FW2	1.3E-03	6.9E-04	6.9E-04	6.9E-04	6.9E-04	6.9E-04	6.9E-04	7.8E-04	2.2E-04
FW3	2.5E-04	0.0E+00							

Table A1.20 Raw experimental data
November 19, 1991

Time	hh:mm	10:10	10:55	11:10	Avg.	Std.
T1	°C	145.2	148.0	146.6	146.6	1.1
T2	°C	135.1	140.0	137.6	137.6	2.0
T3	°C	84.0	101.2	92.6	92.6	7.0
T4	°C	130.9	134.5	132.7	132.7	1.5
T5	°C	38.5	39.8	39.2	39.2	0.5
T6	°C	28.5	28.9	28.7	28.7	0.2
T7	°C	104.0	112.7	108.4	108.4	3.6
T8	°C	17.8	17.8	17.8	17.8	0.0
T9	°C	19.5	19.8	19.7	19.7	0.1
T10	°C	13.4	14.3	13.9	13.9	0.4
T11	°C	20.3	20.4	20.4	20.4	0.0
T12	°C	19.1	19.9	19.5	19.5	0.3
T13	°C	0.8	-5.1	-2.2	-2.2	2.4
T14	°C	26.5	28.3	27.4	27.4	0.7
T15	°C	59.3	67.9	63.6	63.6	3.5
T16	°C	127.3	129.4	128.4	128.4	0.9
T17	°C	27.8	30.2	29.0	29.0	1.0
T18	°C	94.9	104.8	99.9	99.9	4.0
T19	°C	18.2	18.4	18.3	18.3	0.1
T20	°C	9.8	10.8	10.3	10.3	0.4
T21	°C	0.3	5.0	2.7	2.7	1.9
T22	°C	1.7	-1.4	0.2	0.2	1.3
T23	°C	141.6	139.7	140.7	140.7	0.8
T24	°C	129.4	129.6	129.5	129.5	0.1
T25	°C	133.5	135.4	134.5	134.5	0.8
T26	°C	17.1	17.7	17.4	17.4	0.2
T27	°C	22.3	22.6	22.5	22.5	0.1
T28	°C	16.8	17.4	17.1	17.1	0.2
T29	°C	22.9	23.6	23.3	23.3	0.3
T30	°C	16.7	17.4	17.1	17.1	0.3
T31	°C	18.4	19.3	18.9	18.9	0.4
T32	°C	22.9	22.9	22.9	22.9	0.0
PV1	bar	5.9	5.9	5.9	5.9	0.0
PV2	bar	4.4	4.4	4.4	4.4	0.0
P1	bar	9.7	9.7	9.7	9.7	0.0
P2	bar	9.7	9.7	9.7	9.7	0.0
P3	bar	9.8	9.8	9.8	9.8	0.0
P4	bar	9.8	9.8	9.8	9.8	0.0
P5	bar	2.2	2.2	2.2	2.2	0.0
P6	bar	2.2	2.2	2.2	2.2	0.0
P7	bar	1.7	1.7	1.7	1.7	0.0
P8	bar	1.7	1.7	1.7	1.7	0.0
FR1	kg/s	1.3E-05	1.3E-05	1.3E-05	1.3E-05	0.0E+00
FS1	kg/s	6.3E-05	6.3E-05	6.3E-05	6.3E-05	0.0E+00
FW1	kg/s	1.2E-03	1.2E-03	1.2E-03	1.2E-03	0.0E+00
FW2	kg/s	4.4E-04	4.4E-04	4.4E-04	4.4E-04	0.0E+00
FW3	kg/s	2.5E-04	2.5E-04	2.5E-04	2.5E-04	0.0E+00

**Table A1.21 Raw experimental data
November 20, 1991**

Time hh:mm	T1 °C	T2 °C	T3 °C	T4 °C	T5 °C	T6 °C	T7 °C
9:00	147.3	135.6	104.4	132.2	39.7	31.7	107.3
9:30	150.4	144.3	98.9	135.1	43.3	32.9	116.6
10:00	150.3	144.0	87.8	135.2	42.4	32.9	109.4
10:30	152.2	147.0	102.1	137.7	43.9	34.2	120.9
11:00	154.8	152.3	68.4	139.8	41.2	33.7	105.2
11:30	146.6	134.9	73.7	137.3	43.6	35.2	102.4
12:00	152.6	147.6	112.3	138.5	47.8	36.4	120.3
12:30	152.6	147.6	112.3	138.5	47.8	36.4	120.3
13:00	150.6	143.1	94.2	136.6	45.9	37.3	110.3
13:30	152.5	147.8	112.8	137.0	48.9	37.6	117.8
14:00	149.4	137.0	84.8	135.9	48.6	39.0	113.0
14:30	152.6	146.4	104.3	138.4	48.3	38.8	118.4
15:00	154.9	151.4	118.0	140.6	51.6	40.4	120.6
15:30	149.3	137.6	82.1	135.1	50.2	42.4	111.6
16:00	154.3	150.2	109.6	140.2	49.4	40.0	122.8
16:30	151.9	144.9	116.1	137.8	48.2	39.6	115.0
17:00	152.0	146.0	95.9	137.6	46.1	39.1	118.7
17:30	150.6	142.0	85.1	136.2	47.0	40.6	108.3
18:00	156.6	153.9	111.1	141.7	47.3	36.3	121.0
18:30	153.4	149.2	98.0	138.3	44.4	34.8	121.8
19:00	150.0	143.1	83.1	135.2	44.6	35.6	115.2
19:30	153.3	148.9	106.1	138.6	47.1	37.7	122.2
20:00	152.1	146.2	103.3	137.6	47.9	38.6	117.8
20:30	152.1	144.9	94.9	137.6	47.7	39.4	115.2
21:00	148.7	136.9	78.6	134.0	45.9	38.7	107.0
Avg.	151.6	144.9	97.5	137.3	46.4	37.2	115.2
Std.	2.3	5.1	13.6	2.1	2.8	2.7	5.8

**Table A1.21 Raw experimental data
November 20, 1991 (continued..)**

Time hh:mm	T8 °C	T9 °C	T10 °C	T11 °C	T12 °C	T13 °C	T14 °C	T15 °C	T16 °C
9:00	19.9	15.8	15.3	9.0	17.4	3.4	32.8	69.2	129.8
9:30	20.7	17.7	13.3	19.2	18.6	-4.4	29.4	68.6	127.7
10:00	20.5	18.7	13.9	19.8	19.6	-3.6	27.0	60.6	120.7
10:30	22.6	19.6	15.5	20.4	20.6	-3.0	30.6	60.6	127.8
11:00	23.1	20.3	16.7	21.1	21.5	-1.6	28.1	65.5	125.2
11:30	24.1	20.7	18.4	20.1	21.2	-4.8	28.4	57.8	124.8
12:00	24.7	20.9	17.2	21.6	21.8	-2.2	35.6	78.1	134.2
12:30	24.7	20.9	17.2	21.6	21.8	-2.2	35.6	78.1	134.2
13:00	26.1	21.9	20.3	22.5	22.6	-3.9	33.7	76.8	133.7
13:30	26.6	32.4	21.6	23.0	23.1	-0.4	37.5	81.7	136.7
14:00	26.8	22.9	22.5	23.3	23.4	4.1	34.8	65.0	135.0
14:30	18.1	23.1	22.8	23.4	23.1	1.6	36.1	72.0	134.6
15:00	29.6	23.7	23.4	23.8	23.7	-1.2	42.9	88.2	136.9
15:30	30.2	24.1	23.9	24.1	23.4	-3.8	37.3	62.0	134.5
16:00	28.6	23.8	23.7	23.8	22.9	-0.8	41.8	79.7	126.7
16:30	29.9	23.9	23.7	23.7	22.7	-5.2	39.9	77.7	136.9
17:00	29.4	23.7	23.6	23.4	21.3	-5.7	33.9	67.7	129.4
17:30	29.6	23.5	23.6	23.3	21.2	-2.4	33.2	50.9	131.3
18:00	26.0	23.2	23.4	23.3	20.9	-0.9	30.7	79.9	129.6
18:30	24.2	22.2	22.6	22.6	20.1	-1.5	26.9	61.0	131.2
19:00	23.6	21.6	21.7	21.9	19.7	-1.7	26.4	53.2	131.2
19:30	24.1	20.7	21.0	21.1	18.2	-7.3	31.2	4.9	132.6
20:00	26.1	20.6	20.8	20.7	17.3	-8.8	35.2	73.1	135.9
20:30	27.2	20.6	21.0	20.6	17.3	-3.6	33.2	76.5	133.6
21:00	27.0	19.4	20.1	19.5	15.2	-1.8	31.8	57.9	129.6
Avg.	25.3	21.8	20.3	21.5	20.7	-2.5	33.4	66.7	131.4
Std.	3.3	3.0	3.3	2.9	2.3	2.9	4.4	15.8	4.1

Table A1.21 Raw experimental data
November 20, 1991 (continued..)

Time hh:mm	T17 °C	T18 °C	T19 °C	T20 °C	T21 °C	T22 °C	T23 °C	T24 °C
9:00	28.6	103.6	19.2	3.8	-3.4	-2.3	131.4	131.0
9:30	32.0	104.4	20.7	8.6	6.7	1.2	144.9	139.3
10:00	34.8	94.4	20.8	10.7	10.5	-3.6	143.5	142.0
10:30	34.7	104.0	22.0	10.1	-5.3	-6.6	144.7	140.3
11:00	50.0	102.5	22.7	9.3	-8.3	-3.1	153.2	135.6
11:30	36.4	89.2	23.5	-3.9	14.7	-6.1	143.2	141.3
12:00	36.7	113.9	24.3	-6.1	-7.2	-1.7	146.7	143.0
12:30	36.7	113.9	24.3	-6.1	-7.2	-1.7	146.7	143.3
13:00	37.7	97.2	25.6	-8.2	-6.2	-2.5	142.4	142.0
13:30	37.9	119.1	26.4	-6.4	-9.7	-1.0	148.0	142.3
14:00	37.3	89.9	26.2	-7.9	-5.2	-3.6	140.7	138.2
14:30	39.5	104.8	27.6	-7.4	-8.6	0.4	146.3	143.2
15:00	40.3	118.9	28.6	8.1	-8.4	-0.6	148.2	146.2
15:30	41.8	83.3	28.9	3.2	-10.3	-2.4	140.3	138.2
16:00	38.0	101.3	28.1	9.7	-7.9	0.8	140.1	138.2
16:30	40.2	112.6	28.7	4.3	-11.5	-3.8	140.1	138.2
17:00	40.3	94.8	28.3	2.7	-10.2	-4.4	144.0	141.8
17:30	39.9	88.7	27.3	3.7	-10.4	-3.1	139.7	138.1
18:00	38.4	112.3	24.6	8.2	-6.1	-1.0	151.4	145.3
18:30	35.7	102.6	23.3	6.7	-7.7	-2.0	148.0	142.0
19:00	35.9	84.1	23.0	3.4	-10.1	-2.6	141.1	139.2
19:30	37.2	109.9	23.5	1.6	-13.2	-6.4	147.6	143.2
20:00	37.5	105.0	24.8	-0.1	-16.2	-7.9	144.8	142.2
20:30	38.4	98.6	24.7	1.9	-12.9	-4.1	144.0	141.2
21:00	37.9	78.9	24.8	3.9	-10.8	-1.6	135.3	133.0
AVG.	37.8	101.0	24.9	2.2	-6.6	-2.8	143.9	140.3
STD.	3.7	11.0	2.6	6.1	7.0	2.3	4.7	3.5

Table A1.21 Raw experimental data
November 20, 1991 (continued..)

Time hh:mm	T25 °C	T26 °C	T27 °C	T28 °C	T29 °C	T30 °C	T31 °C	T32 °C
9:00	131.3	18.8	35.2	18.4	25.6	18.4	20.3	25.6
9:30	138.3	20.4	34.5	20.1	26.3	20.1	21.7	26.3
10:00	137.3	20.6	34.6	20.3	26.2	20.2	21.7	26.2
10:30	140.4	21.6	35.4	21.4	28.0	21.2	22.7	28.0
11:00	131.8	22.1	36.3	21.9	24.9	21.8	22.9	24.9
11:30	134.0	22.0	36.0	21.9	29.8	21.8	23.5	29.8
12:00	142.3	23.6	35.6	23.3	29.5	23.2	25.1	29.5
12:30	142.3	23.6	34.6	23.3	29.5	23.2	25.1	29.5
13:00	138.9	24.8	34.6	24.7	31.7	24.5	26.1	31.7
13:30	141.7	25.1	34.5	24.7	30.3	24.0	26.7	30.3
14:00	136.7	25.4	35.3	25.3	33.1	25.1	27.0	33.1
14:30	142.2	26.9	35.7	26.6	33.7	26.4	27.9	33.7
15:00	144.4	28.0	36.8	27.6	33.7	27.3	29.1	33.7
15:30	134.9	28.7	35.3	28.4	36.1	28.1	29.8	28.2
16:00	141.6	27.6	35.6	27.5	35.2	27.4	29.4	27.4
16:30	139.3	27.9	35.8	27.8	34.4	27.6	29.1	27.6
17:00	141.2	27.8	36.1	27.6	35.8	27.5	28.7	27.5
17:30	136.8	27.1	25.6	26.8	31.5	26.6	27.7	26.6
18:00	143.4	23.7	28.9	23.3	27.6	23.3	24.7	23.3
18:30	141.7	22.6	25.9	22.2	28.7	22.2	23.5	22.2
19:00	138.1	22.9	25.6	22.7	31.5	22.7	24.0	22.7
19:30	142.2	23.7	35.2	23.7	30.3	23.7	25.1	23.7
20:00	141.2	24.9	26.5	24.8	32.2	24.7	26.3	24.7
20:30	139.8	25.2	26.1	25.1	32.3	25.0	26.3	25.0
21:00	133.2	25.6	26.1	25.6	33.9	25.4	26.6	25.4
AVG.	139.0	24.4	32.9	24.2	30.9	24.1	25.6	27.5
STD.	3.6	2.6	4.1	2.6	3.2	2.6	2.6	3.2

Nomenclature for Tables A1.23 TO A1.28

TFB1	Point 1 at fluidised bed HX see Fig. 6.1	°C
TFB2	Point 1 at fluidised bed HX see Fig. 6.1	°C
TFB3	Point 1 at fluidised bed HX see Fig. 6.1	°C
TFB4	Point 1 at fluidised bed HX see Fig. 6.1	°C
TFB5	Point 1 at fluidised bed HX see Fig. 6.1	°C
TFB6	Point 1 at fluidised bed HX see Fig. 6.1	°C
TFB7	Point 1 at fluidised bed HX see Fig. 6.1	°C
Twi	water entering to the fluidised bed HX	°C
Two	water leaving the fluidised bed HX	°C
Fb	brine flowing in fluidised bed HX	kg s ⁻¹
Fwr	water flowing in fluidised bed HX	kg s ⁻¹
Ps	separation system	bar
Pi	inlet of fluidised bed HX	bar
Po	outlet of the fluidised bed HX	bar

Table A1.23 Raw experimental data
February 25, 1992

HORA	TFB1	TFB2	TFB3	TFB4	TFB5	TFB6	TFB7
13:05	23.4	21.0	97.4	88.0	26.9	28.9	92.6
13:10	24.4	21.1	127.7	120.7	39.1	41.7	122.2
13:15	26.0	21.9	126.8	122.8	51.8	52.9	122.4
13:20	30.4	22.9	122.8	119.4	66.9	63.1	117.3
13:25	30.8	25.1	122.5	119.2	72.9	69.4	117.8
13:30	30.7	25.2	126.5	122.0	80.0	75.7	122.2
13:35	33.7	26.4	127.8	123.9	85.5	79.9	123.9
13:40	36.0	27.3	129.6	125.1	90.6	84.2	124.2
13:45	36.0	28.3	129.3	125.2	94.3	86.9	124.5
13:50	37.9	29.2	130.4	126.2	97.8	89.6	126.7
13:55	38.2	30.0	131.3	127.6	99.3	91.5	127.1
07:35	34.4	33.3	132.4	127.4	109.9	96.1	126.2

Table A1.24 Raw experimental data
February 27, 1992

Time	TFB1	TFB2	TFB3	TFB4	TFB5	TFB6	TFB7
13:09	24.2	23.4	53.2	24.6	22.4	23.7	28.3
13:15	25.4	24.5	74.8	56.5	28.6	29.4	62.5
13:30	28.3	26.8	75.7	65.4	41.3	41.9	69.2
13:35	29.5	27.6	80.6	73.2	45.6	45.4	75.3
13:40	30.2	28.3	98.4	89.8	52.7	51.8	92.7
13:45	32.3	29.1	110.6	103.1	60.5	58.9	105.1
14:00	36.6	30.9	116.7	111.3	84.1	78.3	110.7

Table A1.25 Raw experimental data
February 28, 1992

Time	TFB1	TFB2	TFB3	TFB4	TFB5	TFB6	TFB7
09:35	34.8	30.2	120.0	112.4	97.8	86.8	111.1
10:00	35.2	29.8	118.8	112.3	94.7	82.3	110.3
11:00	38.0	31.1	117.0	110.8	98.4	83.9	109.6
11:30	38.0	32.0	116.6	98.6	82.1	82.2	109.4
12:00	39.7	32.6	117.1	110.6	99.1	85.4	109.7
12:20	38.7	34.1	118.4	102.3	44.8	54.1	83.9
12:40	35.5	34.2	118.9	82.1	42.5	51.1	83.8
13:20	37.3	29.6	116.5	104.3	94.2	104.1	102.7
13:50	39.6	31.2	116.3	109.1	104.2	104.6	107.4

Table A1.26 Raw experimental data
March 4 and 5, 1992

Time	TFB1	TFB2	TFB3	TFB4	TFB5	TFB6	TFB7
14:10	40.3	35.8	129.3	112.6	110.7	116.6	114.5
14:20	43.2	36.1	130.0	115.2	107.3	116.7	114.7
14:30	36.9	36.2	128.1	112.1	108.2	116.6	114.0
07:35	32.2	36.6	91.6	70.1	72.7	77.6	71.9
08:05	34.2	34.1	109.1	84.3	90.2	93.3	87.7
08:35	33.7	33.9	110.8	90.9	93.3	98.6	94.2
09:05	34.1	33.1	107.8	87.4	90.1	95.1	90.8
09:35	35.8	32.4	105.9	87.2	88.9	94.1	89.2
10:05	34.3	32.1	104.7	86.0	87.5	92.7	88.7
10:35	34.3	32.0	103.0	84.1	86.0	91.1	86.4
11:05	35.4	32.2	103.1	83.1	85.4	90.5	85.4
11:35	37.2	32.4	103.6	84.6	85.4	90.5	86.2
13:10	37.4	33.7	101.4	80.9	85.8	90.7	84.1
13:40	33.9	33.7	101.5	81.3	83.8	88.3	83.7
14:10	38.3	34.1	100.6	80.2	83.4	87.8	83.1

Table A1.27 Raw experimental data
March 9 and 10, 1992

Time	TFB1	TFB2	TFB3	TFB4	TFB5	TFB6	TFB7	Twi	Two	Fb	Fwr
08:05	14.9	16.9	112.1	62.1	31.1	51.4	99.5				
08:20	16.8	17.9	114.8	97.2	33.0	55.1	97.8				
08:35	17.9	20.5	116.9	98.5	37.1	61.3	99.7				
08:55	21.2	23.1	117.4	101.7	39.8	64.8	101.1	16.6	66.7	0.43	0.14
09:15	23.6	25.4	117.7	100.4	49.1	74.3	102.4	17.9	79.7		
09:30	26.0	27.1	123.4	110.6	57.2	87.3	108.9				
09:45	27.0	28.4	119.7	107.4	58.3	86.3	107.3				
10:00	27.2	29.4	125.0	113.1	62.1	93.4	111.6	16.9	79.1		
10:20	30.6	30.9	131.1	119.3	69.9	104.1	118.2				
10:40	32.1	31.6	130.8	111.3	62.7	90.1	114.9				
11:00	31.1	32.1	130.4	117.4	68.2	98.2	116.4				
11:20	31.8	32.6	130.9	116.1	59.8	84.0	114.8				
13:00	33.9	34.6	130.6	117.8	57.2	80.4	112.1				
13:15	32.9	34.8	133.3	115.4	54.2	73.3	113.6			0.42	0.2
13:30	33.8	35.1	130.3	111.9	55.2	74.9	110.1				
13:45	35.1	35.3	131.1	115.7	57.2	78.4	114.0			0.43	
14:00	35.6	35.3	131.8	115.5	58.4	81.6	112.7				
14:15	36.6	35.4	132.3	115.7	59.4	83.7	113.4				
14:30	36.8	35.6	132.2	115.9	59.9	84.6	115.9			80.8	0.13
07:45	29.8	33.7	123.8	96.2	59.2	80.3	99.8	18	66.0	0.33	
08:15	30.7	33.7	129.6	103.9	62.4	79.6	104.4				
09:00	29.9	32.9	129.6	98.2	58.5	69.7	99.5				
09:30	29.8	32.9	128.1	97.9	59.7	70.8	99.7				
10:00	31.3	33.4	127.1	97.1	59.8	71.1	98.9				
10:30	32.9	33.8	128.3	98.4	60.7	72.0	100.1				

Table A1.28 Raw experimental data
March 26, 1992

Time	TFB1	TFB2	TFB3	TFB4	TFB5	TFB6	TFB7	Ps	Pi	Po	Fb
09:00	34.7	43.9	125.6	113.4	91.3	103.2	113.2	5.1	2.7	1.7	0.474
09:30	36.2	45.2	127.7	115.8	93.4	104.8	114.3	5.0	2.6	2.0	0.457
10:00	37.1	47.7	128.6	117.6	101.9	109.8	116.0	5.0	2.5	2.0	0.411
10:30	33.3	44.1	123.6	111.4	94.6	104.2	110.1	5.0	2.5	2.0	
11:00	31.3	44.7	123.1	109.3	91.9	102.6	108.2	5.0	2.5	2.0	0.465
11:30	33.6	44.9	125.7	112.1	92.1	102.9	109.9	5.0	2.6	2.1	
12:00	30.5	43.4	120.6	105.5	88.3	98.2	104.8	5.0	2.5	2.0	0.462
12:30	31.6	44.3	123.6	108.1	90.2	100.9	107.4	5.0	2.6	2.0	
13:00	30.5	42.3	120.6	105.2	88.2	98.6	105.2	4.9	2.5	2.0	0.455
13:30	32.8	47.1	125.6	111.2	92.1	103.2	110.7	4.9	2.5	2.2	
14:00	32.6	45.8	122.8	107.1	90.4	100.7	106.8	4.9	2.4	1.9	0.428

APPENDIX 2

SOFTWARE GENERATED

A2.1 NH3H2O00 MODEL

A2.1.1 Introduction

In previous experimental work, the data analysis was difficult and laborious because the ammonia-water properties had to be obtained from experimental tables or calculated with algorithms which have significant errors, from experimental data tables [Heard (1990)].

An application programme (worksheet) was developed using Lotus 1-2-3, release 3, [Lotus 1989] spreadsheet programme. Among the features that made the programme attractive for this application were, its extensive number of users, and its ability to run on a wide variety of personal computers (PC) and microcomputers, supporting numerous output devices [Bond G.C. et al (1990)], [Boone M (1988)]. This programme or worksheet called NH3H2O00.WK3 is a tool which helps to calculate the ammonia-water properties for experimental data, [Institute of Gas Technology (1964)] and [Bogard (1981)] using an algorithm. These properties can be used in other calculations in the same worksheet.

A2.1.2 Programme Description

The column/row environment of a spreadsheet can be used as a table of values, for example, liquid concentration as a function of temperature and pressure, the

pressure increases every row and the temperature every column and a corresponding concentration value can be obtained for specific column and row values.

Nine data tables were typed into the worksheet and a programme was developed in order to select the desired table, read the input data and calculate the thermodynamic property.

To calculate these properties an algorithm was development using INDEX Lotus function [QUE Corporation (1989)]. INDEX is a function that retrieves data from a specified location. It requires indication of the column-offset and row-offset. Because the data tables have specific increments of values in rows or columns, it is necessary to interpolate between rows, columns or both, to obtain the desired value.

A2.1.3 How to Use the Programme

To begin a session using the worksheet, the Lotus spreadsheet must be entered and a file called NH3H2O00.WK3 must be retrieved.

At the beginning, the programme reads a "macro" instruction which moves the cell pointer to cell A1 and displays a message in the mode indicator "Press keys Alt-c to calculate the ammonia properties".

When Alt-c are pressed a "language" programme is activated and the main menu

is shown in the panel (at the top and left side of the screen). Then an option (1 to 7 or other and 8, 9 or previous) must be chosen. Options descriptions can be read from the screen.

After the option is chosen, a menu of unit types is shown. U.S. customary or SI units are used. Then the necessary input data are fed in. Finally a subroutine calculates the property value and it is shown at the bottom of the screen. At this moment the property value can be read from the screen.

A final menu is activated in order to do more calculations or to quit the programme. If the "quit" option is activated the cell pointer is moved to cell A1. At this moment the property value can be used in other applications by its variable name (see nomenclature). Figures 1 and 2 show the programme flowchart.

A2.1.4 Conclusions

Using the NH3H2O00.WK3 programme as a general purpose programme is easy and accurate.

The programme will help to save time in subsequent experimental data analysis. Based on the programme, more versions can be developed for specific applications with a saving of effort.

The techniques used in this programme can be added together with other studies to build additional applications such as design for commercial scale units and their

economic analysis.

A2.1.5 References

- A2.1 1-2-3 Release 3, Lotus Development Corporation, Cambridge MA, USA, (1989).
- A2.2 Institute of Gas Technology, Physical and thermodynamic properties of ammonia-water mixtures, Chicago IL, USA, (1964).
- A2.3 Bogart M., Ammonia absorption refrigeration in industrial process, Gulf Publish Company, (1981).
- A2.4 C.L. Heard, Personal communication.
- A2.5 G.C. Bond, T.A. Alliott and S.W. Pearce, Developing a custom Lotus 1-2-3 application for multisite process monitoring and analysis, American Biotechnology Laboratory, Vol. 8, Num. 11, (1990).
- A2.6 D. Boone, Reservoir Engineering made easy with PC spreadsheet, Petroleum Engineer International, October (1988).
- A2.7 QUE Corporation, Using 1-2-3 release 3, p. 243, (1989)

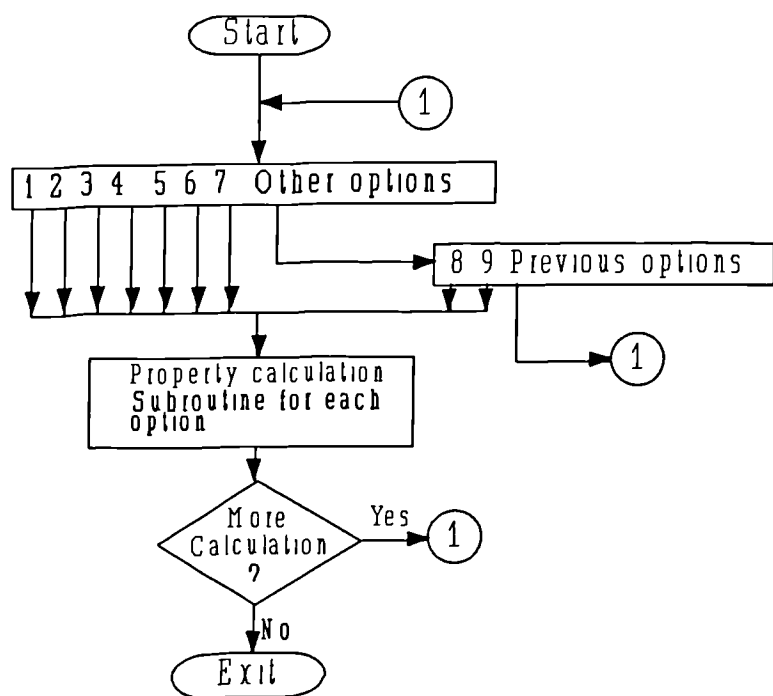


Fig. A2.1 Main programme flowchart NH3H2O.

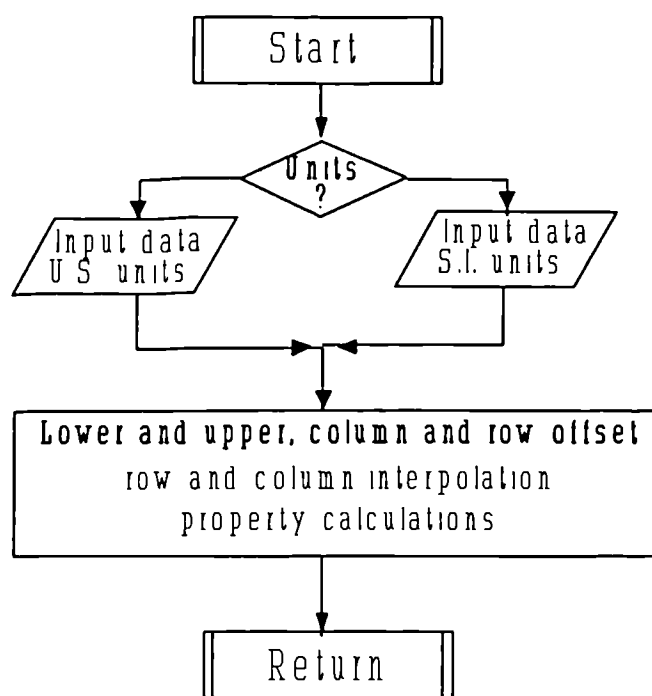


Fig. A2.2 Subroutines NH3H2O flowchart

Table A2.1

NH3H2O programme ranges named and their localization in the worksheet

Range name	Address	Range name	Address
CONCL	AV4..AV4	PAG35	HQ8003..IA80
CWVAP	AX3..AX3	PAG36	HQ7903..IA79
DY	AX4..AX4	PAG37	HQ7803..IA78
EXIT	BT40..BT40	PAG38	HQ7703..IA77
FINISH	BT35..BT35	PAG39	HQ7603..IA76
HLBTU	AX5..AX5	PAG40	HQ7503..IA75
HLKJ	AX6..AX6	PAG41	HQ7403..IA74
HVBTU	AX7..AX7	PAG42	HQ7303..IA73
HVKJ	AX8..AX8	PAGTP	AJ8002..CD80
INDE1	AV10..AV10	PBTC	BT67..BT67
NDE2	AV11..AV11	PBX	BT18..BT18
INDE3	AV12..AV12	PPTF	BT64..BT64
INDE4	AV13..AV13	PPX	BT15..BT15
INX1	AV14..AV14	PRESSCON	BT11..BT11
INX2	AV15..AV15	PRESSTEMP	BT60..BT60
INY1	AV16..AV16	PRESSY	BT21..BT21
INY2	AV17..AV17	PRESSY1	BT75..BT75
LIMITP	BT55..BT55	PSBAR	AV7..AV7
LIMITT	BT50..BT50	PSPSIA	AV6..AV6
MAIN	BE8..BE8	ROW1	AV8..AV8
MOREOP	BN8..BN8	ROW2	AV9..AV9
NO	BT46..BT46	TCX	BT8..BT8
OPT1	BE172..BE172	TEMCON	BT1..BT1
OPT2	BE14..BE14	TEMPC	AV5..AV5
OPT3	BE34..BE34	TEMPPF	AV3..AV3
OPT4	BE54..BE54	TFX	BT5..BT5
OPT5	BE74..BE74	UPLIMY	AX9..AX9
OPT6	BE94..BE94	YES	BT44..BT44
OPT7	BE114..BE114	\0	BE1..BE1
OPT8	BE134..BE134	\C	BE3..BE3
OPT9	BE154..BE152		

A2.1.6**Nomenclature***Variables*

concl	ammonia concentration in liquid [fraction]
cwvap	water amount in the saturated vapor [percent]
dy	row interval in the specific table [dimensionless]
hlbtu	saturated liquid enthalpy [btu lb ⁻¹]
hlkj	saturated liquid enthalpy [kJ kg ⁻¹]
hvbtu	saturated vapor enthalpy [btu lb ⁻¹]
hvkj	saturated vapor enthalpy [kJ kg ⁻¹]
inde1	data value of lower column offset and lower row offset
inde2	data value of upper column offset and lower row offset
inde3	data value of upper column offset and upper column offset
inde4	data value of upper column offset and upper column offset
inx1	lower column offset
inx2	upper column offset
iny1	lower row offset
iny2	upper row offset
psbar	saturation pressure [bar]
pspsia	saturation pressure [psia]
row1	interpolation value between inde1 and inde3
row2	interpolation value between inde2 and inde4
tempc	saturation temperature [°C]
tempf	saturation temperature [°F]
uplimy	upper limit value of row values [°F or psia]

Subroutines

finish	displays options for more calculations or quit the programme
limitp	comparison pressure value against maximum in this table
limitt	comparison temperature value against maximum in this table
no	moves cell point to A1 and quit the programme
pbtc	inputs pressure [bar] and temperature [°C] values
pbx	inputs pressure [bar] and concentration [wt fract.] values
pptf	inputs pressure [psia] and temperature [°F] values
ppx	inputs pressure [bar] and concentration [wt fract.] values
pressy	assigns row offset in function of pressure value in specific range for [2] tables
pressy1	assigns row offset in function of pressure value in specific range for [Bogard (1981)] tables
tcx	inputs temperature [°C] and concentration [wt fract.] values
tfx	inputs temperature [°F] and concentration [wt fract.] values
yes	returns to the main menu
opt1	calculates liquid concentration as a function of pressure and temperature
opt2	calculates saturated vapor pressure as a function of saturation temperature and liquid concentration
opt3	calculates boiling points as a function of saturation pressure and liquid concentration
opt4	calculates water amount in saturated vapour as a function of

	saturation temperature and liquid concentration
opt5	calculates water amount in saturated vapour as a function of saturation pressure and liquid concentration
opt6	calculates saturated liquid enthalpy as a function of saturation temperature and liquid concentration
opt7	calculates saturated liquid enthalpy as a function of saturation pressure and liquid concentration
opt8	calculates saturated vapor enthalpy as a function of saturation temperature and liquid concentration.
opt9	calculates saturated vapor enthalpy as a function of saturation pressure and liquid concentration
<i>Menus</i>	
main	displays 7 options and more options
moreopt	displays 8, 9 options and previous options
tempcon	displays units for temperature and concentration
presscon	displays units for pressure and concentration
presstem	displays units for pressure and temperature
exit	displays yes, no options

A2.1.7 Programme Listing

```

\0  {home}~{indicate "Press (ALT C ), keys to calculate ammonia properties"}

\c  {indicate}{home}{goto}x1-
{Indicate " Select an option and press enter key to continue "}{menucall main}
{finish}
{quit}

main  1      2      3      4      5      6      7      More options
legend legend legend legend legend legend legend
{opt1} {opt2} {opt3} {opt4} {opt5} {opt6} {opt7} {menucall moreop}
{return}

moreopt 8      9      Previous options
legend legend
{opt8} {opt9} {menucall main}

opt2  {pgdn}{menucall temcon}
{if concl=1}{let inx1,concl/.1}{let inx2,inx1}{branch be17}
{let inx1,concl/.1}{let inx2,concl/.1+1}
{let iny1,tempf/10+6}{let iny2,tempf/10+7}
{let uplimy,470}{limitp}
{let inde1,(@index($pag35,inx1,iny1))}
{let inde3,(@index($pag35,inx2,iny1))}
{let inde2,(@index($pag35,inx1,iny2))}
{let inde4,(@index($pag35,inx2,iny2))}
{let row1,(inde3-inde1)*(concl*10-@int(concl*10))+inde1}
{let row2,(inde4-inde2)*(concl*10-@int(concl*10))+inde2}
{let psp sia,(row2-row1)*(tempf/10-@int(tempf/10))+row1}{let psbar,psp sia/14.4}-
{return}

opt3  {pgdn 2}{menucall presscon}
{if psp sia>=40}{branch be37}
{pressy}{branch be39}
{let iny1,psp sia/10+8}{let iny2,psp sia/10+9}{let dy,10}
{limitp}
{if concl=0 #or# concl=1}{let inx1,concl/.1}{let inx2,inx1}{branch be41}
{let inx1,concl/.1}{let inx2,concl/.1+1}
{let inde1,(@index($pag36,inx1,iny1))}
{let inde3,(@index($pag36,inx2,iny1))}
{let inde2,(@index($pag36,inx1,iny2))}
{let inde4,(@index($pag36,inx2,iny2))}
{let row1,(inde3-inde1)*(concl*10-@int(concl*10))+inde1}
{let row2,(inde4-inde2)*(concl*10-@int(concl*10))+inde2}
{let tempf,(row2-row1)*(psp sia/dy-@int(psp sia/dy))+row1}{let tempc,(tempf-32)*1.8
{return}

opt4  {pgdn 3}{menucall temcon}
{if concl=0 #or# concl=1}{let inx1,concl/.1}{let inx2,inx1}{branch be57}
{let inx1,concl/.1}{let inx2,concl/.1+1}
{let iny1,tempf/10+6}{let iny2,tempf/10+7}
{let uplimy,420}{limitp}
{let inde1,(@index($pag37,inx1,iny1))}
{let inde3,(@index($pag37,inx2,iny1))}
{let inde2,(@index($pag37,inx1,iny2))}
{let inde4,(@index($pag37,inx2,iny2))}
{let row1,(inde3-inde1)*(concl*10-@int(concl*10))+inde1}
{let row2,(inde4-inde2)*(concl*10-@int(concl*10))+inde2}
{let cwvap,(row2-row1)*(tempf/10-@int(tempf/10))+row1}-
{return}

opt5  {pgdn 4}{menucall presscon}
{if psp sia>=40}{branch be77}
{pressy}{branch be79}
{let iny1,psp sia/10+8}{let iny2,psp sia/10+9}{let dy,10}
{limitp}
{if concl=0 #or# concl=1}{let inx1,concl/.1}{let inx2,inx1}{branch be81}
{let inx1,concl/.1}{let inx2,concl/.1+1}
{let inde1,(@index($pag38,inx1,iny1))}
{let inde3,(@index($pag38,inx2,iny1))}
{let inde2,(@index($pag38,inx1,iny2))}
{let inde4,(@index($pag38,inx2,iny2))}
{let row1,(inde3-inde1)*(concl*10-@int(concl*10))+inde1}
{let row2,(inde4-inde2)*(concl*10-@int(concl*10))+inde2}

```

```

(let cwwap,(row2-row1)*(pspsia/dy-@int(pspsia/dy))+row1)-
{return}

opt6 {pgdn 5}{menucall temcon}
{if concl=1}{let inx1,concl/.1}{let inx2,inx1}{branch be97}
{let inx1,concl/.1}{let inx2,concl/.1+1}
{let iny1,tempf/10+6}{let iny2,tempf/10+7}
{let uplimy,470}{limit}
{let inde1,(@index($pag39,inx1,iny1))}
{let inde3,(@index($pag39,inx2,iny1))}
{let inde2,(@index($pag39,inx1,iny2))}
{let inde4,(@index($pag39,inx2,iny2))}
{let row1,(inde3-inde1)*(concl*10-@int(concl*10))+inde1}
{let row2,(inde4-inde2)*(concl*10-@int(concl*10))+inde2}
{let hlbtu,(row2-row1)*(tempf/10-@int(tempf/10))+row1)-{let hlkj,hlbtu*2.326}-
{return}

opt7 {pgdn 6}{menucall presscon}
{if pspsia>=40}{branch be117}
{pressy}{branch be119}
{let iny1,pspsia/10+8}{let iny2,pspsia/10+9}{let dy,10}
{limitp}
{if concl=1}{let inx1,concl/.1}{let inx2,inx1}{branch be121}
{let inx1,concl/.1}{let inx2,concl/.1+1}
{let inde1,(@index($pag40,inx1,iny1))}
{let inde3,(@index($pag40,inx2,iny1))}
{let inde2,(@index($pag40,inx1,iny2))}
{let inde4,(@index($pag40,inx2,iny2))}
{let row1,(inde3-inde1)*(concl*10-@int(concl*10))+inde1}
{let row2,(inde4-inde2)*(concl*10-@int(concl*10))+inde2}
{let hlbtu,(row2-row1)*(pspsia/dy-@int(pspsia/dy))+row1)-{let hlkj,hlbtu*2.326}-
{return}

opt8 {pgdn 7}{menucall temcon}
{if concl=1}{let inx1,concl/.1}{let inx2,inx1}{branch be137}
{let inx1,concl/.1}{let inx2,concl/.1+1}
{let iny1,tempf/10+6}{let iny2,tempf/10+7}
{let uplimy,470}{limit}
{let inde1,(@index($pag42,inx1,iny1))}
{let inde3,(@index($pag42,inx2,iny1))}
{let inde2,(@index($pag42,inx1,iny2))}
{let inde4,(@index($pag42,inx2,iny2))}
{let row1,(inde3-inde1)*(concl*10-@int(concl*10))+inde1}
{let row2,(inde4-inde2)*(concl*10-@int(concl*10))+inde2}
{let hvbtu,(row2-row1)*(tempf/10-@int(tempf/10))+row1)-{let hvkj,hvbtu*2.326}-
{return}

opt9 {pgdn 8}{menucall presscon}
{if pspsia>=40}{branch be157}
{pressy}{branch be159}
{let iny1,pspsia/10+8}{let iny2,pspsia/10+9}{let dy,10}
{limitp}
{if concl=1}{let inx1,concl/.1}{let inx2,inx1}{branch be161}
{let inx1,concl/.1}{let inx2,concl/.1+1}
{let inde1,(@index($pag41,inx1,iny1))}
{let inde3,(@index($pag41,inx2,iny1))}
{let inde2,(@index($pag41,inx1,iny2))}
{let inde4,(@index($pag41,inx2,iny2))}
{let row1,(inde3-inde1)*(concl*10-@int(concl*10))+inde1}
{let row2,(inde4-inde2)*(concl*10-@int(concl*10))+inde2}
{let hvbtu,(row2-row1)*(pspsia/dy-@int(pspsia/dy))+row1)-{let hkj,hvbtu*2.326}-
{return}

opt1 {pgdn 9}{menucall presstemp}
{if pspsia>=30}{branch be175}
{pressy1}{branch be177}
{let iny1,pspsia/10+4}{let iny2,pspsia/10+5}{let dy,10}
{limitp}
{let inx1,tempf/10+5}{let inx2,tempf/10+6}
{let inde1,(@index($pagtp,inx1,iny1))}
{let inde3,(@index($pagtp,inx2,iny1))}
{let inde2,(@index($pagtp,inx1,iny2))}
{let inde4,(@index($pagtp,inx2,iny2))}
{let row1,(inde3-inde1)*(tempf/10-@int(tempf/10))+inde1}
{let row2,(inde4-inde2)*(tempf/10-@int(tempf/10))+inde2}
{let concl,(row2-row1)*(pspsia/dy-@int(pspsia/dy))+row1)-{let concl,concl/100}-
{return}

```

```

temcon T °F x T °C x
TemperatuTemperature (°C), Concentration (fraction)
{tx} {tcx}

{tx} {getnumber "temperature (°F); ",tempf}~{getnumber "ammonia in liq. concentration 0-1;
",concl}
~{let tempc,(tempf-32)/1.8}~

{tcx} {getnumber "temperature (°C); ",tempc}~{getnumber "ammonia in liq. concentration 0-1
; ",concl}
~{let tempf,(tempc*1.8)+32}

presscon Press (psia), x Press (bar), x
Pressure .. Pressure in (bar) and Concentration in fraction (0-1).
{px} {pbx}

{px} {getnumber "Pressure (psia); ",pspsia}~{getnumber "Amonia in liq. concentration (0-1);
",concl}
~{let psbar,pspsia/15.4}~

{pbx} {getnumber "Pressure (bar); ",psbar}~{getnumber "Amonia in liq. concentration (0-1);
",concl}~{let pspsia,psbar*15.4}~

pressy {if pspsia<2}{let iny1,0}{let iny2,iny1+1}{let dy,1}{branch bt33}
{if pspsia<4}{let iny1,1}{let iny2,iny1+1}{let dy,2}{branch bt33}
{if pspsia<6}{let iny1,2}{let iny2,iny1+1}{let dy,2}{branch bt33}
{if pspsia<8}{let iny1,3}{let iny2,iny1+1}{let dy,2}{branch bt33}
{if pspsia<10}{let iny1,4}{let iny2,iny1+1}{let dy,2}{branch bt33}
{if pspsia<12}{let iny1,5}{let iny2,iny1+1}{let dy,2}{branch bt33}
{if pspsia<15}{let iny1,6}{let iny2,iny1+1}{let dy,3}{branch bt33}
{if pspsia<20}{let iny1,7}{let iny2,iny1+1}{let dy,5}{branch bt33}
{if pspsia<25}{let iny1,8}{let iny2,iny1+1}{let dy,5}{branch bt33}
{if pspsia<30}{let iny1,9}{let iny2,iny1+1}{let dy,5}{branch bt33}
{if pspsia<35}{let iny1,10}{let iny2,iny1+1}{let dy,5}{branch bt33}
{if pspsia<40}{let iny1,11}{let iny2,iny1+1}{let dy,5}{branch bt33}
{return}

finish {indicate " Do you want to do another calculation ? "}
{menubranch exit}

Exit Yes No
{yes} {no}

{yes} {indicate}{branch \c}

{no} {indicate}{paneloff}
{home}{quit}~

limitt {if tempf<-60 #OR# tempf>uplimy}{Indicate " Data out of range wait a second... "}
{wait &now+&time(0,0,5)}{return}
{if tempf=uplimy}{let iny2,tempf/10+6}

limitp {if pspsia<0 #OR# pspsia>500}{Indicate " Data out of range wait a second... "}
{wait &now+&time(0,0,5)}{return}
{if pspsia=500}{let iny2,pspsia/10+8}

presstem P (psia),P (bar), T (°C)
Pressure Pressure in (bar) and Temperature in (°C).
{pptf} {pbtc}

pptf {getnumber "Pressure (psia); ",pspsia}~{getnumber "Temperature (°F); ",tempf}
{let psbar,pspsia/15.4}{let tempc,(tempf-32)/1.8}

pbtc {getnumber "Pressure (bar); ",psbar}~{getnumber "Temperature (°C); ",tempc}
{let pspsia,psbar*15.4}~{let tempf,(tempc*1.8)+32}~

pressy1 {if pspsia<6}{let iny1,0}{let iny2,iny1+1}{let dy,6-pspsia}{branch bt84}
{if pspsia<8}{let iny1,0}{let iny2,iny1+1}{let dy,2}{branch bt84}
{if pspsia<10}{let iny1,1}{let iny2,iny1+1}{let dy,2}{branch bt84}
{if pspsia<12}{let iny1,2}{let iny2,iny1+1}{let dy,2}{branch bt84}
{if pspsia<15}{let iny1,3}{let iny2,iny1+1}{let dy,3}{branch bt84}
{if pspsia<20}{let iny1,4}{let iny2,iny1+1}{let dy,5}{branch bt84}
{if pspsia<25}{let iny1,5}{let iny2,iny1+1}{let dy,5}{branch bt84}
{if pspsia<30}{let iny1,6}{let iny2,iny1+1}{let dy,5}{branch bt84}
{return}

```

A2.2 REFRI00 MODEL

A2.2.1 Introduction

In previous experimental work, the data analysis was difficult and laborious because ammonia-water properties had to be obtained from experimental tables or calculated with algorithms. Furthermore, a complicated method had to be followed to calculate the main thermodynamic parameters in order to evaluate the performance of the ammonia-water absorption refrigerator.

An applications computer programme (worksheet) was developed using LOTUS 1-2-3, rel.3, [LOTUS 1989] spreadsheet programme. This programme or worksheet called REFRI00.WK3 is a tool which helps to: input experimental data in the order taken in the field, calculate the main thermodynamic parameters for ammonia-water absorption refrigeration using subroutines described in the NH3H2O00.WK3 programme, and save or print results and experimental data.

A2.2.2 Thermodynamic Considerations

The main parameters that define the performance of an absorption refrigeration system are defined in section 2.3 and 2.4.

A2.2.3 REFRI00 Programme Description

The worksheet is a LOTUS file that has two sheets "A" and "B". A sheet is empty, B sheet contains the programme to calculate the main thermodynamic parameters and the experimental tables to calculate concentration, enthalpies, specific gravity and amount of water in the vapour [Bogart (1981)].

When the programme is read, the programme writes the experimental data in sheet **A**, and when the option "Save" is chosen, only data and results ranges are saved in a file. At this point a file name is required. Figure A2.2 shows the programme flow diagram. Next are the programme nomenclature and then are the programme listing and Table A2.1 shows range names and their addresses in the worksheet.

A2.2.3 How to Use the Programme

To begin a session using the worksheet it is necessary to enter a LOTUS spreadsheet and retrieve the file called REFRI00.WK3.

At the beginning, the programme reads a "macro" instruction which moves the cell pointer to **B:X1** and displays a message in the mode indicator "**choose the option or ESC to cancel**". In the control panel display there are six options: "**Input Calculate Modify Save Print Leave**", and on the screen there is a window which shows option descriptions. To choose an option just press the first letter and the option is automatically activated. When the ESC key is pressed the cell pointer is moved to **A:A1** and the mode indicator displays the message "**Press keys < Alt-c > for main menu**".

Input option is a "language" programme which asks for the test date, then the time and continues with temperatures, pressures and flowrates. Input data must be in the corresponding field units and the programme converts them to S.I. units. At the end of every data set, a menu is activated to choose more data or no. If the **Yes** option is activated it returns to ask for the time. If the **No** option is activated

it returns to the main menu.

When the **Calculate** option is chosen, a programme is activated to calculate the average values of every experimental data point and this value is used to calculate the main thermodynamics parameters. In this option a series of calculations are activated and the thermodynamic properties are calculated from their temperature, pressure and ammonia solution concentration. In addition to the options described in the NH3H2O00.WK3 programme, specific gravity was added to the present programme. The specific gravity calculation is based on a graph from Bogart [Bogart (1981)], which was converted to a range of values that could be read into the programme, see table 2.

The **modify** option is used to leave the main menu and the cell pointer is moved to A:A7 in order to modify or check the experimental data. After modifications it is necessary to use the **calculate** option.

The **save** option is to save the calculated and experimental data in a LOTUS file.

The **print** option is used to print the results range. Appendix A shows an example of this printout.

Leave, this option is the final option used to leave the programme and LOTUS. Be sure that the experimental data were previously saved, using **Save** option before leaving the programme.

A2.2.4 Conclusions

Using the REFRI00.WK3 programme for this specific application is easy and accurate.

The programme will help to save time in subsequent experimental data analysis and to have the same format for all the experimental tests.

Techniques used in this programme can be added to other studies to build additional applications such as the design of commercial size units and their economic analysis.

A2.2.5 References

A2.8 1-2-3 Release 3, LOTUS Development Corporation, Cambridge MA, USA, (1989).

A2.9 Institute of Gas Technology, Physical and thermodynamic properties of ammonia-water mixtures, Chicago IL, USA, (1964).

A2.10 Bogart M., Ammonia absorption refrigeration in industrial process, Gulf Publishing Company, (1981).

A2.11 R. Best, C. L. Heard, H. Fernandez and J. Siqueiros, Developments in geothermal energy in Mexico-Part five: The commissioning of an ammonia/water absorption cooler operating on low enthalpy geothermal energy, J. Heat Recovery Systems 6(3), 209-216 (1986).

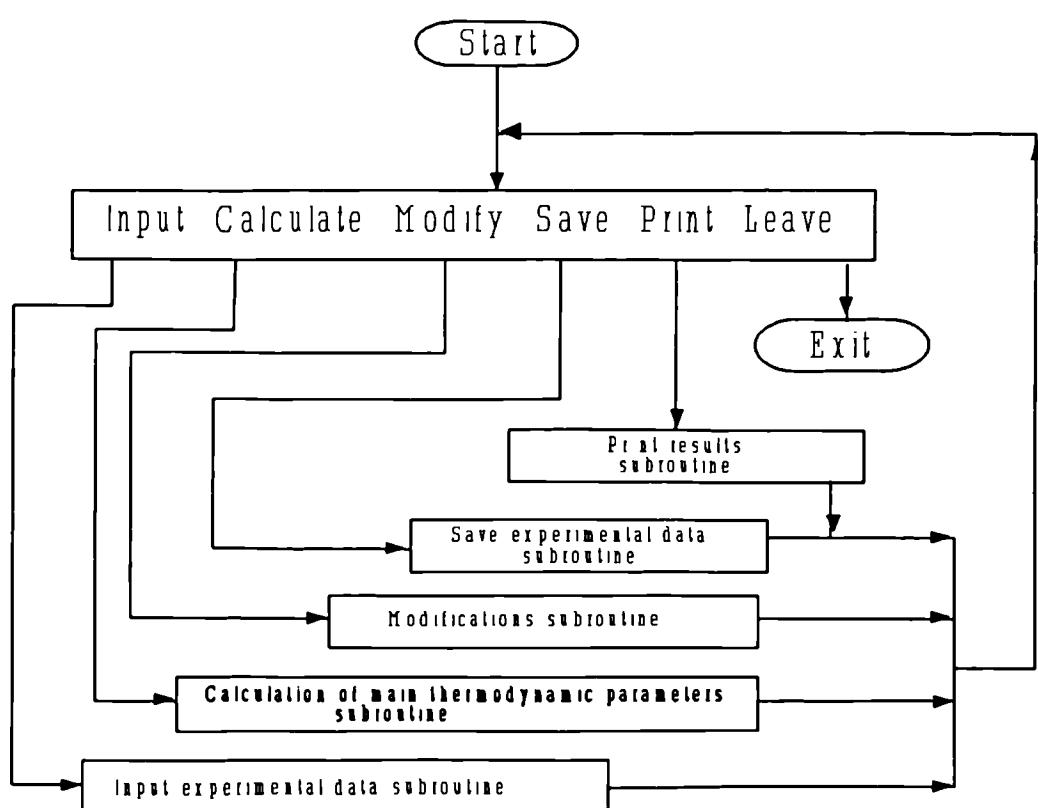


Fig. A2.3 Flow diagram of REFRI00 programme

Table A2.2

REFRI00 programme ranges named and their localization in the worksheet

range	address	range	address
abpreb	b:au11..B:au11	hva8	b:aw3..B:aw3
abtemc	b:au10..B:au10	hva8v	b:aw23..B:aw23
answer	b:au23..B:au23	hvbtu	b:au7..B:au7
calculate	b:j2..B:j2	hvkj	b:au8..B:au8
concl	b:as4..B:as4	inde1	b:as10..B:as10
copa	b:aw7..B:aw7	inde2	b:as11..B:as11
copcc1	b:aw8..B:aw8	inde3	b:as12..B:as12
copecl	b:aw9..B:aw9	inde4	b:as13..B:as13
copreb	b:au18..B:au18	input	b:q115..B:q115
cotemc	b:au17..B:au17	inx1	b:as14..B:as14
cwvap	b:au3..B:au3	inx2	b:as15..B:as15
data	a:a7..A:av107	iny1	b:as16..B:as16
densol	b:as24..B:as24	iny2	b:as17..B:as17
dy	b:au4..B:au4	limitp	b:bq55..B:bq55
evdukw	b:au22..B:au22	mab	b:as23..B:as23
evliconf	b:au15..B:au15	modify	b:q123..B:q123
evpreb	b:au14..B:au14	moredata	b:r100..B:r100
evtemc	b:au13..B:au13	mr	b:as22..B:as22
evvaconf	b:au16..B:au16	nge	b:aw13..B:aw13
exit	b:q138..B:q138	ngen	b:aw13..B:aw13
flr1	b:an47..B:an47	nre	b:aw12..B:aw12
flra	b:aw10..B:aw10	nrec	b:aw12..B:aw12
fls1	b:an48..B:an48	opt1	b:bb14..B:bb14
flw1	b:an49..B:an49	opt4	b:bb31..B:bb31
flw2	b:an50..B:an50	opt6	b:bb45..B:bb45
flw3	b:an51..B:an51	opt7	b:bb58..B:bb58
fra	b:aw11..B:aw11	opt8	b:bb74..B:bb74
genconf	b:aw17..B:aw17	opt9	b:bb88..B:bb88
genexqf	b:au21..B:au21	optden	b:bb1..B:bb1
gentemc	b:au20..B:au20	options	b:q109..B:w109
gravran	b:dw4..B:eg34	pag37	b:hn7803..B:hx7851
hlbtu	b:au5..B:au5	pag39	b:hn7603..B:hx7656
hli11	b:aw16..B:aw16	pag40	b:hn7503..B:hx7561
hli15	b:as21..B:as21	pag41	b:hn7403..B:hx7461
hli16	b:aw14..B:aw14	pag42	b:hn7303..B:hx7356
hli4	b:aw19..B:aw19	pagtp	b:ag8002..B:ca8036
hli43	b:aw18..B:aw18	pre1	b:an39..B:an39
hli5	b:aw20..B:aw20	pre2	b:an40..B:an40
hli7	b:aw6..B:aw6	pre3	b:an41..B:an41
hli8	b:aw4..B:aw4	pre4	b:an42..B:an42
hli8v	b:aw22..B:aw22	pre5	b:an43..B:an43

Table A2.2 (continued)

REFRI00 programme ranges named and their localization in the worksheet

range	address	range	address
prev1	b:an37..B:an37	tem20	b:an24..B:an24
hlkj	b:au6..B:au6	pre6	b:an44..B:an44
hmi8	b:aw5..B:aw5	pre7	b:an45..B:an45
hmi8v	b:aw21..B:aw21	pre8	b:an46..B:an46
hva10	b:aw15..B:aw15	pressy	b:bq21..B:bq21
hva17	b:as19..B:as19	pressy1	b:bq75..B:bq75
prev2	b:an38..B:an38	tem21	b:an25..B:an25
print	b:q135..B:q135	tem22	b:an26..B:an26
psbar	b:as7..B:as7	tem23	b:an27..B:an27
pspsia	b:as6..B:as6	tem24	b:an28..B:an28
pst1	b:an37..B:an37	tem25	b:an29..B:an29
pst2	b:an38..B:an38	tem26	b:an30..B:an30
rectemc	b:au19..B:au19	tem27	b:an31..B:an31
row1	b:as8..B:as8	tem28	b:an32..B:an32
row2	b:as9..B:as9	tem29	b:an33..B:an33
save	b:q127..B:q127	tem3	b:an7..B:an7
start	b:b43..B:b43	tem30	b:an34..B:an34
startd	b:b45..B:b45	tem31	b:an35..B:an35
stconf	b:au12..B:au12	tem32	b:an36..B:an36
tdate	b:as18..B:as18	tem4	b:an8..B:an8
tem1	b:an5..B:an5	tem5	b:an9..B:an9
tem10	b:an14..B:an14	tem6	b:an10..B:an10
tem11	b:an15..B:an15	tem7	b:an11..B:an11
tem12	b:an16..B:an16	tem8	b:an12..B:an12
tem13	b:an17..B:an17	tem9	b:an13..B:an13
tem14	b:an18..B:an18	tempc	b:as5..B:as5
tem15	b:an19..B:an19	tempf	b:as3..B:as3
tem16	b:an20..B:an20	time	b:an4..B:an4
tem17	b:an21..B:an21	uplimy	b:au9..B:au9
tem18	b:an22..B:an22	weconf	b:as20..B:as20
tem19	b:an23..B:an23	\0	b:b37..B:b37
tem2	b:an6..B:an6	\c	b:b37..B:b37

Table A2.3

**Density of aqua ammonia solutions as a function
of liquid concentration (%), and temperature**

Ammonia in liquid, wt %

Saturation Temperature	0	0.1	0.2	0.3	0.4	0.5	0.6	0.7	0.8	0.9	1	
°C	°F			Specific gravity								
-46	-50	1	1	1	0.915	0.895	0.866	0.837	0.801	0.765	0.728	0.692
-40	-40	1	1	1	0.913	0.893	0.864	0.834	0.798	0.761	0.725	0.688
-34	-30	1	1	0.94	0.912	0.891	0.861	0.831	0.793	0.755	0.718	0.680
-29	-20	1	1	0.94	0.911	0.89	0.859	0.828	0.789	0.751	0.712	0.673
-23	-10	1	1	0.939	0.91	0.888	0.856	0.825	0.785	0.746	0.706	0.667
-18	0	1	1	0.937	0.908	0.885	0.853	0.821	0.781	0.740	0.700	0.660
-12	10	1	0.965	0.933	0.907	0.881	0.849	0.816	0.776	0.735	0.695	0.654
-7	20	1	0.963	0.931	0.905	0.879	0.846	0.813	0.772	0.731	0.689	0.648
-1	30	1	0.961	0.93	0.902	0.876	0.842	0.809	0.766	0.724	0.682	0.640
4	40	0.999	0.96	0.929	0.9	0.873	0.838	0.804	0.760	0.717	0.673	0.630
10	50	0.999	0.959	0.927	0.897	0.87	0.835	0.800	0.756	0.713	0.669	0.625
16	60	0.998	0.958	0.925	0.894	0.868	0.832	0.796	0.751	0.707	0.662	0.617
21	70	0.997	0.955	0.922	0.891	0.863	0.827	0.791	0.746	0.700	0.655	0.610
27	80	0.995	0.953	0.916	0.889	0.86	0.823	0.786	0.739	0.693	0.646	0.600
32	90	0.993	0.95	0.92	0.884	0.854	0.816	0.779	0.732	0.685	0.638	0.591
38	100	0.992	0.949	0.918	0.88	0.85	0.812	0.773	0.726	0.678	0.630	0.582
43	110	0.99	0.946	0.915	0.875	0.846	0.807	0.768	0.719	0.671	0.622	0.573
49	120	0.989	0.943	0.912	0.87	0.84	0.801	0.761	0.712	0.663	0.614	0.565
54	130	0.987	0.94	0.906	0.865	0.833	0.793	0.754	0.704	0.654	0.605	0.555
60	140	0.983	0.935	0.901	0.86	0.826	0.786	0.746	0.696	0.645	0.595	0.545
66	150	0.98	0.933	0.896	0.854	0.82	0.779	0.738	0.687	0.636	0.584	0.533
71	160	0.978	0.93	0.892	0.85	0.815	0.774	0.732	0.680	0.629	0.577	0.525
77	170	0.974	0.925	0.887	0.843	0.805	0.763	0.721	0.668	0.615	0.563	0.510
82	180	0.97	0.92	0.882	0.838	0.796	0.754	0.711	0.659	0.606	0.553	0.500
88	190	0.963	0.916	0.877	0.83	0.79	0.747	0.703	0.649	0.595	0.540	0.486
93	200	0.96	0.912	0.87	0.825	0.78	0.736	0.691	0.636	0.581	0.525	0.470
99	210	0.957	0.91	0.864	0.82	0.77	0.726	0.681	0.626	0.571	0.515	0.460
104	220	0.953	0.905	0.86	0.812	0.76	0.715	0.671	0.615	0.559	0.504	0.448
110	230	0.95	0.9	0.853	0.807	0.751	0.705	0.659	0.602	0.545	0.487	0.430
116	240	0.946	0.894	0.85	0.798	0.742	0.695	0.649	0.590	0.532	0.473	0.415
121	250	0.94	0.89	0.84	0.782	0.733	0.685	0.638	0.578	0.519	0.459	0.400

A2.2.6 REFRI00.WK3 Programme Print Out

Test Date	8/30/90		
Experimental data:		Thermodynamic results:	
absorption temperature (°C)	43.1	actual coefficient of performance (COP)	0.34
absorption pressure (bar)	2.4	Carnot for cooling (COP)	-0.17
strong solution concentration	34.72%	enthalpy based for cooling (COP)	-1.33
weak solution concentration	27.34%		
solution flow (m³/s)	9.46E-05	flow ratio (FR)	11.08
refrigerant flow (m³/s)	1.14E-05	actual flow ratio (FRA)	10.13
evaporation temperature (°C)	-11.7	recuperator efficiency (NREC)	0.66
evaporation pressure (bar)	2.4	generator efficiency (NGE)	1.01
evaporator liq. conc.	87.94%		
evaporator vap. conc.	99.68%	heat balances	
condenser temperature (°C)	32.6	evaporator duty (kW)	10.93
condenser pressure (bar)	14.8		
rectification temperature (°C)	99.3	generator exit quality	0.08
generation temperature (°C)	118.6		

A2.2.7 Programme Nomenclature

<i>Variable</i>	<i>Description</i>
abpreb	absorption pressure [bar]
abtemc	absorption temperature [°C]
answer	answer value [Y/N]
concl	ammonia concentration in liquid [fraction]
copa	actual coefficient of performance [dimensionless]
copccl	Carnot for cooling coefficient of performance [dimensionless]
copecl	enthalpy based for cooling coefficient of performance [dimensionless]
copreb	condenser pressure [bar]
cotemc	condenser temperature [°C]
cwvap	water amount in the saturated vapour [%]
data	data range in first sheet to be erased [a:a7..A:av107]
densol	relativity density of the solution
dy	row interval in the specific table [dimensionless]
evdukw	evaporator duty [kW]
evlconf	evaporator liquid concentration [fraction]
evpreb	evaporation pressure [bar]
evtemc	evaporation temperature [°C]
evvaconf	evaporator vapour concentration [fraction]
frl	liquid refrigerant flow rate [$m^3 \text{ s}^{-1}$]
fra	thermodynamic flow ratio [dimensionless]
fsl	weak solution flow ratio [$m^3 \text{ s}^{-1}$]
flw1	cooling water to absorber [$m^3 \text{ s}^{-1}$]
flw2	cooling water to rectifier [$m^3 \text{ s}^{-1}$]
flw3	cooling water to condenser [$m^3 \text{ s}^{-1}$]
fra	actual flow ratio [dimensionless]
genconf	generator concentration [fraction]
genexqf	generator exit quality [fraction]
gentemc	generation temperature [°C]
hlbtu	saturated liquid enthalpy [Btu lb ⁻¹]
hli11	saturated liquid enthalpy of 11 stream [Btu lb ⁻¹]
hli15	saturated liquid enthalpy of 15 stream [Btu lb ⁻¹]
hli16	saturated liquid enthalpy of 16 stream [Btu lb ⁻¹]
hli4	saturated liquid enthalpy of 4 stream [Btu lb ⁻¹]
hli43	saturated liquid enthalpy of 43 stream [Btu lb ⁻¹]
hli5	saturated liquid enthalpy of 5 stream [Btu lb ⁻¹]
hli7	saturated liquid enthalpy of 7 stream [Btu lb ⁻¹]
hli8	saturated liquid enthalpy of 8 stream [Btu lb ⁻¹]
hli8v	saturated liquid enthalpy of 8 stream [Btu lb ⁻¹]
hmi8	two-phase mix enthalpy of 8 stream [Btu lb ⁻¹]
hmi8v	two-phase mix enthalpy of 8 stream [Btu lb ⁻¹]
hva10	saturated vapour enthalpy of stream 10 [Btu lb ⁻¹]
hva17	saturated vapour enthalpy of stream 17 [Btu lb ⁻¹]
hva8	saturated vapour enthalpy of stream 8 [Btu lb ⁻¹]
hva8v	saturated vapour enthalpy of stream 8 at [Btu lb ⁻¹]
hvbtu	saturated vapour enthalpy [Btu lb ⁻¹]
inde1	data value of lower column offset and lower row offset
inde2	data value of upper column offset and lower row offset
inde3	data value of upper column offset and upper column offset
inde4	data value of upper column offset and upper column offset
inx1	lower column offset
inx2	upper column offset
iny1	lower row offset
iny2	upper row offset
mab	absorber mass flow rate [kg s^{-1}]
mr	liquid refrigerant mass flow rate [kg s^{-1}]
nge	generator efficiency [dimensionless]
nrec	recuperator efficiency [dimensionless]
pre1	rectifier pressure [bar]
pre2	weak solution accumulator pressure [bar]
pre3	condenser pressure [bar]

<i>Variable</i>	<i>Description</i>
pre4	refrigerant leaving condenser pressure [bar]
pre5	weak solution entering to mixer pressure [bar]
pre6	strong solution pressure [bar]
pre7	refrigerant entering evaporator pressure [bar]
pre8	refrigerant leaving evaporator pressure [bar]
prev1	geothermal steam pressure [bar]
prev2	shell side generator pressure [bar]
psbar	saturation pressure [bar]
pssia	saturation pressure [psia]
rectempc	rectification temperature [°C]
row1	interpolation value between inde1 and inde3
row2	interpolation value between inde2 and inde4
sconf	strong solution concentration [fraction]
tdate	test date [mm/dd/yy]
tem1	geothermal fluid entering generator temperature [°C]
tem10	refrigerant leaving evaporator temperature [°C]
tem11	cold storage temperature [°C]
tem12	ambient temperature [°C]
tem13	refrigerant vapour entering mixer temperature [°C]
tem14	weak refrigerant solution entering mixer temperature [°C]
tem15	weak refrigerant solution leaving economizer temperature [°C]
tem16	weak refrigerant solution entering economizer temperature [°C]
tem17	strong refrigerant solution entering economizer temperature [°C]
tem18	strong refrigerant solution entering economizer temperature [°C]
tem19	liquid refrigerant entering precooler temperature [°C]
tem2	geothermal fluid leaving generator temperature [°C]
tem20	liquid refrigerant leaving precooler temperature [°C]
tem21	refrigerant vapour entering precooler temperature [°C]
tem22	refrigerant vapour leaving precooler temperature [°C]
tem23	two-phase mixture entering separator-rectifier temperature [°C]
tem24	refrigerant vapour leaving separator-rectifier temperature [°C]
tem25	weak refrigerant solution leaving separator-rectifier temperature [°C]
tem26	cooling water entering separator-rectifier temperature [°C]
tem27	cooling water leaving separator-rectifier temperature [°C]
tem28	cooling water entering condenser temperature [°C]
tem29	cooling water leaving condenser temperature [°C]
tem3	strong refrigerant solution entering generator temperature [°C]
tem30	cooling water entering absorber temperature [°C]
tem31	cooling water leaving absorber temperature [°C]
tem32	cooling water temperature [°C]
tem4	two-phase mixture leaving generator temperature [°C]
tem5	solution-vapour mixture entering absorber [after mixer] temperature [°C]
tem6	solution leaving absorber temperature [°C]
tem7	refrigerant vapour entering condenser temperature [°C]
tem8	refrigerant leaving condenser temperature [°C]
tem9	refrigerant entering evaporator temperature [°C]
tempc	saturation temperature [°C]
tempf	saturation temperature [°F]
time	time [hh:mm]
uplimy	upper limit value of row values [°F or psia]
weconf	weak solution concentration

Subroutines

print	sent to a printer results range
save	save experimental data and results to a file
start	begin to ask experimental data including date
startd	begin to ask experimental data
optden	calculates specific gravity as a function of temperature and liquid concentration
options	display the main menu
moredata	display yes/no options
modify	sent to data range
input	sent to start subroutine and end with moredata subroutine
exit	quit the programme and leave LOTUS
limitp	comparison pressure value against maximum in this table
limitt	comparison temperature value against maximum in this table
pressay	assigns row offset in function of pressure value in specific range for [2] tables
pressyl1	assigns row offset in function of pressure value in specific range for [Bogart (1981)] tables
opt1	calculates liquid concentration as a function of pressure and temperature
opt4	calculates water amount in saturated vapour as a function of saturation temperature and liquid concentration
opt6	calculates saturated liquid enthalpy as a function of saturation temperature and liquid concentration
opt7	calculates saturated liquid enthalpy as a function of saturation pressure and liquid concentration
opt8	calculates saturated vapour enthalpy as a function of saturation temperature and liquid concentration.
opt9	calculates saturated vapour enthalpy as a function of saturation pressure and liquid concentration

Menus

main	displays options
-------------	------------------

A2.2.8 Programme Listing

```

\c      {goto}b:~{home}{bigright 4}{indicate "Choose the option; or ESC to cancel"}
{menucall options}
{ps}{home}{indicate "Press < Alt c > for the main menu "}

{options}Input  Calculate Modify  Save   Print   Leave
          Input expCalculateModify cuSave expePrint maLeave programme and LOTUS
          {branch i{branch c{branch m{branch s{branch p{branch exit}

{input} {indicate "This option clean the sheet do you want to continue"}
{getlabel "Are you sure Y/N ;",answer}
{indicate}{if answer="y"#{OR#answer="Y"}{branch b:q119}
{branch \c}
/redata~{branch start}

start {goto}a:a7-
{getlabel "Test Date (mm/dd/yy) ;",tdate}

startd {indicate}{getlabel "Time (HH:MM); ",time}~/rvtime--{right}
{indicate " Temperatures, (°C) "}
{getnumber "Geothermal fluid entering generator, T1; ",tem1}~+tem1{calc}~{right}
{getnumber "Geothermal fluid leaving generator, T2; ",tem2}+tem2{calc}~{right}
{getnumber "Strong refrigerant solution entering generator, T3;
",tem3}~+tem3{calc}~{right}
{getnumber "Two-phase mixture leaving generator, T4 ; ",tem4}~+tem4{calc}~{right}
{getnumber "Solution-vapour mixture entering absorber (after mixer), T5;
",tem5}~+tem5{calc}
{getnumber "Solution leaving absorber, T6; ",tem6}~+tem6{calc}~{r}
{getnumber "Refrigerant vapour entering condenser, T7; ",tem7}~+tem7{calc}~{r}
{getnumber "Refrigerant leaving condenser, T8; ",tem8}~+tem8{calc}~{r}
{getnumber "Refrigerant entering evaporator, T9; ",tem9}~+tem9{calc}~{r}
{getnumber "Refrigerant leaving evaporator, T10; ",tem10}~+tem10{calc}~{r}
{getnumber "Cold storage, T11; ",tem11}~+tem11{calc}~{r}
{getnumber "Ambient temperature, T12; ",tem12}~+tem12{calc}~{r}
{getnumber "Refrigerant vapour entering mixer, T13; ",tem13}~+tem13{calc}~{r}
{getnumber "Weak refrigerant solution entering mixer, T14; ",tem14}~+tem14{calc}~{r}
{getnumber "Weak refrigerant solution leaving economizer, T15; ",tem15}~+tem15{calc}~{r}
{getnumber "Weak refrigerant solution entering economizer, T16; ",tem16}~+tem16{calc}~{r}
{getnumber "Strong refrigerant solution entering economizer, T17;
",tem17}~+tem17{calc}~{r}
{getnumber "Strong refrigerant solution leaving economizer, T18;
",tem18}~+tem18{calc}~{r}
{getnumber "Liquid refrigerant entering precooler, T19; ",tem19}~+tem19{calc}~{r}
{getnumber "Liquid refrigerant leaving precooler, T20; ",tem20}~+tem20{calc}~{r}
{getnumber "Refrigerant vapour entering precooler, T21; ",tem21}~+tem21{calc}~{r}
{getnumber "Refrigerant vapour leaving precooler, T22; ",tem22}~+tem22{calc}~{r}
{getnumber "Two-phase mixture entering separator-rectifier, T23;
",tem23}~+tem23{calc}~{r}
{getnumber "Refrigerant vapour leaving separator-rectifier, T24;
",tem24}~+tem24{calc}~{r}
{getnumber "Weak refrigerant solution leaving separator-rectifier, T25;
",tem25}~+tem25{cal}
{getnumber "Cooling water entering separator-rectifier, T26; ",tem26}~+tem26{calc}~{r}
{getnumber "Cooling water leaving separator-rectifier, T27; ",tem27}~+tem27{calc}~{r}
{getnumber "Cooling water entering condenser, T28; ",tem28}~+tem28{calc}~{r}
{getnumber "Cooling water leaving condenser, T29; ",tem29}~+tem29{calc}~{r}
{getnumber "Cooling water entering absorber, T30; ",tem30}~+tem30{calc}~{r}
{getnumber "Cooling water leaving absorber, T31; ",tem31}~+tem31{calc}~{r}
{getnumber "Cooling water, T32; ",tem32}~+tem32{calc}~{r}{indicate " Pressure (kg/cm²)
"}
{getnumber "Geothermal steam, Pv1; ",prev1}-
{let prev1,(prev1+0.96784)*0.98067}~+prev1{calc}~{r}
{getnumber "Shell side generator, Pv2; ",prev2}-
{let prev2,(prev2+0.96784)*0.98067}~+prev2{calc}~{r}
{getnumber "Rectifier pressure, P1; ",pre1}-
{let pre1,(pre1+0.96784)*0.98067}~+pre1{calc}~{r}
{getnumber "Weak solution accumulator, P2; ",pre2}-
{let pre2,(pre2+0.96784)*0.98067}~+pre2{calc}~{r}
{getnumber "Condenser, P3; ",pre3}-
{let pre3,(pre3+0.96784)*0.98067}~+pre3{calc}~{r}
{getnumber "Refrigerant leaving condenser, P4; ",pre4}-
{let pre4,(pre4+0.96784)*0.98067}~+pre4{calc}~{r}
{getnumber "Weak solution entering to mixer, P5; ",pre5}-
{let pre5,(pre5+0.96784)*0.98067}~+pre5{calc}~{r}
{getnumber "Strong solution, P6; ",pre6}-
{let pre6,(pre6+0.96784)*0.98067}~+pre6{calc}~{r}

```

```

{getnumber "Refrigerant entering evaporator, P7; ",pre7}-
{let pre7,(pre7+0.96784)*0.98067}~+pre7{calc}~{r}
  {getnumber "Refrigerant leaving evaporator, P8; ",pre8}~{indicate " Flow rate (GPM )
  "}
{let pre8,(pre8+0.96784)*0.98067}~+pre8{calc}~{r}
{getnumber "Liquid refrigerant, Fr1; ",flr1}-
{let flr1,(flr1*3.785/60)/1000+flr1{calc}~{r}
{getnumber "Weak refrigerant solution, Fs1; ",fls1}-
{let fls1,(fls1*3.785/60)/1000+fls1{calc}~{r}
{getnumber "Cooling water to absorber, Fw1; ",flw1}-
{let flw1,(flw1*3.785/60)/1000+flw1{calc}~{r}
{getnumber "Cooling water to rectifier, Fw2; ",flw2}-
{let flw2,(flw2*3.785/60)/1000+flw2{calc}~{r}
{getnumber "Cooling water to condenser, Fw3; ",flw3}-
{let flw3,(flw3*3.785/60)/1000+flw3{calc}~{d}{end}{l}
{indicate Do you want to write more data ?}{menucall moredata}
{indicate}
{branch \c}

calculate{indicate "Working..... Please wait"}
{ps}{home}{goto}a7-
{end}{d}{d}
{d}{r}{avg}({u 2}.{end}{u})-
{d}{std}({u 3}.{end}{u})-
{u}/{c}{d}-{r}.({u 2}{end}{r}{d 3})-
/rv{end}{r}~{u}-
{u}/rt{end}{r}-b:an5-
/re{end}{r}~{l}{d}^AVG.-{d}^STD.-
{let tempf,tem25*1.8+32}
{let pspia,pre2*14.503}{opt1}{let weconf,concl}
{let abtemc,tem6}{let abtemc}{let abpreb,pre6}{let psbar,pre6}
{let tempf,tempc*1.8+32}
weconf {let pspia,psbar*14.503}{opt1}{let stconf,concl}
{let evtemc,tem9}{let tempc,tem9}{let evpreb,pre6}{let psbar,pre6}
{let tempf,tempc*1.8+32}
{let pspia,psbar*14.503}{opt1}{let evliconf,concl}
{opt4}{let evvaconf,1-cwvap}
{let cotemc,tem8}{let copreb,pre3}
{let gentemc,tem4}{let rectemc,tem24}
hv17 {let tempf,tem10*1.8+32}{let concl,evliconf}
{opt8}{let hva17,hvbtu}
h115 {let tempf,tem20*1.8+32}{let concl,evliconf}
{opt6}{let hli15,hlbtu}
mr {let tempf,tem8*1.8+32}{let concl,evliconf}{optden}
{let mr,flr1*densol*1000}
mab {let tempf,tem15*1.8+32}{let concl,weconf}{optden}
{let mab,fls1*densol*1000}
h8 {let tempf,tem4*1.8+32}{let concl,weconf}{opt8}{let hva8,hvbtu}
{let pspia,pre1*14.503}{opt7}{let hli8,hlbtu}
{let hmi8,hva8*(flr1/(flr1+fls1))+hli8*(fls1/(flr1+fls1)))}
h7 {let tempf,tem3*1.8+32}{let concl,stconf}{opt6}{let hli7,hlbtu}
copa {let copa,mr*(hva17-hli15)/(Hab*(hmi8-hli7))}
copccl {let copccl,((tem4-tem6)/tem4)*(tem9/(tem8-tem9)))
h10 {let pspia,pre1*14.503}{let concl,evliconf}{opt9}{let hva10,hvbtu}
h11 {let tempf,tem25*1.8+32}{let concl,weconf}{opt6}{let hli11,hlbtu}
flra {let flra,mab/mr}
geconf {let pspia,pre1*14.503}{let tempf,tem4*1.8+32}{opt1}{let genconf,concl}
fra {let fra,(evliconf-genconf)/(stconf-genconf)}
copecl {let copecl,(hva17-hli15)/(hva10-hli11-(hli11-hli7)*fra)}
hli4 {let pspia,pre1*14.503}{let tempf,tem15*1.8+32}{opt1}
{opt6}{let hli4,hlbtu}
hli43 {let tempf,tem17*1.8+32}{opt6}{let hli43,hlbtu}
hli5 {let tempf,tem16*1.8+32}{let concl,weconf}{opt6}{let hli5,hlbtu}
nrec {let nrec,(hli5-hli4)/(hli5-hli43)}
hli8v {let tempf,tem2*1.8+32}{let concl,weconf}{opt8}{let hva8v,hvbtu}
{let tempf,tem2*1.8+32}{opt6}{let hli8v,hlbtu}
{let hmi8v,hva8*(flr1/(flr1+fls1))+hli8v*(fls1/(flr1+fls1)))}
Ngen {let ngen,(hli7-hmi8)/(hli7-hmi8v)}
hli16 {let tempf,tem9}{let concl,evliconf}{opt6}{let hli16,hlbtu}
evdukw {let evdukw,mr*(hva17-hli16)/0.454*3600*0.29307/1000}
genexqf {let genexqf,mr/(mr+mab)}
{beep 1}{indicate " OK I "}{branch \c}

{modify} {ps}{indicate "Press < Alt c > to return the menu"}
{home}{goto}a7~{quit}

```

```

(save) {ps}{home}/wic{r 4}~/rvb:a1..b:e35~~
/wcs33-{r 2}/wcs5-{r}/wcs41-
{home}{indicate "Type a new filename and press < enter >"}
/fxv{esc}{?}-a:a1..a:ba54-{indicate "Press <enter> to continue"}{?}-{indicate}
{home}/wdc{r 4}-
{branch \c}

(print) /pponu~ad{indicate "Choose the printer to use"}n{?}-{indicate}
qqagpq

(exit) {indicate}
/qyy

optden {if concl=1}{let inx1,concl/.1}{let inx2,inx1}{branch bb3}
{let inx1,concl/.1}{let inx2,concl/.1+1}
{let iny1,tempf/10+5}{let iny2,tempf/10+6}
{let inde1,(@index(gravran,inx1,iny1))}
{let inde3,(@index(gravran,inx2,iny1))}
{let inde2,(@index(gravran,inx1,iny2))}
{let inde4,(@index(gravran,inx2,iny2))}
{let row1,(inde3-inde1)*(concl*10-@int(concl*10))+inde1}
{let row2,(inde4-inde2)*(concl*10-@int(concl*10))+inde2}
{let densol,(row2-row1)*(tempf/10-@int(tempf/10))+row1}
{return}

opt1 {if psp sia>=30}{branch b:bb16}
{pressy1}{branch b:bb17}
{let iny1,pspsia/10+4}{let iny2,pspsia/10+5}{let dy,10}
{let inx1,tempf/10+5}{let inx2,tempf/10+6}
{let inde1,(@index($pagtp,inx1,iny1))}
{let inde3,(@index($pagtp,inx2,iny1))}
{let inde2,(@index($pagtp,inx1,iny2))}
{let inde4,(@index($pagtp,inx2,iny2))}
{let row1,(inde3-inde1)*(tempf/10-@int(tempf/10))+inde1}
{let row2,(inde4-inde2)*(tempf/10-@int(tempf/10))+inde2}
{let concl,(row2-row1)*(pspsia/dy-@int(psp sia/dy))+row1}-{let concl,concl/100}-
{return}

opt4 {if concl=0 #or# concl=1}{let inx1,concl/.1}{let inx2,inx1}{branch b:bb33}
{let inx1,concl/.1}{let inx2,concl/.1+1}
{let iny1,tempf/10+6}{let iny2,tempf/10+7}
{let inde1,(@index($pag37,inx1,iny1))}
{let inde3,(@index($pag37,inx2,iny1))}
{let inde2,(@index($pag37,inx1,iny2))}
{let inde4,(@index($pag37,inx2,iny2))}
{let row1,(inde3-inde1)*(concl*10-@int(concl*10))+inde1}
{let row2,(inde4-inde2)*(concl*10-@int(concl*10))+inde2}
{let cwvp,(row2-row1)*(tempf/10-@int(tempf/10))+row1}-
{return}

opt6 {if concl=1}{let inx1,concl/.1}{let inx2,inx1}{branch bb47}
{let inx1,concl/.1}{let inx2,concl/.1+1}
{let iny1,tempf/10+6}{let iny2,tempf/10+7}
{let inde1,(@index($pag39,inx1,iny1))}
{let inde3,(@index($pag39,inx2,iny1))}
{let inde2,(@index($pag39,inx1,iny2))}
{let inde4,(@index($pag39,inx2,iny2))}
{let row1,(inde3-inde1)*(concl*10-@int(concl*10))+inde1}
{let row2,(inde4-inde2)*(concl*10-@int(concl*10))+inde2}
{let hlbtu,(row2-row1)*(tempf/10-@int(tempf/10))+row1}-{let hlkj,hlbtu*2.326}-
{return}

opt7 {if psp sia>=40}{branch bb60}
{pressy}{branch bb61}
{let iny1,pspsia/10+8}{let iny2,pspsia/10+9}{let dy,10}
{if concl=1}{let inx1,concl/.1}{let inx2,inx1}{branch bb63}
{let inx1,concl/.1}{let inx2,concl/.1+1}
{let inde1,(@index($pag40,inx1,iny1))}
{let inde3,(@index($pag40,inx2,iny1))}
{let inde2,(@index($pag40,inx1,iny2))}
{let inde4,(@index($pag40,inx2,iny2))}
{let row1,(inde3-inde1)*(concl*10-@int(concl*10))+inde1}
{let row2,(inde4-inde2)*(concl*10-@int(concl*10))+inde2}
{let hlbtu,(row2-row1)*(pspsia/dy-@int(psp sia/dy))+row1}-{let hlkj,hlbtu*2.326}-
{return}

opt8 {if concl=1}{let inx1,concl/.1}{let inx2,inx1}{branch bb76}
{let inx1,concl/.1}{let inx2,concl/.1+1}
{let iny1,tempf/10+6}{let iny2,tempf/10+7}

```

```

(let inde1,(@index($pag42,inx1,iny1)))
(let inde3,(@index($pag42,inx2,iny1)))
(let inde2,(@index($pag42,inx1,iny2)))
(let inde4,(@index($pag42,inx2,iny2)))
(let row1,(inde3-inde1)*(conc *10-a nt(concl*10))+inde1)
(let row2,(inde4-inde2)*(conc*10-a nt(conc *10))+inde2)
(let hvbtu,(row2-row1)*(tempf/10-a nt(tempf/10))+row1)-(let hvkj,hvbtu*2.326)-
{return}

opt9 {if ppsia>=40}{branch bb90}
{pressy}{branch bb91}
(let iny1,ppsia/10+8){ et my2,pps a/10+9}{ et dy,10}
{if concl=1}{let inx1,conc /.1}{ et mx2, mx1}{branch bb93}
(let inx1,concl/.1){ et mx2,conc / 1+1}
(let inde1,(@index($pag41, mx1, iny1)))
(let inde3,(@index($pag41, mx2, ny' )))
(let inde2,(@index($pag41, mx1, ny2)))
(let inde4,(@index($pag41, mx2, ny2)))
(let row1,(inde3-inde1)*(conc *10-a nt(conc *10))+ inde1)
(let row2,(inde4-inde2)*(conc *10-a nt conc *10))+ inde2)
(let hvbtu,(row2-row1)*(pps a/dy-a nt(pps a/0/))+row1)-(let hvkj,hvbtu*2.326)-
{return}

```